15

MARYLAND

COLLEGE PARK CAMPUS

STUDY OF SUPERCONVERGENCE BY A COMPUTER-BASED APPROACH.

SUPERCONVERGENCE OF THE GRADIENT IN FINITE ELEMENT SOLUTIONS OF LAPLACE'S AND POISSON'S EQUATIONS

by

I. Babuška
T. Strouboulis
C. S. Upadhyay
S. K. Gangaraj

Technical Note BN-1155

and

CMC Report No. 93-07
Texas Engineering Experiment Station
The Texas A&M University System

November 1993

INSTITUTE FOR PHYSICAL SCIENCE AND TECHNOLOGY

SECURITY CLASSIFICATION OF THIS PAGE (When Data Entered)

REPORT DOCUMENTATION PAGE		READ INSTRUCTIONS BEFORE COMPLETING FORM
1. REPORT NUMBER Technical Note BN-1155	2. GOVT ACCESSION NO.	3. RECIPIENT'S CATALOG NUMBER
4. TITLE (and Subtitle) Study of Superconvergence by a Computer-Based Approach. Superconv;rgence of the Gradient in Finite Element Solutions of Laplace's and Poisson's Equations		5. TYPE OF REPORT & PERIOD COVERED Final Life of Contract 6. PERFORMING ORG. REPORT NUMBER
7. AUTHOR(s) I. Babuska[1] - T. Strouboulis[2] - C. S. Upadhyay[2] - S. K. Gangaraj[2]		8. CONTRACT OR GRANT NUMBER(s) [1]ONR N00014-90-J-1030 [2]USARO DAAL03-G-028 & NSF MSS-9025110 & TARP-71071
9. PERFORMING ORGANIZATION NAME AND ADDRESS Institute for Physical Science and Technology University of Maryland College Park, MD 20742-2431		10. PROGRAM ELEMENT, PROJECT, TASK AREA & WORK UNIT NUMBERS
11. CONTROLLING OFFICE NAME AND ADDRESS Department of the Navy Office of Naval Research Arlington, VA 22217		12. REPORT DATE November 1993 13. NUMBER OF PAGES 59 + Figures
14. MONITORING AGENCY NAME & ADDRESS(if different from Controlling Office)		15. SECURITY CLASS. (of this report) 15a. DECLASSIFICATION/ DOWNGRADING SCHEDULE

16. DISTRIBUTION STATEMENT (of this Report)

Approved for public release: distribution unlimited

17. DISTRIBUTION STATEMENT (of the abstract entered in Block 20, if different from Report)

18. SUPPLEMENTARY NOTES

19. KEY WORDS (Continue on reverse side if necessary and identify by block number)

20. ABSTRACT (

This paper addresses the problem of existence of the superconvergence points by a computer based proof. We prove a basic mathematical theorem that the superconvergence point exists if and only if it can be found by certain numerical algorithm. We address the problem of the superconvergence points for the gradient of the finite element solution of the Laplace and Poisson equations. Our study shows that the sets of superconvergence points are very different for these two cases. We consider triangular as well as quadrilateral elements of degree p, $1 \leq p \leq 7$. In the case of quadrilateral elements we analyze, among others, the tensor-product and the serendipity elements.

DD FORM 1 JAN 73 1473 EDITION OF 1 NOV 65 IS OBSOLETE

S N 0102-LF-014-6601

SECURITY CLASSIFICATION OF THIS PAGE (When Data Entered)

Study of Superconvergence by a Computer-Based Approach. Superconvergence of the Gradient in Finite Element Solutions of Laplace's and Poisson's Equations

I. Babuška*
Institute for Physical Science and Technology and Department of Mathematics,
University of Maryland, College Park, MD 20742, U.S.A.

T. Strouboulis†, C.S. Upadhyay† and S.K. Gangaraj†
Department of Aerospace Engineering, Texas A&M University,
College Station, TX 77843, U.S.A.

November 1993

*The work of this author was supported by the U.S. Office of Naval Research under Contract N00014-90-J-1030 and by the National Science Foundation under Grant CCR-88-20279.

†The work of these authors was supported by the U.S. Army Research Office under Grant DAAL03-G-028, by the National Science Foundation under Grant MSS-9025110 and by the Texas Advanced Research Program under Grant TARP-71071.

Abstract:

This paper addresses the problem of existence of the superconvergence points by a computer based proof. We prove a basic mathematical theorem that the superconvergence point exists if and only if it can be found by certain numerical algorithm. We address the problem of the superconvergence points for the gradient of the finite element solution of the Laplace and Poisson equations. Our study shows that the sets of superconvergence points are very different for these two cases. We consider triangular as well as quadrilateral elements of degree p, $1 \leq p \leq 7$. In the case of quadrilateral elements we analyze, among others, the tensor-product and the serendipity elements.

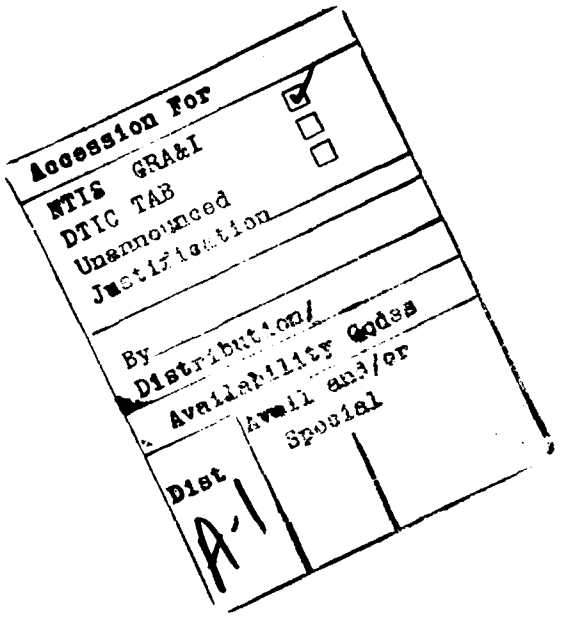

1 Introduction.

Let u_h be a one parameter sequence of finite element solutions of a problem which are computed using a sequence of meshes $\mathcal{T} = \{T_h\}$ and let u denote the exact solution. Let us assume that we are interested in the values of the solution or its derivatives or combinations of these quantities i.e. in the linear functional $F(u)(x)$. Let us assume that for every element τ of the mesh T_h a special point $\bar{x}$, which depends on the geometry (but not the size) of the element, is given. Then denoting

$$\Psi(u - u_h) = \max_{x \in \tau} |F(u - u_h)(x)| \tag{1.1}$$

we are interested in the values of

$$\Theta(\bar{x}; F; u, u_h, h, \tau) = \frac{|F(u - u_h)(\bar{x})|}{\Psi(u - u_h)} \tag{1.2}$$

If the point $\bar{x}$ is such that

$$\Theta(\bar{x}; F; u, u_h, h, \tau) \longrightarrow 0 \quad \text{as} \quad h \longrightarrow 0 \tag{1.3}$$

then $\bar{x}$ will be called a *u-superconvergence point* relatively to the exact solution u and the family of meshes $\mathcal{T}$. Consider now a family $\mathcal{U}$ of solutions; the point $\bar{x}$ will be a *$\mathcal{U}$-superconvergence point* if it is u-superconvergence point for every $u \in \mathcal{U}$. Obviously $\Theta(\bar{x}; F; u, u_h, h, \tau) \leq 1$. If $\Psi(u - u_h) = 0$ in τ then we define $\Theta(\bar{x}; F; u, u_h, h, \tau) = 0$. Practically we can be interested only in the case that

$$\Theta(\bar{x}; F; u, u_h, h, \tau) \leq \eta < 1 \tag{1.4}$$

uniformly for all $u \in \mathcal{U}$ and $T_h \in \mathcal{T}$. In the present paper we will address the case of superconvergence in the sense (1.3). The superconvergence of this type was studied by many investigators; see for example [1-27] and the citations in these papers. The η-superconvergence was not analyzed in the literature; we will address this type of superconvergence for meshes of triangles (resp. meshes of quadrilaterals) in [28] (resp. [29]).

In this paper we will study the superconvergence problem when $F(u)$ is a derivative of u. Here we will address in detail only the cases of the Laplace and the Poisson equation for meshes of triangular and quadrilateral elements of degree p. We will address the elasticity problem in [30].

Our approach is completely different than all other studies of superconvergence. In particular our approach is *computer-based proof*: We prove a theorem that *the superconvergence point exists if and only if it can be found by a numerical algorithm.* Based on this theorem we wrote a computer program, by employing this program we can decide whether the $\mathcal{U}$- or u-superconvergence points exist or not and if so where they are located. By this approach we can handle automatically elements of arbitrary degree and $\mathcal{U}$-superconvergence for any class of solutions. This is essential because often in practice we treat only homogeneous differential equations.

Given a family of finite-element meshes and a corresponding family of conforming piecewise polynomial spaces of degree p, the superconvergence points (for a quantity of interest) in an element in the interior of the domain may or may not exist depending on

1. *The geometry of the grid.*
2. *The class of solutions of interest.*
3. *The span of the local polynomial spaces in each element.*

Following this Introduction we outline the model problem of orthotropic heat-conduction; here we study in detail the superconvergence for the isotropic case (i.e. Laplace's and Poisson's equations) but the same approach can be employed for the general orthotropic case. We present the theoretical setting of the study and describe the computer-based approach which gives the asymptotic properties of the gradient of the error in the interior of the grid. We then demonstrate that the numerical approach can be employed to find the classical superconvergence points (if they exist) in the interior of *locally periodic* finite element meshes of triangular or square elements of any polynomial degree.

2 Preliminaries.

2.1 The model problem

Let us consider the model problem of heat-conduction in orthotropic medium with mixed boundary conditions. Let $\Omega \subseteq \mathbf{R}^2$ be a bounded polygonal domain and let its boundary $\partial\Omega$ be split into two parts Γ_D and Γ_N. Let u be the solution of the problem

$$\mathcal{L}(u) := -\sum_{k,l=1}^{2} \frac{\partial}{\partial x_k}\Big(K_{kl}\frac{\partial u}{\partial x_l}\Big) = \bar{f} \quad \text{in } \Omega, \tag{2.1a}$$

$$u = 0 \quad \text{on } \Gamma_D\,, \tag{2.1b}$$

$$\sum_{k=1}^{2} q_k(u) n_k = \bar{g} \quad \text{on } \Gamma_N \,. \tag{2.1c}$$

Here $K_{k\ell}$, $k, \ell = 1, 2$ are the entries of the *thermal-conductivity* matrix which satisfy the conditions

$$K_{k\ell} = K_{\ell k} \,, \qquad k, \ell = 1, 2 \tag{2.2a}$$

$$0 < K_{\min}(\xi_1^2 + \xi_2^2) \le \sum_{k,\ell=1}^{2} K_{k\ell}\, \xi_k\, \xi_\ell \le K_{\max}(\xi_1^2 + \xi_2^2) \quad \forall\, \boldsymbol{\xi} = (\xi_1, \xi_2) \in \mathbf{R}^2 \,, \tag{2.2b}$$

where $K_{\min}$, $K_{\max}$ are the principal thermal conductivities;

$$q_k(u) := \sum_{\ell=1}^{2} K_{k\ell} \frac{\partial u}{\partial x_\ell} \,, \quad k = 1, 2 \tag{2.3}$$

are the components of the flux (*heat-flux*); n_k, $k = 1, 2$ are the components of the unit outer vector to $\partial\Omega$; $\bar{f} \in L^2(\Omega)$, $\bar{g} \in L^2(\Gamma_N)$ are given data.

Remark 2.1. The majority of the numerical results will be presented for the case of Poisson's equation for which $K_{k\ell} = \delta_{k\ell}$, where $\delta_{k\ell}$ is Kronecker's delta.

Let $H^1_{\Gamma_D}(\Omega) := \left\{ u \in H^1(\Omega) \mid u = 0 \text{ on } \Gamma_D \right\}$. Then the above problem may be put in the variational form: Find $u \in H^1_{\Gamma_D}(\Omega)$ such that

$$B_\Omega(u, v) = L_\Omega(v) \qquad \forall\, v \in H^1_{\Gamma_D}(\Omega) \tag{2.4}$$

where

$$B_\Omega(u, v) := \int_\Omega \sum_{k,\ell=1}^{2} K_{k\ell} \frac{\partial u}{\partial x_\ell} \frac{\partial v}{\partial x_k} \,, \tag{2.5a}$$

and

$$L_\Omega(v) := \int_\Omega \bar{f} v + \int_{\Gamma_N} \bar{g} v \,. \tag{2.5b}$$

If $\Gamma_D = \emptyset$ we assume that the data $\bar{f}, \bar{g}$ satisfy the *consistency condition*

$$\int_\Omega \bar{f} + \int_{\partial\Omega} \bar{g} = 0 \tag{2.6}$$

We define the *energy-norm* by

$$|||u|||_\Omega^2 := B_\Omega(u,u) \tag{2.7}$$

Let $\mathcal{T} := \{T_h\}$ be a *regular-family* of meshes of triangles or quadrilaterals. (For the meshes of triangles it is assumed that for any elements τ_i, $\tau_j \in T_h$, the intersection $\tau_i \cap \tau_j$ is either empty, a vertex or a common edge, and that the minimal angle of all the elements is bounded below by a positive constant, the same for all meshes. For the meshes of quadrilaterals we employ similar assumptions as in [8], [9]. The meshes T_h are not assumed to be quasiuniform.) We introduce the conforming finite-element spaces

$$S_h^p := \left\{ u \in C^0(\Omega) \,\middle|\, u|_{\tau_k} \circ F_{\tau_k} \in \hat{S}^p(\hat{\tau}), \qquad k = 1, \ldots, M(T_h) \right\}, \tag{2.8}$$

where F_{τ_k} is a vector-valued mapping function for the k-th finite element (for the proper assumptions on the smoothness of the transformation see [8], [9], [20], [26]); $\hat{S}^p(\hat{\tau})$ denotes the element-space of polynomials defined over the master-element $\hat{\tau}$; $M(T_h)$ is the number of elements in the mesh T_h.

Below we will consider the following choices for the element-space $\hat{S}^p(\hat{\tau})$:

a. Complete polynomial space up to degree p.

In the case of triangular elements we have $\hat{S}_p(\hat{\tau}) = \hat{\mathcal{P}}_p(\hat{\tau})$ where

$$\hat{\mathcal{P}}_p(\hat{\tau}) := \left\{ \hat{P} \mid \hat{P}(\hat{x}_1, \hat{x}_2) = \sum_{\substack{i,j \\ 0 \le i+j \le p}} \alpha_{i,j}\, \hat{x}_1^i\, \hat{x}_2^j \right\}. \tag{2.9}$$

In the case of quadrilaterals we will consider the following choices for the definition of the polynomial space $\hat{S}_p(\hat{\tau})$ (see also [31]).

b. Tensor-product (bi-p) polynomial space of degree p.

$$\hat{S}^{(p,p)}(\hat{\tau}) := \left\{ \hat{P} \mid \hat{P}(\hat{x}_1, \hat{x}_2) = \sum_{\substack{i,j \\ 0 \le i,j \le p}} \alpha_{i,j}\, \hat{x}_1^i\, \hat{x}_2^j \right\} \tag{2.10}$$

c. Serendipity (trunc) polynomial space of degree p.

$$(2.11)\qquad \hat{\mathcal{S}}^p(\hat{\tau}) := \left\{ \hat{P} \mid \hat{P}(\hat{x}_1,\hat{x}_2) = \sum_{\substack{i,j \\ 0\le i+j\le p}} \alpha_{i,j}\,\hat{x}_1^i\,\hat{x}_2^j + \alpha_{p,1}\,\hat{x}_1^p\,\hat{x}_2 + \alpha_{1,p}\,\hat{x}_1\,\hat{x}_2^p \right\}$$

d. Intermediate polynomial space of degree p.

$$(2.12)\quad \hat{\mathcal{S}}'^p(\hat{\tau}) := \left\{ \hat{P} \mid \hat{P}(\hat{x}_1,\hat{x}_2) = \sum_{\substack{i,j \\ 0\le i+j\le p}} \alpha_{i,j}\,\hat{x}_1^i\,\hat{x}_2^j + \sum_{k=0}^{p-1} \alpha_{p-k,k+1}\,\hat{x}_1^{p-k}\,\hat{x}_2^{k+1} \right\}$$

Remark 2.2. Let $\hat{\tau}$ denote the master square-element. We note that:

$$(2.13a)\qquad \hat{\mathcal{S}}^{(1,1)}(\hat{\tau}) = \hat{\mathcal{S}}^1(\hat{\tau}) = \hat{\mathcal{S}}'^1(\hat{\tau}),$$

$$(2.13b)\qquad \hat{\mathcal{S}}^2(\hat{\tau}) = \hat{\mathcal{S}}'^2(\hat{\tau})$$

while for $p \ge 3$ all three spaces are distinct.

We let $S^p_{h,\Gamma_D} := S^p_h \cap H^1_{\Gamma_D}(\Omega)$. The finite element solution u_h of the model problem satisfies: Find $u_h \in S^p_{h,\Gamma_D}$ such that

$$(2.14)\qquad B_\Omega(u_h, v_h) = L_\Omega(v_h) \qquad \forall\ v_h \in S^p_{h,\Gamma_D}$$

We let $e_h := u - u_h$ denote the error of this approximation. We assume that one of the above mentioned spaces is employed with $p \ge 1$.

2.2 The class of locally periodic meshes

We now present the definition of a special class of locally periodic meshes. In the following Section we will prove several results for the asymptotic behavior of the error for these grids. Let us consider a locally periodic grid defined as follows:

Let $0 < H < H^0$, $x^0 = (x_1^0, x_2^0) \in \Omega$,

$$(2.15)\qquad S(x^0,H) := \left\{ x = (x_1,x_2) \,\middle|\, |x_i - x_i^0| < H, \quad i = 1,2 \right\}$$

and assume H^0 is sufficiently small such that $\bar{S}(x^0, H^0) \subset \Omega$. Further, let γ be a set of multi-indices (i,j), $x^{(i,j)} = (x_1^{(i,j)}, x_2^{(i,j)}) \in \Omega$ and

$$c(x^{(i,j)}, h) := S(x^{(i,j)}, h) \subset S(x^0, H), \qquad (i,j) \in \gamma \tag{2.16}$$

be the set of the h-cells (or cells) which cover exactly $S(x^0, H)$ i.e.

$$\bigcup_{(i,j)\in\gamma} \bar{c}(x^{(i,j)}, h) = \bar{S}(x^0, H) \tag{2.17a}$$

$$c(x^{(i_1,j_1)}, h) \cap c(x^{(i_2,j_2)}, h) = \emptyset \quad \text{for} \quad (i_1, j_1) \neq (i_2, j_2) \tag{2.17b}$$

We will refer to $S(x^0, H)$ as *the subdomain of periodicity of the mesh centered at* x^0. Denoting by

$$\tilde{c} := \left\{ (x_1, x_2) \,\middle|\, |x_1| < 1,\ |x_2| < 1 \right\} \tag{2.18}$$

the *unit-* (*master-*) cell $\tilde{c}$, the h-cell is an h-scaled and translated master-cell.

Let $\tilde{T}$ be a triangular mesh on the master-cell (the master-mesh) and $\tilde{T}_h^{(i,j)}$ be the mesh on $c(x^{(i,j)}, h)$ which is the scaled and translated image of $\tilde{T}$. We will consider the family $\mathcal{T}$ of *locally periodic meshes*. Let $T_h \in \mathcal{T}$ and $T_h(x^0, H)$ be the restriction of T_h on $S(x^0, H)$ and $T_h^{(i,j)}$ the restriction of $T_h(x^0, H)$ on $c(x^{(i,j)}, h)$. We assume that $T_h^{(i,j)} = \tilde{T}_h^{(i,j)}$, $(i,j) \in \gamma$ i.e. $T_h(x^0, H)$ is made by the periodic repetition of the h-scaled master mesh. An example of such a mesh is shown in Fig. 1a where the master-mesh is shown in Fig. 2(a). Note that the parameter $2h$ has the meaning of the length of the cell side in $S(x^0, H)$. In $\Omega - S(x^0, H)$ it has, in general, nothing common with the size of the elements used.

Below we will study the asymptotic properties of the error in the locally periodic mesh for h-cells well within the interior of $S(x^0, H)$. By asymptotic properties we mean the properties in the limit as h tends to zero. Moreover, it will be assumed that $H \geq Ch^\alpha$, with $0 < \alpha < 1$ i.e. the subdomain of periodicity of the mesh in the neighborhood of x^0, $S(x^0, H)$, can shrink to zero but at a slower rate than the size h of the cells. Nevertheless, for simplicity, we will assume that H is fixed and independent of h. We underline that changing h does not change the geometry of the mesh in $S(x^0, H)$.

3 Theoretical setting

3.1 Preliminaries

We will here for simplicity address only the case of Poisson's equation ($K_{kl} = \delta_{kl}$ in (2.1)). Nevertheless, the results could be easily generalized to the general setting for orthotropic medium.

The solution of the problem is understood in the sense of (2.14). In (2.7) we defined the energy-norm which, for K unit-matrix, is

$$|||u|||_\Omega = \| \, |\nabla u| \, \|_\Omega \tag{3.1}$$

where $\| \cdot \|$ is the usual L^2-norm. The fact that we deal in some cases with the seminorm instead of the norm will not play any role. For a specified domain $S \subset \Omega$ we will also use the norms (seminorms) $|||\cdot|||_S$, $\|\cdot\|_S$ with obvious meaning as well as the notation $B_S(u,v)$ with $|||u|||_S^2 := B_S(u,u)$. Given a function u and the multi-index $\alpha := (\alpha_1, \alpha_2)$ we define

$$D^\alpha u := \frac{\partial^{|\alpha|} u}{\partial x_1^{\alpha_1} \, \partial x_2^{\alpha_2}}, \qquad |\alpha| := \alpha_1 + \alpha_2 \tag{3.2a}$$

$$(\mathcal{D}^k u)(x) := \left[\Big(\sum_{|\alpha|=k} |D^\alpha u|^2 \Big)(x) \right]^{\frac{1}{2}}, \quad k \geq 0, \text{ integer} \tag{3.2b}$$

and hence we can write

$$|||u|||_S^2 = \sum_{|\alpha|=1} \|D^\alpha u\|_S^2 = \| \, |\nabla u| \, \|_S^2 = \|\mathcal{D}^1 u\|_S^2 . \tag{3.3}$$

Further we denote by $|\cdot|$ the usual L^∞-norm and $\| u \| = \max\limits_{|\alpha|=1} | D^\alpha u |$.

3.2 The basic properties of the finite element solution

Let $H^0 > H > H_1 > H_2 > H_3$; we have $\Omega \supset \bar{S}(x^0, H^0)$, $S(x^0, H^0) \supset \bar{S}(x^0, H)$, and $S(x^0, H_\ell) \supset \bar{S}(x^0, H_m)$, $\ell < m$. We will deal with $S(x^0, H_\ell)$, $\ell = 1,2,3$, with various $H_\ell < H$. We will assume that H_ℓ are such that

$$\bar{S}(x^0, H_\ell) = \bigcup_{(i,j)\in\gamma_\ell} \bar{c}(x^{(i,j)}, h)\,, \quad \ell = 1,2,3\,. \tag{3.4a}$$

where

$$\gamma_\ell := \left\{(i,j) : c(x^{(i,j)}, h) \subseteq S(x^0, H_\ell)\right\}\,. \tag{3.4b}$$

This means that $S(x^0, H_\ell)$ can be partitioned into the set of cells. In Fig. 1b we give an example of the subdomains $S(x^0, H)$, $S(x^0, H_\ell)$, $\ell = 1,2$, for the mesh shown in Fig. 1a.

We will make the following assumptions about the exact solution u:

Assumption I

On $\bar{S}(x^0, H)$

$$|\, D^\alpha u \,| \le K < \infty, \quad 0 \le |\alpha| \le p+2 \tag{3.5}$$

Remark 3.1. Assumption I states that the solution is smooth in the subdomain $\bar{S}(x^0, H)$ i.e. the subdomain should be sufficiently far from boundaries, material-interfaces and points where the data are rough.

Assumption II

If $a_\alpha := (D^\alpha u)(x^0), \quad \alpha = (\alpha_1, \alpha_2), \quad |\alpha| \le p+1$ then

$$R^2 = \sum_{|\alpha|=p+1} a_\alpha^2 > 0 \tag{3.6}$$

Further, we assume that the mesh $T(\Omega, h)$ is such that:

Assumption III

On $S(x^0, H_2), \quad H_2 < H_1 < H < H^0$

$$\|e_h\|_{S(x^0,H_2)} \le C h^\beta H_2 \tag{3.7}$$

with $\beta \ge (p+1) - \epsilon$, where $0 < \epsilon < 1$ will be specified later, and where C is independent of $T(\Omega, h)$, H_2, but it depends on K and R.

Remark 3.2. We do not assume that u is smooth in Ω outside of $S(x^0, H)$. For example, Ω can have a boundary with corners (as in Fig. 1(a)) and hence u can be unsmooth in the neighborhood of these corners. Nevertheless assumption III makes an implicit requirement on the (refinement of the) mesh in the neighborhood of these corners. If u is smooth in a convex Ω and the mesh is quasi-uniform then

$$|e_h|_\Omega \le Ch^{p+1}|lnh|^r \, |D^{p+1}u|_\Omega, \qquad r \ge 0 \tag{3.8}$$

and hence in the assumption III we can take $\beta < p+1$ arbitrary.

Remark 3.3. Assumptions II, III imply that the principal part of the error in $S(x^0, H_2)$ is related to the non-zero $(p+1)$-derivatives of the exact solution at x^0.

In the following we prove a series of lemmas and the theorems. *We will assume everywhere below that H_1 is sufficiently small (depending on K, R) independent of h.* For simplicity we will address explicitly only the case of triangular meshes although the arguments are general.

Lemma 1.

$$|||e_h|||_{c(x^{(i,j)},h)} \ge Ch^{p+1} \qquad \forall\ c(x^{(i,j)},h) \subset S(x^0, H_1) \tag{3.9a}$$

$$\| e_h \|_{c(x^{(i,j)},h)} \ge Ch^{p} \qquad \forall\ c(x^{(i,j)},h) \subset S(x^0, H_1) \tag{3.9b}$$

$$|||e_h|||_{S(x^0,H_i)} \ge Ch^p H_i\ , \qquad i = 1,2,3 \tag{3.10a}$$

$$\| e_h \|_{S(x^0,H_i)} \ge Ch^p\ , \qquad i = 1,2,3 \tag{3.10b}$$

where C depends only on H_1, R, K and the master-cell mesh, but is independent of h.

Proof. Using assumptions I and II the lemma follows immediately from the fact that $D^{p+1}u$ is bounded below on $S(x^0, H_1)$, and therefore on $c(x^{(i,j)}, h)$, by a positive constant, which depends on R, H_1 and K. □

Remark 3.4. The lower estimates in lemma 1, as given above, hold only for the case of triangular elements of degree p (the span of the shape-functions in each element

includes all monomials up to degree p). In the case of quadrilateral elements the span of the element shape-functions is larger and includes monomials of degree greater than p (see [31]). Hence here we have to understand lemma 1 in the sense that (3.9a), (3.9b), (3.10a), (3.10b) are valid for the solutions which are not in the span of the element-space.

Remark 3.5. We also remark that in (3.9b) we have

$$\max\Big(\Big| \frac{\partial e_h}{\partial x_1} \Big|_{c(x^{(i,j)},h)} , \Big| \frac{\partial e_h}{\partial x_2} \Big|_{c(x^{(i,j)},h)} \Big) \geq C h^p \tag{3.11}$$

and not

$$\Big| \frac{\partial e_h}{\partial x_i} \Big|_{c(x^{(i,j)},h)} \geq C h^p , \qquad i = 1,2 . \tag{3.12}$$

Nevertheless later we will assume that

$$\Big| \frac{\partial e_h}{\partial x_i} \Big|_{c(x^{(i,j)},h)} \geq \bar{c} \, \| e_h \|_{c(x^{(i,j)},h)} \tag{3.13}$$

with $\bar{c}$ uniform for the entire class of functions under consideration. This can be achieved by imposing additional assumptions on a_α in assumption II.

Lemma 2. There is a polynomial Q of degree $p+1$ on $S(x^0, H_2)$, $H_2 < H_1$

$$|||u - Q|||_{S(x^0,H_2)} \leq C \, H_2^{p+2} \tag{3.14a}$$

$$| D^\alpha (u - Q) |_{S(x^0,H_2)} \leq C H_2^{p+2-|\alpha|} , \qquad 0 \leq |\alpha| \leq p+2 \tag{3.14b}$$

Proof. Q is the Taylor expansion of u up to degree $p+1$. □

Lemma 3. Let Q be a polynomial of degree $p+1$ defined on $S(x^0, H)$ and let Q_h^{INT} be its interpolant of degree p on the mesh $T_h(x^0, H)$. Denote

$$\rho := Q - Q_h^{\mathrm{INT}} \tag{3.15}$$

then ρ is a periodic function on $S(x^0, H)$ with period $2h$, $\rho \in H^1(S(x^0, H))$, and hence

$$(3.16) \qquad \begin{cases} \rho(x_1^{(i,j)} + h, x_2) = \rho(x_1^{(i,j)} - h, x_2), & |x_2 - x_2^{(i,j)}| < h \\ \rho(x_1, x_2^{(i,j)} + h) = \rho(x_1, x_2^{(i,j)} - h), & |x_1 - x_1^{(i,j)}| < h \end{cases}$$

Proof. The lemma follows immediately from the observation that the $(p+1)$-derivatives of Q are constant in $S(x^0, H)$. Note that we are dealing with elements which are able to reproduce any polynomial of degree p on $c(x^{(i,j)}, h)$. □

In the following we will consider polynomials of degree $(p+1)$

$$(3.17) \qquad Q(x_1, x_2) := \sum_{0 \le |\alpha| \le p+1} b_\alpha (x_1 - x_1^0)^{\alpha_1} (x_2 - x_2^0)^{\alpha_2}, \qquad \alpha = (\alpha_1, \alpha_2)$$

and we assume that

$$(3.18) \qquad 0 < \mu_1^2 \le \sum_{|\alpha| = p+1} b_\alpha^2 \le \mu_2^2 < \infty$$

Lemma 4. Let ρ be given by (3.15); then

$$(3.19a) \qquad C_1 h^{p+2-j} \le \|\mathcal{D}^j \rho\|_{c(x^{(i,j)}, h)} \le C_2 h^{p+2-j}, \qquad j = 0,\ 1$$

$$(3.19b) \qquad C_1 h^{p+1-j} \le |\mathcal{D}^j \rho|_{c(x^{(i,j)}, h)} \le C_2 h^{p+1-j}, \qquad j = 0,\ 1$$

where C_1, C_2 depend on μ_1 and μ_2 and the master mesh but are independent of h.

Proof. The lemma follows from the basic properties of the interpolant, (3.18) and lemma 1. □

We now define the periodic finite element problem on $c(x^{(i,j)}, h)$. Let

$$(3.20) \qquad H^1_{\text{PER}}\big(c(x^{(i,j)}, h)\big) := \Big\{ u \in H^1\big(c(x^{(i,j)}, h)\big) : u \text{ satisfies (3.16)} \Big\}$$

and

$$S^p_{h,\mathrm{PER}}\left(c(x^{(i,j)},h)\right) := \left\{u \in H^1_{\mathrm{PER}}\left(c(x^{(i,j)},h)\right) : u|_\tau \in \mathcal{P}_p,\ \tau \in T_h^{(i,j)}\right\} \tag{3.21}$$

Let $\varphi \in H^1_{\mathrm{PER}}\left(c(x^{(i,j)},h)\right)$; then we denote $z_h^\varphi \in S^p_{h,\mathrm{PER}}\left(c(x^{(i,j)},h)\right)$ such that

$$B_{c(x^{(i,j)},h)}(z_h^\varphi, v_h) = B_{c(x^{(i,j)},h)}(\varphi, v_h) \qquad \forall\, v_h \in S^1_{h,\mathrm{PER}}\left(c(x^{(i,j)},h)\right) \tag{3.22}$$

and

$$\int_{c(x^{(i,j)},h)} (\varphi - z_h^\varphi) = 0 \tag{3.23}$$

The function z_h^φ will be called the *periodic finite element solution*. Let us remark that by scaling and translating the mesh we can solve the finite element problem in the master cell using the master mesh.

Lemma 5. Let $\varphi \in H^1_{\mathrm{PER}}\left(c(x^{(i,j)},h)\right)$ and let $\tilde{\varphi}$ be the periodic extension of φ on $S(x^0, H_\ell)$, $H_\ell < H_1$, $\ell = 2,3$. Further let $\tilde{z}_h^\varphi$ be the periodic extension of z_h^φ on $S(x^0, H_\ell)$. Then

$$B_{S(x^0,H_\ell)}(\tilde{z}_h^\varphi, v_h) = B_{S(x^0,H_\ell)}(\tilde{\varphi}, v_h) \qquad \forall\, v_h \in S^p_{h,0}\left(S(x^0,H_\ell)\right) \tag{3.24}$$

where

$$S^p_{h,0}\left(S(x^0,H_\ell)\right) := \left\{v_h \in S^p_h(\Omega) :\ v_h \text{ has its support in } \bar{S}(x^0,H_\ell)\right\} \tag{3.25}$$

Proof. We will write

$$B_{S(x^0,H_\ell)}(\tilde{z}_h^\varphi, v_h) = \sum_{(i,j)\in\gamma_\ell} B_{c(x^{(i,j)},h)}(\tilde{z}_h^\varphi, v_h) \tag{3.26}$$

Using the periodicity of $\tilde{z}_h^\varphi$ and $\tilde{\varphi}$ we have

$$\begin{aligned} \sum_{(i,j)\in\gamma_\ell} B_{c(x^{(i,j)},h)}(\tilde{z}_h^\varphi, v_h) &= B_{c(x^0,h)}\Big(z_h^\varphi, \sum_{(i,j)\in\gamma_\ell} v_h(x + x^{(i,j)})\Big) = \\ &= B_{c(x^0,h)}\Big(\tilde{\varphi}, \sum_{(i,j)\in\gamma_\ell} v_h(x + x^{(i,j)})\Big) \end{aligned} \tag{3.27}$$

Realizing that

$$\sum_{(i,j)\in\gamma_\ell} v_h(x + x^{(i,j)}) \in S^p_{h,\mathrm{per}}\left(c(x^0,h)\right) \tag{3.28}$$

we get (3.24). □

Let us now use $\varphi = \rho$, where ρ has been defined in (3.15). Then by lemma 4 we have $\varphi \in H^1_{\mathrm{per}}\left(c(x^{(i,j)},h)\right)$, $\rho = \tilde{\rho}$ and denoting

$$\psi := \tilde{\rho} - \tilde{z}^\rho_h \tag{3.29}$$

we have:

Lemma 6.

$$B_{S(x^0,H_\ell)}(\psi, v_h) = 0 \qquad \forall\, v_h \in S^p_{h,0}\left(S(x^0,H_\ell)\right) \tag{3.30}$$

and

$$C_3\, h^{p+1-j} H_\ell \le \|\mathcal{D}^j\psi\|_{S(x^0,H_\ell)} \le C_4\, h^{p+1-j} H_\ell\,, \qquad j = 0,\ 1 \tag{3.31a}$$

$$C_3\, h^{p+1-j} \le |\,\mathcal{D}^j\psi\,|_{S(x^0,H_\ell)} \le C_4\, h^{p+1-j}|\ell n h|^r\,, \qquad j = 0,\ 1\,, \quad r \ge 0 \tag{3.31b}$$

where C_3, C_4 depend on μ_1, μ_2, H_1 and the master mesh.

Proof. We have $B_{S(x^0,H_\ell)}(\rho - \tilde{z}^\rho_h, v_h) = B_{S(x^0,H_\ell)}(\rho, v_h) - B_{S(x^0,H_\ell)}(\tilde{z}^\rho_h, v_h) = 0$ by lemma 5, and (3.30) is proven.

From (3.22) and lemma 4 we get

$$|||\psi|||_{c(x^{(i,j)},h)} = |||\rho - z^\rho_h|||_{c(x^{(i,j)},h)} \le |||\rho|||_{c(x^{(i,j)},h)} \le Ch^{p+1} \tag{3.32}$$

and applying the duality principle we get

$$\|\psi\|_{c(x^{(i,j)},h)} = \|z^\rho_h - \rho\|_{c(x^{(i,j)},h)} \le Ch|||\rho|||_{c(x^{(i,j)},h)} \tag{3.33}$$

where C is independent of ρ and h. Realizing that there are H_l^2/h^2 cells in $S(x^0, H_l)$ we get

$$|||\psi|||^2_{S(x^0,H_l)} \leq Ch^{2(p+1)}\frac{H_l^2}{h^2} \leq CH_l^2h^{2p}$$

$$\|\psi\|^2_{S(x^0,H_l)} \leq Ch^{2(p+2)}\frac{H_l^2}{h^2} \leq CH_l^2h^{2(p+1)}$$

which proves the right-hand side of (3.31a).

Because $\mathcal{D}^{p+1}\psi = C'(\mu_1) > 0$ on every $\tau \in T_h^{(i,j)}$, it can be readily seen that

$$\|\mathcal{D}^1\psi\|_{c(x^{(i,j)},h)} \geq C\,C'(\mu_1)h^{p+1}$$

$$\|\psi\|_{c(x^{(i,j)},h)} \geq C\,C'(\mu_1)h^{p+2}$$

from which the left hand side of (3.31a) follows.

The proof for the norms $|\cdot|, \|\cdot\|$ follows analogous steps using the standard theory of L^∞ estimates. □

Lemma 7. Let Q be a polynomial of degree $(p+1)$ on $S(x^0, H_2)$, $H_2 < H_1$ and $Q_h \in S_h^1\left(S(x^0, H_2)\right)$ such that

$$\inf_{\chi \in S_h^1\left(S(x^0,H_2)\right)} |||Q - \chi|||_{S(x^0,H_2)} = |||Q - Q_h|||_{S(x^0,H_2)} \tag{3.34a}$$

$$\int_{S(x^0,H_2)} (Q - Q_h) = 0 \tag{3.34b}$$

Further let $H_3 = \pi H_2$, $0 < \pi < 1$, $d_2 := H_2 - H_3 = (1-\pi)H_2$. Then

$$\| Q - Q_h \|_{S(x^0,H_3)} = \| \psi \|_{S(x^0,H_3)}\left(1 + \lambda C\frac{hH_2}{d_2^2}\right) \tag{3.35}$$

where $|\lambda| \leq 1$ and C is independent of h, H_1 and ψ.

Proof. We have $Q - Q_h - \psi = \tilde{z}_h^\rho + Q_h^{\mathrm{INT}} - Q_h \in S_h^p(S(x^0, H_2))$ and

$$B_{S(x^0,H_2)}(Q - Q_h - \psi, v_h) = 0 \qquad \forall\ v_h \in S_{h,0}^p(S(x^0, H_2))$$

and using Lemma 9 (see below) we get

$$\| Q - Q_h - \psi \|_{S(x^0,H_3)} \leq \frac{C}{d_2^2} \| Q - Q_h - \psi \|_{S(x^0,H_2)} \leq$$

$$\leq \frac{C}{d_2^2} \left(\| Q - Q_h \|_{S(x^0,H_2)} + \| \psi \|_{S(x^0,H_2)} \right) \leq C \frac{h}{d_2^2} |||\rho|||_{S(x^0,H_2)}$$

The above follows by using the duality principle ($S(x^0, H_2)$ is convex domain) and by observing that

$$|||Q - Q_h|||_{S(x^0,H_2)} \leq |||Q - Q_h^{\mathrm{INT}}|||_{S(x^0,H_2)} = |||\rho|||_{S(x^0,H_2)}$$

and that

$$|||\psi|||_{S(x^0,H_2)} = |||\rho - z_h^\rho|||_{S(x^0,H_2)} \leq |||\rho|||_{S(x^0,H_2)}$$

Moreover $|||\rho|||_{S(x^0,H_2)} \leq C h^p H_2$ and thus

$$\| Q - Q_h - \psi \|_{S(x^0,H_3)} \leq C \frac{h^{p+1} H_2}{d_2^2} \tag{3.36}$$

From lemma 6

$$\| \psi \|_{S(x^0,H_3)} \geq C h^p$$

and hence

$$\| Q - Q_h - \psi \|_{S(x^0,H_3)} \leq C \frac{h H_2}{d_2^2} \| \psi \|_{S(x^0,H_3)}$$

Moreover

$$\| Q - Q_h \|_{S(x^0,H_3)} \leq \| \psi \|_{S(x^0,H_3)} + \| Q - Q_h - \psi \|_{S(x^0,H_3)}$$

$$\| Q - Q_h \|_{S(x^0,H_3)} \geq \| \psi \|_{S(x^0,H_3)} - \| Q - Q_h - \psi \|_{S(x^0,H_3)}$$

and hence

$$\| Q - Q_h \|_{S(x^0,H_3)} = \| \psi \|_{S(x^0,H_3)} \left(1 + \lambda C \frac{h H_2}{d_2^2} \right)$$

which completes the proof of the lemma. □

We will now summarize the theorems on interior error estimates which we use in this Section. For the proofs see [38].

Lemma 8. Let $x \in S(x^0, H_i)$, $d_i := H_{i-1} - H_i \geq Ch$. Let $u_h \in S_h^p(S(x^0, H_1))$,

$$B_{S(x^0,H_{i-1})}(u - u_h, v) = 0 \qquad \forall\ v \in S_{h,0}^p\Big(S(x^0, H_{i-1})\Big) \tag{3.37a}$$

Then

$$|\nabla e_h(x)| \leq C \min_{\chi \in S_h^p(S(x^0,H_{i-1}))}\Big(\| u - \chi \|_{S(x^0,H_{i-1})} + \frac{1}{d_i} | u - \chi |_{S(x^0,H_{i-1})}\Big)$$

$$+ \frac{C}{d_i^2}||u - u_h||_{S(x^0,H_{i-1})} \tag{3.37b}$$

Lemma 9. Let $w_h \in S_h^p\Big(S(x^0, H_{i-1})\Big)$ and

$$B_{S(x^0,H_{i-1})}(w_h, v_h) = 0 \qquad \forall\ v_h \in S_{h,0}^p\Big(S(x^0, H_{i-1})\Big) \tag{3.38a}$$

Then

$$\| w_h \|_{S(x^0,H_i)} \leq \frac{C}{d_i^2}\ ||w_h||_{S(x^0,H_{i-1})} \tag{3.38b}$$

Let us now prove the main theorem of the paper.

Theorem 1. Let $H_3 < H_2 < H_1 < H < H^0$ and the assumptions I-III hold with

$$C_1 H_3^\alpha \leq h \leq C_2 H_3^\alpha\ ,\ \alpha = \frac{6p+1}{6p}\ , \nu = \frac{1}{6(6p+1)}\ ,\ \beta = p + 1 - \epsilon\ ,\ \epsilon = \nu\ . \tag{3.39}$$

Then for any $x \in S(x^0, H_3)$

$$\Big|\frac{\partial e_h}{\partial x_i}(x)\Big| = \Big|\frac{\partial \psi}{\partial x_i}(x)\Big| + \lambda C h^{p+\nu} \tag{3.40}$$

with $|\lambda| \leq 1$ and C independent of h.

Proof: Let $H_3 = (1 - h^{2\nu})H_2$, $H_2 < H_1$. We have

$$e_h = u - u_h = u - Q + Q - Q_h + Q_h - u_h$$

and hence

$$\| e_h \|_{S(w^0,H_2)} \le \| u_h - Q_h - (u - Q) \|_{S(w^0,H_2)} + \| Q - Q_h \|_{S(w^0,H_2)}$$

Let us estimate $\| u_h - Q_h - (u - Q) \|_{S(w^0,H_2)}$. Noting that

$$B_{S(w^0,H_2)}(u_h - Q_h - (u - Q), v) = 0 \qquad \forall\ v \in S^p_{h,0}\Big(S(w^0, H_2)\Big)$$

and using lemma 8 we get

$$\| u_h - Q_h - (u - Q) \|_{S(w^0,H_2)} \le C \min_{\chi \in S^p_h(S(w^0,H_2))} \Big(\| u - Q - \chi \|_{S(w^0,H_2)} +$$

$$+ \frac{1}{d_2} | u - Q - \chi |_{S(w^0,H_2)} \Big) + \frac{C}{d_2^2} \| u_h - Q_h - (u - Q) \|_{S(w^0,H_2)}$$

Using for χ the interpolant of $u - Q$ we get

$$\| u - Q - \chi \|_{S(w^0,H_2)} \le C H_2 h^p, \qquad | u - Q - \chi |_{S(w^0,H_2)} \le C H_2 h^{p+1}$$

Further we have

$$\| u_h - Q_h - (u - Q) \|_{S(w^0,H_2)} \le \| u_h - u \|_{S(w^0,H_2)} + \| Q_h - Q \|_{S(w^0,H_2)}$$

and using assumption III, the duality principle and lemma 4 we get using lemma 2

$$\| u_h - Q_h - (u - Q) \|_{S(w_0,H_2)} \le C(h^\beta H_2 + h^{p+1} H_2)$$

and hence

$$\| u_h - Q_h - (u - Q) \|_{S(w^0,H_3)} \le C\Big(H_2 h^p + \frac{H_2 h^{p+1}}{d_2} + \frac{h^\beta H_2}{d_2^2} + \frac{h^{p+1} H_2}{d_2^2} \Big) \le C h^\mu$$

where

$$\mu = \min\Big\{ p + \frac{1}{\alpha},\quad p + 1 - 2\nu,\quad \beta - \frac{1}{\alpha} - 4\nu,\quad p + 1 - \frac{1}{\alpha} - 4\nu \Big\}$$

From lemma 7 we get

$$\| Q - Q_h \|_{S(w^0,H_3)} = \| \psi \|_{S(w^0,H_3)} \left(1 + C\lambda h^{1-\frac{1}{\alpha}-4\nu}\right)$$

where $|\lambda| < 1$. Moreover from lemma 6

$$C_1 h^p \leq \| \psi \|_{S(w^0,H_3)} \leq C_2 h^p$$

Hence

$$\| e_h \|_{S(w^0,H_3)} \leq \| \psi \|_{S(w^0,H_3)} \left(1 + C\, h^{\mu-p}\right)$$

and analogously the other inequality so we get

$$\| e_h \|_{S(w^0,H_3)} = \| \psi \|_{S(w^0,H_3)} \left(1 + \lambda C h^{\hat{\mu}}\right)$$

where

$$\hat{\mu} = \min\left\{ \frac{1}{\alpha},\ 1-2\nu,\ \beta - \frac{1}{\alpha} - 4\nu - p,\ 1 - \frac{1}{\alpha} - 4\nu \right\}$$

Assuming that $\beta \geq p + 1 - \epsilon$,

$$0 < \epsilon \leq \sigma_0\,, \qquad \alpha = 1 + \frac{1}{6p} = \frac{6p+1}{6p}\,, \qquad \nu = \frac{1}{6(6p+1)}$$

we get with $\sigma_0 = \nu$,

$$\frac{1}{\alpha} = \frac{6p}{6p+1} \geq \sigma_0\,, \qquad 1 - 2\nu \geq \sigma_0\,,$$

$$\beta - \frac{1}{\alpha} - 4\nu - p = p + 1 - \epsilon - \frac{6p}{6p+1} - \frac{4}{6(6p+1)} - p =$$

$$= 1 - \frac{36p+4}{6(6p+1)} - \epsilon = \frac{2}{6(6p+1)} - \epsilon \geq \frac{1}{6(6p+1)} \geq \sigma_0\,,$$

$$1 - \frac{1}{\alpha} - 4\nu = 1 - \frac{6p}{6p+1} - \frac{4}{6(6p+1)} = \frac{6(6p+1) - 36p - 4}{6(6p+1)} = \frac{2}{6(6p+1)} \geq \sigma_0$$

when

$$\frac{1}{6(6p+1)} = \epsilon = \nu = \sigma_0 \geq 0 .$$

We thus have

$$\| e_h \|_{S(x^0,H_3)} = \| \psi \|_{S(x^0,H_3)} \left(1 + \lambda C h^{\sigma_0}\right) .$$

Further we have for any $x \in S(x^0, H_3)$

$$\frac{\partial e_h}{\partial x_i}(x) = \frac{\partial}{\partial x_i}\Big((u - Q) - (u_h - Q_h)\Big)(x) + \frac{\partial}{\partial x_i}(Q - Q_h)(x)$$

and so proceeding in the same way we get

$$\frac{\partial e_h}{\partial x_i}(x) = \frac{\partial \psi}{\partial x_i}(x) + \lambda C h^{\sigma_0 + p} .$$

□

Remark 3.6. Let us now comment briefly on the meaning of the theorem. We will assume that the mesh is periodic in a small region in the interior of the domain and that the solution is smooth. Outside the square we assume neither that the mesh is periodic nor that the solution is smooth. We only assume that the pollution in the periodic mesh-subdomain is controlled. Then the superconvergence is directly related to the function ψ which can be computed in the master-cell.

Remark 3.7. Note that the fact that we have used square cells is not essential. It is only essential that the mesh is translation-invariant. Let us also underline that the assumption that K is the identity matrix was made only for simplicity. The theorem holds for general matrix K, which is allowed to vary smoothly throughout the domain.

Remark 3.8. Theorem 1 allows us to make a computer-based proof of the existence of the superconvergence points for the case when $F(u) = \dfrac{\partial u}{\partial x_i}$ (see introduction). We see from (3.40) that if and only if $\dfrac{\partial}{\partial x_i}\psi(x) = 0$ we have

$$\left|\frac{\partial e_h}{\partial x_i}(x)\right| \leq C h^{p+\sigma_0}, \qquad \sigma_0 > 0 \tag{3.41}$$

and C is independent of h. Further we know from the construction of ψ that (after scaling) the function ψ is independent of h. Hence the relative position of x in τ where $\dfrac{\partial}{\partial x_i}\psi(x) = 0$ is independent of the mesh. On the other hand with the exception of very special cases we have

$$(3.42) \qquad \left| \frac{\partial e_h}{\partial x_i} \right|_\tau \geq \bar{c} \, \| e_h \|_\tau \geq C h^p \quad \bar{c} > 0$$

In this case (which is always assumed in the classical superconvergence theories) our theorem says that *a point x in the element τ is a superconvergence point for* $F(u) = \dfrac{\partial u}{\partial x_i}$ *if and only if* $\dfrac{\partial \psi}{\partial x_i}(x) = 0$. Because we are interested in a $\mathcal{U}$-superconvergence point for $\mathcal{U}$ being a sufficiently large set of solutions, the condition (3.42) is not restrictive.

Remark 3.9. We discussed above only the heat-conduction problem. We will address the superconvergence for the elasticity problem in a forthcoming paper [30].

Remark 3.10. Although in general the superconvergence points do not exist, a region of points where the accuracy of the gradient is much larger than the maximal error in the element still could exist. This question is addressed in forthcoming papers ([28], [29]) in which we introduce and analyze the notion of η-superconvergence points, $0 \leq \eta \leq 1$. The case $\eta = 0$ coincides with the classical superconvergence (see also (1.4)).

4 The methodology for finding the superconvergence points

In this paper superconvergence is treated as local behavior and hence we are making assumptions about the local behavior of the solution in the interior of the domain. We will consider the class of solutions which are locally smooth in $S(x^0, H)$, namely,

$$(4.1) \qquad \mathcal{U}^G := \left\{ u \in H^1(\Omega) \Big| \quad | D^\alpha u |_{S(x^0,H)} < K, \qquad 0 \leq |\alpha| \leq p+2 \right\}$$

where $S(x^0, H)$ denotes an interior subdomain of interest in which the mesh is locally periodic as described above (the subdomain must be a finite distance away from the boundary and points of roughness of the source term). In many instances we are only interested in the subclass of solutions in $\mathcal{U}^G$ which are "harmonic" (we say that u is "harmonic" if it satisfies the homogeneous differential equation), namely,

$$(4.2) \qquad \mathcal{U}^{"H"} := \left\{ u \in \mathcal{U}^G \;\Big|\; \mathcal{L}(u) = 0 \quad \text{in} \quad \Omega \right\}$$

We may also assume that the functions are "harmonic" in a subdomain which is slightly bigger than $S(x^0, H)$ and which includes $S(x^0, H)$ in its interior.

In the previous Section we proved that we can obtain the asymptotic values of the error for any smooth solution in the interior of a periodic mesh-subdomain by solving a periodic boundary-value problem, using the master-mesh $\tilde{T}$ over the master-cell $\tilde{c}$, with data obtained from the local $(p+1)$-degree Taylor-series expansion of the exact solution. Based on this result we will construct a numerical procedure to determine the superconvergence points (which may not exist) for a given class of smooth solutions by employing the corresponding class of $(p+1)$-degree monomials.

a. The classes of $(p+1)$-degree monomial solutions.

Let us assume that for a given locally periodic grid with corresponding periodic master-mesh $\tilde{T}$, given material orthotropy and given class of smooth solutions $\mathcal{U}$ we consider

$$(4.3) \qquad \mathcal{Q} := \left\{ Q \;\middle|\; Q(x_1, x_2) = \sum_{k=1}^{nd} \alpha_k Q_k(x_1, x_2),\ Q_k(x_1, x_2) = \sum_{\ell=0}^{p+1} \beta_\ell\, x_1^\ell\, x_2^{p+1-\ell} \right\}$$

the class of $(p+1)$-degree monomials which occur in all $(p+1)$-degree Taylor-series expansions about x^0 of functions from $\mathcal{U}$. Here Q_k, $k = 1, \ldots, nd$ denotes a set of linearly independent monomials which span $\mathcal{Q}$. For example let us assume that $\mathcal{U}$ is the class of smooth solutions $\mathcal{U}^G$ given in (4.1); in this case we may choose

$$(4.4) \qquad Q_k(x_1, x_2) := x_1^{p+2-k} x_2^{k-1}, \qquad 1 \le k \le nd = p+2$$

and we obtain the class of all $(p+1)$-degree monomials $\mathcal{Q}^G$.

In many practical applications we are interested only in the class of "harmonic" solutions $\mathcal{U}^{"H"}$ given in (4.2). Then $\mathcal{Q}$ is the two-dimensional space of "harmonic" monomials and will be denoted by $\mathcal{Q}^{"H"}$. For example in the case of Laplace's equation ($K_{k\ell} = \delta_{k\ell}$, $k, \ell = 1, 2$) we have

$$(4.5a) \qquad \mathcal{Q}^H := \left\{ Q^H \;\middle|\; Q^H(x_1, x_2) = \sum_{k=1}^{2} \alpha_k\, Q_k^H(x_1, x_2) \right\},$$

$$(4.5b) \qquad Q_1^H(x_1, x_2) = \mathcal{R}e(z^{p+1}), \quad Q_2^H(x_1, x_2) = \mathcal{I}m(z^{p+1}), \quad z = x_1 + i x_2 .$$

Note that in this case we do not use the quotes since the functions are harmonic in the classical sense (i.e. they satisfy Laplace's equation).

b. The error in the periodic finite-element solution.

For a given exact solution $Q \in \mathcal{Q}$, material-orthotropy matrix $\boldsymbol{K}$, periodic grid $\tilde{T}$ we obtain the error in $\tilde{T}$ by solving the following periodic boundary-value problem:

Find $z_h^\rho \in H_{\mathrm{per}}^h(\tilde{c})$ such that

$$B_{\tilde{c}}(z_h^\rho, v_h) = B_{\tilde{c}}(\rho, v_h) \qquad \forall\ v_h \in S_{h,\mathrm{PER}}^\rho(\tilde{c}) \tag{4.6a}$$

where $\rho, S_{h,\mathrm{PER}}^\rho(\tilde{c})$ are defined in (3.15), (3.20), respectively, and

$$\int_{\tilde{c}} z_h^\rho = \int_{\tilde{c}} \rho \tag{4.6b}$$

and we obtain the error

$$\psi = \rho - z_h^\rho\ . \tag{4.7}$$

· Let $F(u)$ denote the solution-quantity of interest; for example below we will consider $F(u) = \dfrac{\partial u}{\partial x_1}$ or $F(u) = q_1(u) = K_{11}\dfrac{\partial u}{\partial x_1} + K_{12}\dfrac{\partial u}{\partial x_2}$.

c. Superconvergence points of $F(u)$ for the class $\mathcal{Q}$.

We will say that $\bar{\boldsymbol{x}}$ is a superconvergence point in the element $\tau \in \tilde{T}$ for the functional $F(u)$ and the class of solutions $\mathcal{Q}$ if

$$F(\psi)(\bar{\boldsymbol{x}}) = 0 \qquad \forall\ Q \in \mathcal{Q} \tag{4.8}$$

Here ψ is the error which corresponds to the solution Q.

To determine the superconvergence points for $F(u)$, in $\tau \in \tilde{T}$ for the class $\mathcal{Q}$ we define the zero-contour for $F(\psi^i)$ corresponding to the linearly independent monomials Q_i, $i = 1 \ldots, nd$ in the element $\tau \in \tilde{T}$ and for the material-orthotropy $\boldsymbol{K}$

$$C_{F(u)}(Q_i; \tau, \tilde{T}; \boldsymbol{K}) := \left\{ \boldsymbol{x} \in \tau \,\middle|\, F(\psi^i)(\boldsymbol{x}) = 0 \right\}, \tag{4.9}$$

where $\{Q_i\}_{i=1}^{nd}$ is a basis for $\mathcal{Q}$ and ψ^i denotes the error corresponding to Q_i. The set of superconvergence points in the element τ is given by

$$\bar{X}_{F(u)}(Q;\tau,\tilde{T};K) := \bigcap_{i=1}^{nd} C_{F(u)}(Q_i;\tau,\tilde{T};K)\,. \tag{4.10}$$

In the implementations the contours $C_{F(u)}(Q_i;\tau,\tilde{T};K)$ were approximated by piecewise linear continuous lines in each element τ using a background mesh of linear triangles. The initial approximations of the superconvergence points were obtained from the intersections of the approximate contours. In order to find more accurate values of the superconvergence points we constructed the function

$$G_{F(u)}(Q;\tau,\tilde{T};K) := \sum_{i=1}^{nd} \left|F(\psi^i)\right| \tag{4.11}$$

The superconvergence points, if they exist, are located at the zeros of this function. A minimization algorithm was employed to improve the initial approximations of the superconvergence points obtained from the intersections of the approximate contours by minimizing $G_{F(u)}$.

Remark 4.1. Note that the superconvergence points for the functional $F(u)$ and the class Q may not exist in the element τ i.e. the set $\bar{X}_{F(u)}(Q;\tau,\tilde{T};K)$ may be empty. This is indeed the case when the function $G_{F(u)}$ does not have any zeros. In the case that Q is the class of harmonic monomials, we have only two families of zero-contours which, in general, will intersect. Thus we can always find superconvergence points for the class of harmonic solutions.

5 Numerical study of superconvergence for periodic meshes of triangles and squares

We will now demonstrate that, by using the methodology outlined in the previous Section, we can find the superconvergence points for the components of the gradient (or the components of the flux in the case of orthotropic material) in the interior of periodic meshes of triangular or square elements. In the numerical examples we will study the following questions:

1. For periodic meshes of triangles with various mesh-topologies and elements of degree p where are the superconvergence points for
   a. the class of harmonic smooth solutions;
   b. the class of general smooth solutions?

2. For meshes of square elements of degree p where are the superconvergence points for

   a. the tensor-product space $\hat{S}^{(p,p)}(\hat{\tau})$;

   b. the serendipity space $\hat{S}^{p}(\hat{\tau})$;

   c. the intermediate space $\hat{S}'^{p}(\hat{\tau})$?

We will answer these questions using the numerical approach.

Remark 5.1. We remark that for unsmooth solutions the superconvergence points do not exist, in general.

Remark 5.2. Although in Section 4 we addressed only the case of triangular elements the theory holds for the general element-spaces we address below.

5.1 Determination of the superconvergence points for periodic meshes of triangles

The majority of the results for the superconvergence points for the triangular elements in the literature are given exclusively for the Regular pattern (which is also known as *the three-directional mesh* and is shown in Fig. 2a) and linear and quadratic elements; see for example [11], [13], [15-26]. To our knowledge there are no systematic results reported in the literature about the superconvergence points for other mesh-patterns and $p \geq 3$. Here we will employ the numerical approach of Section 4 to find the superconvergence points for all the patterns shown in Fig. 2 and for elements of degree p, $1 \leq p \leq 7$. Moreover we will find the superconvergence points for the harmonic class and the general class of smooth solutions.

We determined the superconvergence points for the x_1-derivative of the gradient for the class of harmonic solutions by locating the points of intersection of the contours $C_{\frac{\partial u}{\partial x_1}}(Q_i^H; \tau, \tilde{T}; I)$, $i = 1,2$. We then checked if these points are also superconvergence points for the class of general solutions by computing the values of the x_1-derivative of the error, $\dfrac{\partial \psi}{\partial x_1}$, corresponding to the linearly independent monomials which are needed to complete the basis of the harmonic space Q^H into the basis of the general space Q^G.

In Table 1 we give the set of superconvergence points $\bar{X}_{\frac{\partial u}{\partial x_1}}(U^H; \tau, \tilde{T}; I)$ for the class of harmonic solutions and for the periodic meshes $\tilde{T}$ shown in Figs. 2a, 2b, 2c and the element τ shown with gray-shading in these Figures (note that the points are the same for all three patterns). The superconvergence points for the class of harmonic solutions for the element τ_1 (resp. τ_2) in the Criss-Cross pattern shown in Fig. 2d are given in Table 2 (resp. Table 3). In Tables 4a-4d (resp. 5a-5b) we

indicate which points for Table 1 (resp. Tables 2, 3) are also superconvergence points for the class of general solutions .

In Figs. 3a-3d we give a schematic example of how the superconvergence points for the class of harmonic solutions in the cubic elements and the four mesh-patterns are obtained from the intersections of the zero-contours for $\frac{\partial \psi}{\partial x_1}$ for the two linearly-independent harmonic monomials of degree $(p+1)$. Figs. 3a-3d also show how to interpret the points given in Tables 1-3 for all the elements in each pattern. In Fig. 4a we show the contours of zero-error in the x_1-derivative for the two harmonic monomials for the shaded element from the Regular-pattern while in Fig. 4b we also included the zero-contours for the monomials which are needed to complete the harmonic basis into the general one. We note that there is only one point which is common to the zero-contours of all the monomials, namely the midpoint of the side of the triangle which is parallel to the x_1-axis. As indicated in Table 4a, this point is the only superconvergence point (for the class of general solutions) for the x_1-derivative in element τ in the Regular pattern.

We make the following observations:

a. For the harmonic solutions there are always superconvergence points for the x_1-derivative for all the mesh-patterns. The number of the points increases with the degree p of the elements.

b. Only very few of the superconvergence points for the class of harmonic solutions are also superconvergence points for the class of general solutions. For example

   (i) For even p's, $p \geq 4$ there are no superconvergence points for the class of general solutions.

   (ii) For the odd p's, $p \geq 3$ and the Regular and Chevron pattern there is only one superconvergence point for the class of general solutions. It is located at the mid-point of the side parallel to the x_1-axis.

   (iii) For the Union-Jack pattern there are no superconvergence points for the class of general solutions for elements of any degree p.

c. The superconvergence points for the x_2-component of the gradient for the mesh-patterns shown in Fig. 2 can be obtained using symmetry arguments.

We now demonstrate that when the points given in Tables 1-3 are employed in model computations the superconvergence of the x_1-derivative can be observed for relatively coarse meshes. To study the superconvergence in actual computations we employed the *discrete-norm* suggested in [8,9], namely

$$E := \left[\frac{1}{N}\sum_{k=1}^{nsup}\left(\frac{\partial e^h}{\partial x_1}(\bar{x}_k)\right)^2\right]^{\frac{1}{2}}. \tag{5.1}$$

Here $\{\bar{\boldsymbol{x}}_k\}_{k=1}^N$ denotes the superconvergence points in the triangles of the mesh which participate in the definition of the discrete norm.

We considered the domain $\Omega = (0,1)^2$ which is meshed by a uniform-grid of elements in the Regular pattern. We computed the values of the discrete norm using points from the elements in the subdomain $\Omega_0 = (0.25, 0.75)^2$. We considered meshes with cell-size $h = \frac{1}{4}, \frac{1}{8}, \frac{1}{16}, \frac{1}{32}$ and we computed three types of discrete norms E', E'', E'''. In particular E' includes the superconvergence points given in Table 1 for each element in Ω_0, E'' includes only those points for each element in Ω_0 which are superconvergence points for the x_1-derivative for the class of general solutions (see Table 4) and E''' includes the points from the elements in Ω_0 which are superconvergence points only for the class of harmonic solutions. Thus we expect to see that all three norms are superconvergent if the exact solution is harmonic while only E'' is also superconvergent for solutions which are not harmonic.

In Table 6a (resp. Table 6c) we give the values of $h^{-3}E'$, $h^{-3}E''$, $h^{-3}E'''$ (resp. $h^{-4}E'$, $h^{-4}E''$, $h^{-4}E'''$) computed from the solution of a Dirichlet boundary-value problem in Ω using quadratic (resp. cubic elements) with data consistent with the harmonic solution $u^H(x_1, x_2) = \sin(\pi x_1)\sinh(\pi x_2)$. We note that as h is subdivided the values $h^{-3}E'$, $h^{-3}E''$, $h^{-3}E'''$ (resp. $h^{-4}E'$, $h^{-4}E''$, $h^{-4}E'''$) converge to constants; this shows the superconvergence of all three versions of the discrete-norm.

In Table 6b (resp. Table 6d) we give the values of $h^{-2}E'$, $h^{-3}E''$, $h^{-2}E'''$ (resp. $h^{-3}E'$, $h^{-4}E''$, $h^{-3}E'''$) computed from the solution of a Dirichlet boundary-value problem in Ω using quadratic (resp. cubic) elements with data consistent with the solution $u^G(x_1, x_2) = \sin(\pi x_1)\sin(\pi x_2)$ (which is not harmonic). We note that as h is subdivided the values of $h^{-2}E'$, $h^{-3}E''$, $h^{-2}E'''$ (resp. $h^{-3}E'$, $h^{-4}E''$, $h^{-3}E'''$) converge to constants; this shows that only the values of E'' are superconvergent in this case.

5.2 Determination of the superconvergence points for periodic meshes of squares

We also employed the computer based approach to find the superconvergence points for meshes of square elements. In particular we studied the effect of the choice of the finite-element space (tensor-product, serendipity, intermediate spaces as defined in (2.9), (2.10), (2.11)) on the superconvergence points for the x_1-derivative. For the tensor-product space it is well known that the points of the $(p \times p)$ Gauss-Legendre product rule are the superconvergence points for the x_1- and x_2-derivative simultaneously for elements of degree p (see for example [9]). To our knowledge, superconvergence points for the serendipity family and the intermediate have not been reported in the literature for $p \geq 3$.

We used the numerical approach to determine the superconvergence points for the x_1-derivative for the case of Poisson's equation. We observed the following:

a. For the tensor-product and the intermediate family of element-spaces, superconvergence of the x_1-derivative occurs along the constant $\hat{x}_1$-Gauss lines which pass through the Gauss-Legendre points of degree p along the $\hat{x}_1$-axis.

b. For the serendipity family the superconvergence points for the x_1-derivative are given as follows:

   (i) For $p = 1, 2$ and the class of general solutions the points are exactly the same Gauss-lines as for the tensor-product and the intermediate family.

   (ii) For $p = 3$ and the class of general solutions four superconvergence points and one superconvergence line (the line $\hat{x}_1 = 0$) were found, as reported in Table 7 and shown in Fig. 5. For the class of harmonic solutions three superconvergence lines, which are shown with thick continuous line in Fig. 5, were obtained.

   (iii) For $p \geq 4$ there are no superconvergence points for the class of general solutions. For the class of harmonic solutions several superconvergence points exist; these points are listed in Table 7 and shown schematically in Figs. 6a-6d for p =4, 5, 6, 7, respectively.

To demonstrate the superconvergence of the x_1-derivative for the points in Table 7 for $p = 3$ and 4, we considered a Neumann boundary-value problem in $\Omega = (0,1)^2$ with data consistent with the harmonic solution u^H and the general solution u^G. We computed the discrete norm E using points from the elements in the subdomain $\Omega_0 = (0.25, 0.75)^2$.

In Table 8a we give the value of $h^{-4}E$ where the (3×3) Gauss-Legendre points from each element in Ω_0 were used in the definition of the discrete norm E; the Neumann problem with data obtained from the general solution u^G was solved with elements of degree $p = 3$ using the tensor-product space and the intermediate space. We observe that for both spaces the values of E are superconvergent, as expected.

In Table 8b we give the values of E and $h^{-3}E$ (resp. $h^{-4}E$) computed from the finite element solution of the Neumann problem with data consistent with the general solution u^G and using the (3×3) Gauss-Legendre points from each element in Ω_0 (resp. the four points given in Table 7 and the point (0,0)). We note that the values of E are superconvergent only when the points from Table 7 are employed.

In Table 8c we give the values of $h^{-5}E$ (resp. $h^{-4}E$) computed from the finite element solution of the Neumann problem with data consistent with the harmonic solution u^H (resp. the general solution u^G). Here we used quartic serendipity finite element space and the points given in Table 7 for $p = 4$. We note that the values of the discrete norm E are superconvergent only in the case of the harmonic.

5.3 Effect of the material orthotropy on the superconvergence points for the flux

In the above examples we gave the superconvergence points for the components of the derivative of finite element solution for Poisson's equation. We now study the effect of orthotropy on the superconvergence points.

We considered square cubic elements ($p = 3$). We let the material-orthotropy matrix $\boldsymbol{K} = \boldsymbol{K}(\theta)$ where $\boldsymbol{K}(\theta)$ has ratio of principal values $\frac{K_{\max}}{K_{\min}} = 10$ and θ denotes the angle (measured counterclockwise) between the x_1-axis and the principal-axis of orthotropy corresponding to $K_{\min}$. We considered the class of "harmonic" solutions $\mathcal{U}^{"H"}$ and the corresponding space $Q^{"H"}$ of functions which can be expressed as linear combinations of the "harmonic" monomials

$$(5.2)\quad Q_1^{"H"}(x_1'', x_2'') = \mathcal{R}e(z''^{p+1}), \quad Q_2^{"H"}(x_1'', x_2'') = \mathcal{I}m(z''^{p+1}), \quad z'' = x_1'' + ix_2'',$$

Here x_1'', x_2'' denotes the axes of the coordinate-system for which the differential operator is transformed to isotropic i.e.

$$(5.4a)\qquad \sum_{i,j=1}^{2} \frac{\partial}{\partial x_i}\Big(K_{ij}\frac{\partial u}{\partial x_j}\Big) = \sqrt{\frac{K_{\max}}{K_{\min}}}\Big(\frac{\partial^2 u''}{\partial x_1''^2} + \frac{\partial^2 u''}{\partial x_2''^2}\Big)$$

where

$$(5.4b)\qquad u''(x_1'', x_2'') := u(x_1, x_2).$$

In Fig. 7 we give the zero-contours $C_{q_1(u)}(Q_i^{"H"}; \tau, \tilde{T}; \boldsymbol{K})$, $i = 1, 2$, and the superconvergence points for the tensor-product space $\hat{S}^{(3,3)}$ and the intermediate space $\hat{S}^{[3]}$. We note that the zero-contours for the two-spaces are identical and the superconvergence points do not depend on the material-orthotropy. (The superconvergence points for the components of $\boldsymbol{q}(u)$ for elements of degree p from the tensor-product or the intermediate space are located at the $(p \times p)$ Gauss-Legendre points in the element.)

In Fig. 8 we give the zero-contours $C_{q_1(u)}(Q_i^{"H"}; \tau, \tilde{T}; \boldsymbol{K})$, $i = 1, 2$, and the superconvergence points for the cubic serendipity element and various grid-material orientations. We note that, in general, the points depend on the material-orthotropy (on the ratio $\frac{K_{\max}}{K_{\min}}$ and the grid-material orientation θ). This dependence should also be expected for serendipity elements of higher-degree ($p \geq 4$).

In Figs. 9a-9h we give the zero-contours $C_{\epsilon_i(u)}(Q_i^{*H^*}; \tau, \tilde{T}; \boldsymbol{K})$, $i = 1, 2$, and superconvergence points for quadratic triangular elements and various grid-material orientations $\left(\frac{K_{\max}}{K_{\min}} = 10, \theta \in [0°, 90°]\right)$. In Figs. 9a-9h we show the zero contours and superconvergence points for the element τ (shaded gray in Fig. 2a) for the Regular pattern. From the Figures it is clear that the location and number of superconvergence points depends on the material-orthotropy. Note that for the given orthotropy and $\theta = 0°$ there are two points of superconvergence; for $\theta = 90°$ there are four superconvergence points while for any of the grid-material orientation there is only one superconvergence point. Based on the above results we can conjecture that for meshes of triangles the number and location of the superconvergence points for the "harmonic" class of solutions depend on the grid-material orientation.

6 Summary of conclusions.

1. We presented a computer-based methodology which can be employed to determine the superconvergence points for the derivatives in the interior of any locally periodic mesh of triangles or squares of any degree p.

2. The methodology takes directly into account the topology of the mesh, the element polynomial spaces and the nature of the solution.

3. We employed the methodology to determine the superconvergence points for several cases of practical interest. We made the following observations:

   a. For the class of harmonic solutions the superconvergence points always exist for any mesh-pattern and type of elements.

   b. For the class of general solutions the superconvergence points may not exist.

   c. For the square elements and tensor-product and the intermediate element-spaces of degree p the superconvergence points are the points of the $(p \times p)$ Gauss-Legendre product rule.

   d. For square elements and the serendipity space of degree p the superconvergence points depend on the class of solutions and the material-orthotropy for elements of degree $p \geq 3$.

   e. For triangular elements the superconvergence points depend on the mesh-pattern, the class of solutions and the material-orthotropy.

Acknowledgments

The first author was partially supported by the Office of Naval Research under Grant N00014-Q0-I-1030 and the National Science Foundation under Grant CCR-88-20279.

The second, third and fourth authors acknowledge the support of the National Science Foundation under grant MSS-9025110, the Army Research Office under grant DAAL03-92-G-0268 and the Texas Advanced Research Program under grant TARP-71071.

References

1. L.A. OGANESYAN AND L.A. RUKHOVETS, *Study of the rate of convergence of variational difference schemes for second-order elliptic equations in a two-dimensional field with a smooth boundary*, U.S.S.R. Comput. Math. Math. Phys., 9 (1968), pp. 153-183.

2. J. DOUGLAS, JR., AND T. DUPONT, *Superconvergence for Galerkin methods for the two point boundary problem via local projections*, Numer. Math., 21 (1973), pp. 270-278.

3. J. DOUGLAS, JR., AND T. DUPONT, *Galerkin approximations for the two point boundary problem using continuous piecewise polynomial spaces*, Numer. Math., 22 (1974), pp. 99-109.

4. J. DOUGLAS, JR., T. DUPONT AND M.F. WHEELER, *An L^∞ estimate and a superconvergence result for a Galerkin method for elliptic equations based on tensor products of piecewise polynomials*, RAIRO Anal. Numér., 8 (1974), pp. 61-66.

5. T. DUPONT, *A unified theory of superconvergence for Galerkin methods for two-point boundary problems*, SIAM J. Numer. Anal., 13 (1976), pp. 362-368.

6. J.H. BRAMBLE and A.H. SCHATZ, *Higher order local accuracy by averaging in the finite element method*, Math. Comp., 31 (1977), pp. 94-111.

7. V. THOMÉE *High order local approximations to derivatives in the finite element method*, Math. Comp. 31 (1977), pp. 652-660.

8. M. ZLÁMAL, *Superconvergence and reduced integration in the finite element method*, Math. Comp., 32 (1978), pp. 663-685.

9. P. LESAINT AND M. ZLÁMAL, *Superconvergence of the gradient of finite element solutions*, RAIRO Anal. Numér., 13 (1979), pp. 139-166.

10. R.Z. DAUTOV, A.V. LAPIN AND A.D. LYASHKO, *Some mesh schemes for quasi-linear elliptic equations*, U.S.S.R. Comput. Math. Math. Phys., 20 (1980), pp. 62-78.

11. M. KŘÍŽEK AND P. NEITTAANMÄKI, *Superconvergence phenomenon in the finite element method arising from averaging gradients*, Numer. Math., 45 (1984), pp. 105-116.

12. N. LEVINE, *Superconvergent recovery of the gradient from piecewise linear finite-element approximations*, IMA J. Numer. Anal., 5 (1985), pp. 407-427.

13. M.F. WHEELER AND J.R. WHITEMAN, *Superconvergent recovery of gradients on subdomains from piecewise linear finite-element approximations*, Numer. Methods for PDEs, 3 (1987), pp. 65-82.

14. M.T. NAKAO, *Superconvergence of the gradient of Galerkin approximations for elliptic problems*, RAIRO Math. Model. Numer. Anal., 21 (1987), pp. 679-695.

15. M. KŘÍŽEK AND P. NEITTAANMÄKI, *On superconvergence techniques*, Acta Applic. Math., 9 (1987), pp. 175-198.

16. M. KŘÍŽEK AND P. NEITTAANMÄKI, *On a global superconvergence of the gradient of linear triangular elements*, J. Comput. Appl. Math., 18 (1987), pp. 221-233.

17. I. HLAVÁČEK AND M. KŘÍŽEK, *On a superconvergent finite element scheme for elliptic systems. I. Dirichlet boundary condition*, Aplik. Mat., 32 (1987), pp. 131-154.

18. I. HLAVÁČEK AND M. KŘÍŽEK, *On a superconvergent finite element scheme for elliptic systems. II. Boundary conditions of Newton's or Neumann's type*, Aplik. Mat., 32 (1987), pp. 200-213.

19. I. HLAVÁČEK AND M. KŘÍŽEK, *On a superconvergent finite element scheme for elliptic systems. III. Optimal interior estimates*, Aplik. Mat., 32 (1987), pp. 276-289.

20. A.B. ANDREEV AND R.D. LAZAROV, *Superconvergence of the gradient for quadratic triangular finite elements*, Numer. Methods for PDEs, 4 (1988), pp. 15-32.

21. Q.D. ZHU AND Q. LIN, *Superconvergence Theory of FEM*, Hunan Science Press, 1989.

22. G. GOODSELL AND J.R. WHITEMAN, *A unified treatment of superconvergent recovered gradient functions for piecewise linear finite element approximations*, Internat. J. Numer. Methods Engrg., 27 (1989), pp. 469-481.

23. G. GOODSELL AND J.R. WHITEMAN, *Pointwise superconvergence of recovered gradients for piecewise linear finite element approximations to problems of planar linear elasticity*, Numer. Methods for PDEs, 6 (1990), pp. 59-74.

24. G. GOODSELL AND J.R. WHITEMAN, *Superconvergence of recovered gradients of piecewise quadratic finite element approximations. Part I: L_2-error estimates*, Numer. Methods for PDEs, 7 (1991), pp. 61-83.

25. G. GOODSELL AND J.R. WHITEMAN, *Superconvergence of recovered gradients of piecewise quadratic finite element approximations. Part II: L_∞-error estimates*, Numer. Methods for PDEs, 7 (1991), pp. 85-99.

26. R. DURÁN, M.A. MUSCHIETTI AND R. RODRÍGUEZ, *On the asymptotic exactness of error estimators for linear triangular finite elements*, Numer. Math., 59 (1991), pp. 107-127.

27. R. DURÁN, M.A. MUSCHIETTI AND R. RODRÍGUEZ, *Asymptotically exact error estimators for rectangular finite elements*, SIAM J. Numer. Anal., 29 (1992), pp. 78-88.

28. I. BABUŠKA, T. STROUBOULIS AND C.S. UPADHYAY, *η%-superconvergence of finite element approximations in the interior of general meshes of triangles*, in preparation.

29. I. BABUŠKA, T. STROUBOULIS, S.K. GANGARAJ AND C.S. UPADHYAY, *η%-superconvergence of finite element approximations in the interior of locally refined meshes of quadrilaterals*, in preparation.

30. I. BABUŠKA, T. STROUBOULIS, C.S. UPADHYAY AND S.K. GANGARAJ, *Study of superconvergence by a computer-based approach. Superconvergence of the strain and stress in finite element solutions of the equations of elasticity*, in preparation.

31. B.A. SZABÓ AND I. BABUŠKA, *Finite Element Analysis*, John Wiley & Sons, Inc., New York, 1991.

32. J.A. NITSCHE AND A.H. SCHATZ, *Interior estimates for Ritz-Galerkin methods*, Math. Comp. 28 (1974), pp. 937-958.

33. J.H. BRAMBLE, J.A. NITSCHE AND A.H. SCHATZ, *Maximum-norm estimates for Ritz-Galerkin methods*, Math. Comp. 29 (1975), pp. 677-688.

34. A.H. SCHATZ AND L.B. WAHLBIN, *Interior maximum norm estimates for finite element methods*, Math. Comp. 31 (1977), pp. 414-442.

35. A.H. SCHATZ AND L.B. WAHLBIN, *Maximum norm estimates in the finite element method on plane polygonal domains. Part 1*, Math. Comp. 32 (1978), pp. 73-109.

36. A.H. SCHATZ AND L.B. WAHLBIN, *Maximum norm estimates in the finite element method on plane polygonal domains. Part 2*, refinements, Math. Comp. 33 (1979), pp. 465-492.

37. L.B. WAHLBIN, *Local behavior in finite element methods*, in: P.G. Ciarlet and J.L. Lions, eds., Handbook of Numerical Analysis, Vol. II (North-Holland, Amsterdam, 1991), pp. 357-522.

38. A.H. SCHATZ AND L.B. WAHLBIN, *Interior maximum norm estimates for finite element methods. Part II*, preprint.

List of Figures

Figure 1. Locally periodic grids. (a) An example of a grid with a locally periodic subdomain meshed with the Regular pattern shown in Fig. 2a; (b) The subdomain $S(\boldsymbol{x}^0, H)$ with the subdomains $S(\boldsymbol{x}^0, H_\ell)$, $\ell = 1, 2$, in its interior.

Figure 2. Periodic meshes of triangles: (a) Regular pattern; (b) Chevron pattern; (c) Union-Jack pattern; (d) Criss-Cross pattern.

Figure 3. Superconvergence points for the x_1-derivative for the class of harmonic solutions of Poisson's equation: Cubic triangular elements. The superconvergence points are located at the intersection of the zero-contours $C_{\frac{\partial u}{\partial x_1}}(Q_i^H; \tau, \tilde{T}; I)$, $i = 1, 2$, for the x_1-derivative of the error for the harmonic monomial solutions. In the Figures $C_{\frac{\partial u}{\partial x_1}}(Q_1^H; \tau, \tilde{T}; I)$ (resp. $C_{\frac{\partial u}{\partial x_1}}(Q_2^H; \tau, \tilde{T}; I)$) was drawn using thin (resp. thick) continuous line in each element τ (the element boundaries were drawn using dashed line). The zero-contours and the superconvergence points are given for: (a) The Regular pattern; (b) The Chevron pattern; (c) The Union-Jack pattern; (d) The Criss-Cross pattern.

Figure 4. Superconvergence points for the x_1-derivative for the classes of harmonic and general solutions of Poisson's equation: Cubic triangular element τ from the Regular pattern. (a) The triangle with the zero-contours $C_{\frac{\partial u}{\partial x_1}}(Q_i^H; \tau, \tilde{T}; I)$, $i = 1, 2$ for the quartic harmonic monomials; (b) The triangle with the zero contours $C_{\frac{\partial u}{\partial x_1}}(Q_i; \tau, \tilde{T}; I)$, $i = 1, \ldots, 4$ for all the quartic monomials for which the error in the x_1-derivative does not vanish identically. The zero contours for the harmonic monomials where drawn using thick continuous line; the zero-contours for the other two monomials were drawn using thin continuous line. Note that the midpoint of the horizontal side of the triangle belongs to the zero-contours for all quartic monomials and is a superconvergence point (the only one) for general solutions.

Figure 5. Cubic serendipity element: Superconvergence points for the x_1-derivative for the class of general solutions of Poisson's equation. The superconvergence points are located at the intersection of the zero-contours $C_{\frac{\partial u}{\partial x_1}}(Q_i; \tau, \tilde{T}; I)$, $i = 1, 2$, where $Q_1(x_1, x_2) = x_1^4$ and $Q_2(x_1, x_2) = x_1^4 - 6x_1^2x_2^2 + x_2^4$. The zero-contours for Q_1 (resp. Q_2) were drawn with thin (resp. thick) continuous line. Note that there are four distinct superconvergence points and a superconvergence line (the line indicated by a multitude of points and passes through the center of the element).

Figure 6. Serendipity elements of degree p $(4 \leq p \leq 7)$: Superconvergence points for the x_1-derivative for the class of harmonic solutions of Poisson's equation. The superconvergence points are located at the intersection of the zero-contours

$C_{\frac{\partial u_i}{\partial x_1}}(Q_i^H;\tau,\tilde{T};I)$ $i=1,2$, for the x_1-derivative of the error for the harmonic monomial solutions. In the Figures $C_{\frac{\partial u_1}{\partial x_1}}(Q_1^H;\tau,\tilde{T};I)$ (resp. $C_{\frac{\partial u_2}{\partial x_1}}(Q_2^H;\tau,\tilde{T};I)$ was drawn using thin (resp. thick) continuous line. Zero-contours and superconvergence points for the x_1-derivative for the serendipity square element of degree: (a) Four; (b) Five; (c) Six; (d) Seven. Note that there are no superconvergence points for the class of general solutions for these elements.

Figure 7. Effect of the material orthotropy. Superconvergence points for the x_1-component of the flux, $q_1(u) = K_{11}\dfrac{\partial u}{\partial x_1} + K_{12}\dfrac{\partial u}{\partial x_2}$ for the class of "harmonic" solutions of the equation of orthotropic heat-conduction: Cubic elements. The superconvergence points are located at the intersection of the zero-contours $C_{q_1(u)}(Q_i^{"H"};\tau,\tilde{T};\boldsymbol{K}(\theta))$, $i=1,2$. In the Figures the contours were drawn for matrices $\boldsymbol{K}(\theta)$ with $\dfrac{K_{\max}}{K_{\min}} = 10$ and for grid-material orientations $\theta = 0°, 15°, 30°, 45°$, $60°, 75°$, $90°$. The grid-material orientation is measured by the angle θ between the x_1-axis and the principal-axis corresponding to $K_{\min}$ (measured counterclockwise). (a) Zero-contours and superconvergence points for the tensor-product family; (b) Zero-contours and superconvergence points for the intermediate family. Note that the two Figures are identical. The locations of the superconvergence points (which are at the (3×3)-Gauss-Legendre points) do not depend on the grid-material orientation.

Figure 8. Effect of the material orthotropy. Superconvergence points for the x_1-component of the flux, $q_1(u) = K_{11}\dfrac{\partial u}{\partial x_1} + K_{12}\dfrac{\partial u}{\partial x_2}$ for the class of "harmonic" solutions of the equation of orthotropic heat-conduction: Cubic serendipity elements. The superconvergence points are located at the intersection of the zero-contours $C_{q_1(u)}(Q_i^{"H"};\tau,\tilde{T};\boldsymbol{K}(\theta))$, $i=1,2$. In the Figures the contours were drawn for matrices $\boldsymbol{K}(\theta)$ with $\dfrac{K_{\max}}{K_{\min}} = 10$ and for grid-material orientations $\theta = 0$. The grid-material orientation is measured by the angle θ between the x_1-axis and the principal-axis corresponding to $K_{\min}$ (measured counterclockwise). Zero-contours and superconvergence points for grid material orientation θ: (a) $\theta = 0°$; (b) $\theta = 15°$; (c) $\theta = 30°$; (d) $\theta = 45°$; (e) $\theta = 60°$; (f) $\theta = 75°$; (g) $\theta = 90°$. Note that for $\theta = 0°, 90°$ there are three superconvergence lines. The zero-contours and the superconvergence points for all the above θ's are displayed in Fig. 8h. Note that there is only one superconvergence point, located at the center of the element, which is valid for all grid-material orientations.

Figure 9. Effect of the material orthotropy. Superconvergence points for the x_1-component of the flux, $q_1(u) = K_{11}\dfrac{\partial u}{\partial x_1} + K_{12}\dfrac{\partial u}{\partial x_2}$ for the class of "harmonic"

solutions of the equation of orthotropic heat-conduction: Quadratic triangular elements, Regular pattern. The superconvergence points are located at the intersection of all the zero-contours $C_{q_1(\omega)}(Q_i^{*H^*}; \tau, \bar{T}; \boldsymbol{K}(\theta))$, $i = 1,2$. In the Figures the contours were drawn for matrices $\boldsymbol{K}(\theta)$ with $\frac{K_{\max}}{K_{\min}} = 10$ and for grid-material orientations θ, where θ is the angle between the x_1-axis and the principal-axis corresponding to $K_{\min}$ (measured counterclockwise) for the element τ (shaded gray in Fig. 2a). Zero-contours and superconvergence points for (a) $\theta = 0°$; (b) $\theta = 15°$; (c) $\theta = 30°$; (d) $\theta = 45°$; (e) $\theta = 60°$; (f) $\theta = 75°$; (g) $\theta = 90°$. Note that for $\theta = 0°$ there are two superconvergence points; the $\theta = 90°$ there are four superconvergence points. The zero-contours and superconvergence points for all the angles θ, mentioned above, are plotted in Fig. 9h. Note that there is no common superconvergence points for all the grid-material orientations.

List of Tables

to the superconvergence points given in Tables 1a, 1b for the class of harmonic solutions. The are no superconvergence points for general solutions for this pattern.

Table 5a. Superconvergence points for periodic meshes of triangular elements of degree p ($1 \leq p \leq 6$). General solutions: Criss-Cross pattern. This Table refers to the superconvergence points given in Tables 2a, 2b for the class of harmonic solutions. The points from Tables 2a, 2b which are also superconvergence points for the class of general solutions for the element τ_1 (shown in Fig. 5d) are indicated by the word yes.

Table 5b. Superconvergence points for periodic meshes of triangular elements of degree p ($1 \leq p \leq 6$). General solutions: Criss-Cross pattern. This Table refers to the superconvergence points given in Tables 3a, 3b for for the class of harmonic solutions. There are no superconvergence points for the class of general solutions for the element τ_2 (shown in Fig. 5d).

Table 6a. Superconvergence for meshes of triangular elements. Quadratic elements, Regular pattern, harmonic solution ($u^H(x_1, x_2) = \sin(\pi x_1)\sinh(\pi x_2)$) : Convergence of the discrete norms for various selections of the points. Column 2: Convergence of the discrete norm E' which includes all four points given in Table 1a for $p = 2$. Column 3: Convergence of the discrete norm E'' which includes only the first two points from Table 1a (the points belong to the element boundary). Column 4: Convergence of the discrete norm E''' which includes only the third and fourth points from Table 1a (the points are in the interior of the element). Note that all three discrete norms E', E'', E''' are superconvergent.

Table 6b. Superconvergence for meshes of triangular elements. Quadratic elements, Regular pattern, general solution ($u^G(x_1, x_2) = \sin(\pi x_1)\sin(\pi x_2)$) : Convergence of the discrete norms for various selections of the points. Column 2: Convergence of the discrete norm E' which includes all four points given in Table 1a for $p = 2$. Column 3: Convergence of the discrete norm E'' which includes only the first two points from Table 1a (the points belong to the element boundary). Column 4: Convergence of the discrete norm E''' which includes only the third and fourth points from Table 1a (the points are in the interior of the element). Note that only the discrete norm E'' is superconvergent.

Table 6c. Superconvergence for meshes of triangular elements. Cubic elements, Regular pattern, harmonic solution ($u^H(x_1, x_2) = \sin(\pi x_1)\sinh(\pi x_2)$) : Convergence of the discrete norms for various selections of the points. Column 2: Convergence of the discrete norm E' which includes all six points given in Table 1a for $p = 3$. Column 3: Convergence of the discrete norm E'' which includes only the third point from Table 1a (the mid-point of the the side of the element parallel to the x_1-axis). Column 4: Convergence of the discrete norm E''' which includes all the points from Table 1a except the third one. Note that all three discrete norms E', E'', E''' are superconvergent.

Table 6d. Superconvergence for meshes of triangular elements. Cubic elements, Regular pattern, general solution ($u^G(x_1, x_2) = \sin(\pi x_1)\sin(\pi x_2)$) : Convergence of the discrete norms for various selections of the points. Column 2: Convergence of the discrete norm E' which includes all six points given in Table 1a for $p = 3$. Column 3: Convergence of the discrete norm E'' which includes only the third point from Table 1a (the mid-point of the the side of the element parallel to the x_1-axis). Column 4: Convergence of the discrete norm E''' which includes all the points from Table 1a except the third one. Note that only the discrete norm E'' is superconvergent.

Table 7. Superconvergence points for square-elements of the serendipity family. Superconvergence points for the x_1-derivative for the class of harmonic solutions for elements of degree p ($3 \leq p \leq 7$). The vertices of the square are at (-1.,-1.), (1.,-1.), (1.,1.), (-1.,1.). Note that: a. For $p = 3$ we have three lines of superconvergence for the class of harmonic solutions; the thick continuous line in Fig. 5. In this Table for $p = 3$ we give the four points and the line which are also superconvergent for general solutions; b. For $p \geq 4$ there are no superconvergence points for general solutions.

Table 8a. Superconvergence for meshes of square elements. Cubic elements, general solution ($u^G(x_1, x_2) = \sin(\pi x_1)\sin(\pi x_2)$) : ($3 \times 3$) Gauss-Legendre points. Values of the discrete-norm of the x_1-derivative E and of the product $h^{-4}E$ for uniform subdivisions of the mesh-size h. Note that the values of E are superconvergent for both the tensor-product and the intermediate space.

Table 8b. Superconvergence for meshes of square elements. Cubic serendipity elements, general solution ($u^G(x_1, x_2) = \sin(\pi x_1)\sin(\pi x_2)$) : Effect of the selection of the points. Column 2: Values of the discrete norm of the x_1-derivative E and of the product $h^{-3}E$ for uniform subdivisions of the mesh-size h when the (3×3) Gauss-Legendre points are used in the computation of E. Column 3: Values of the discrete-norm for the x_1-derivative E and of the product $h^{-4}E$ for uniform subdivisions of the mesh-size h when the points given in Table 6a are employed in the computation of E. Note that the values of E are superconvergent only when points from Table 7 are employed.

Table 8c. Superconvergence for meshes of square elements. Quartic serendipity elements, points from Table 7 : Effect of the nature of solution. Column 2: Values of the discrete-norm of the x_1-derivative E and of the product $h^{-5}E$ for uniform subdivisions of the mesh-size h for the harmonic solution $u^H(x_1, x_2) = \sin(\pi x_1)\sinh(\pi x_2)$. Column 3: Values of the discrete-norm of the x_1-derivative E and of the product $h^{-4}E$ for uniform subdivisions of the mesh-size h for the general solution $u^G(x_1, x_2) = \sin(\pi x_1)\sin(\pi x_2)$. Note that the values of E are superconvergent only for the harmonic solution.

Triangular elements					
Superconvergence points for the class of harmonic solutions					
The vertices of the triangle are at (0.0,0.0), (1.0,0.0), (1.0, 1.0)					
Regular, Chevron, Union-Jack patterns					
Points	$p = 1$	$p = 2$	$p = 3$	$p = 4$	$p = 5$
1	0.5000000000, 0.0000000000	0.2113248654, 0.0000000000	0.0000000000, 0.0000000000	0.0118976218, 0.0000000000	0.0000000000, 0.0000000000
2		0.7886751346, 0.0000000000	0.3752181980, 0.0858825088	0.2821230756, 0.0000000000	0.1726731646, 0.0000000000
3		0.7500000000, 0.0458758546	0.5000000000, 0.0000000000	0.7178769244, 0.0000000000	0.5000000000, 0.0000000000
4		0.7500000000, 0.4541241452	0.4715185566, 0.3241733208	0.9881023782, 0.0000000000	0.8273268354, 0.0000000000
5			1.0000000000, 0.0000000000	0.1195044522, 0.0224992688	1.0000000000, 0.0000000000
6			0.8638176260, 0.6824066036	0.7053452590, 0.0071869378	0.4640525316, 0.0103019842
7				0.3095295948, 0.2201118672	0.2328766474, 0.15749286240
8				0.6402277154, 0.5196142358	0.4734766188, 0.3874100850
9				0.9063362308, 0.7871241952	0.7356302926, 0.6425966766
10					0.9343659198, 0.7080184052

Table 1a

Triangular elements		
Superconvergence points for the class of harmonic solutions		
The vertices of the triangle are at (0.0,0.0), (1.0,0.0), (1.0, 1.0)		
Regular, Chevron, Union-Jack patterns		
Points	$p = 6$	$p = 7$
1	0.9871917636, 0.0797658369	0.0000000000, 0.0000000000
2	0.9556960448, 0.7771050728	0.0637900495, 0.0000000000
3	0.8901470515, 0.0000000000	0.9837699874, 0.0278840787
4	0.7965034496, 0.7034683949	0.9671927841, 0.8195293891
5	0.6451460051, 0.0000000000	0.7443785569, 0.0000000000
6	0.5873974006, 0.5156451535	0.8413048661, 0.7026536445
7	0.3658757490, 0.2978238991	0.6689015074, 0.6017629175
8	0.3548540007, 0.0000000000	0.5000000000, 0.0000000000
9	0.2851597869, 0.0102771287	0.4770713108, 0.4203250119
10	0.2807031259, 0.1264409904	0.2949370204, 0.2365148149
11	0.1098529492, 0.0000000000	0.2556214434, 0.0000000000
12		0.2236970856, 0.0897505908
13		0.1620004419, 0.0056060808
14		0.9362099504, 0.0000000000
15		1.0000000000, 0.0000000000

Table 1b

Triangular elements					
Superconvergence points for the class of harmonic solutions					
The vertices of the triangle are at (0.0,0.0), (1.0,0.0), (0.5, 0.5)					
Criss-Cross pattern					
Points	$p = 1$	$p = 2$	$p = 3$	$p = 4$	$p = 5$
1	0.5000000000, 0.0000000000	0.2113248654, 0.0000000000	0.1464466094, 0.0000000000	0.0761088279, 0.0000000000	0.0488705882, 0.0000000000
2		0.7886751346, 0.0000000000	0.5000000000, 0.0000000000	0.3397707358, 0.0000000000	0.2355765633, 0.0000000000
3			0.8535533906, 0.0000000000	0.6602292641, 0.0000000000	0.5000000000, 0.0000000000
4			0.5000000000, 0.5000000000	0.9238911721, 0.0000000000	0.7644234366, 0.0000000000
5				0.5000000000, 0.4887686394	0.9511294118, 0.0000000000
6					0.5000000000, 0.0000000000

Table 2a

Triangular elements	
Superconvergence points for the class of harmonic solutions	
The vertices of the triangle are at (0.0,0.0), (1.0,0.0), (0.5, 0.5)	
Criss-Cross pattern	
Points	$p = 6$
1	0.4554029520, 0.4414423293
2	0.0344614509, 0.0000000000
3	0.5445970478, 0.4414423293
4	0.1716793301, 0.0000000000
5	0.3821587890, 0.0000000000
6	0.6178412109, 0.0000000000
7	0.8283206698, 0.0000000000
8	0.9655385491, 0.0000000000

Table 2b

Triangular elements					
Superconvergence points for the class of harmonic solutions					
The vertices of the triangle are at (0.0,0.0), (1.0,0.0), (0.5, 0.5)					
Criss-Cross pattern					
Points	$p = 1$	$p = 2$	$p = 3$	$p = 4$	$p = 5$
1	0.5000000000, 0.5000000000	0.7886751346, 0.5000000000	0.8750000000, 0.2834936534	0.7621420044, 0.3163540210	0.8368698019, 0.2268165908
2			0.8750000000, 0.5000000000	0.9145863153, 0.3966634454	0.7540881642, 0.3397926069
3			0.8750000000, 0.7165063710	0.8970792676, 0.5000000000	0.6883014452, 0.3781734456
4			0.5000000000, 0.5000000000	0.9145863153, 0.6033365546	0.7811733816, 0.4582804499
5				0.7621420044, 0.6836459789	0.9334689552, 0.5000000000
6					0.7811733816, 0.5417195501
7					0.6883014452, 0.6218265544
8					0.7540881642, 0.6602073930
9					0.8368698019, 0.7731834092
10					0.5000000000, 0.5000000000
11					0.7760422930, 0.5000000000

Table 3a

Triangular elements	
Superconvergence points for the class of harmonic solutions	
The vertices of the triangle are at (0.0,0.0), (1.0,0.0), (0.5, 0.5)	
Criss-Cross pattern	
Points	$p = 6$
1	0.7631964888, 0.2833600514
2	0.8508031659, 0.2069721253
3	0.8678258572, 0.1849536861
4	0.7086428573, 0.5000000000
5	0.8383266448, 0.3701490568
6	0.8284878782, 0.3953625943
7	0.8332694721, 0.500000000
8	0.8284878779, 0.6046374047
9	0.9467769341, 0.5000000000
10	0.8383266448, 0.6298509433
11	0.7631964887, 0.7166399487
12	0.8508031661, 0.7930278749
13	0.8678258572, 0.8150463139

Table 3b

Triangular elements							
Superconvergence points for the class of general solutions							
The vertices of the triangle are at (0.0,0.0), (1.0,0.0), (1.0, 1.0)							
Regular pattern; The point numbers correspond to the points in Tables 1a, 1b							
Points	$p = 1$	$p = 2$	$p = 3$	$p = 4$	$p = 5$	$p = 6$	$p = 7$
1	yes	yes	no	no	no	no	no
2		yes	no	no	no	no	no
3		no	yes	no	yes	no	no
4		no	no	no	no	no	no
5			no	no	no	no	no
6			no	no	no	no	no
7				no	no	no	no
8				no	no	no	yes
9				no	no	no	no
10					no	no	no
11						no	no
12							no
13							no
14							no
15							no

Table 4a

Triangular elements							
Superconvergence points for the class of general solutions							
The vertices of the triangle are at (0.0,0.0), (1.0,0.0), (1.0, 1.0)							
Chevron pattern; The point numbers correspond to the points in Tables 1a, 1b							
Points	$p = 1$	$p = 2$	$p = 3$	$p = 4$	$p = 5$	$p = 6$	$p = 7$
1	yes	no	no	no	no	no	no
2		no	no	no	no	no	no
3		no	yes	no	yes	no	no
4		no	no	no	no	no	no
5			no	no	no	no	no
6			no	no	no	no	no
7				no	no	no	no
8				no	no	no	yes
9				no	no	no	no
10					no	no	no
11						no	no
12							no
13							no
14							no
15							no

Table 4b

Triangular elements							
Superconvergence points for the class of general solutions							
The vertices of the triangle are at (0.0,0.0), (1.0,0.0), (1.0, 1.0)							
Union-Jack pattern; The point numbers correspond to the points in Tables 1a, 1b							
Points	$p = 1$	$p = 2$	$p = 3$	$p = 4$	$p = 5$	$p = 6$	$p = 7$
1	no	no	no	no	no	no	no
2		no	no	no	no	no	no
3		no	no	no	no	no	no
4		no	no	no	no	no	no
5			no	no	no	no	no
6			no	no	no	no	no
7				no	no	no	no
8				no	no	no	no
9				no	no	no	no
10					no	no	no
11						no	no
12							no
13							no
14							no
15							no

Table 4c

Triangular elements						
Superconvergence points for the class of general solutions						
The vertices of the triangle are at (0.0,0.0), (1.0,0.0), (0.5, 0.5)						
Criss-Cross pattern; The point numbers correspond to the points in Tables 2a, 2b (For the element τ_1 in the pattern)						
Points	$p = 1$	$p = 2$	$p = 3$	$p = 4$	$p = 5$	$p = 6$
1	yes	yes	no	no	no	no
2		yes	yes	no	no	no
3			no	no	yes	no
4			no	no	no	no
5				no	no	no
6					no	no
7						no
8						no

Table 5a

Triangular elements						
Superconvergence points for the class of general solutions						
The vertices of the triangle are at (0.0,0.0), (1.0,0.0), (0.5, 0.5)						
Criss-Cross pattern; The point numbers correspond to the points in Tables 3a, 3b (For the element τ_2 in the pattern)						
Points	$p = 1$	$p = 2$	$p = 3$	$p = 4$	$p = 5$	$p = 6$
1	no	no	no	no	no	no
2			no	no	no	no
3			no	no	no	no
4			no	no	no	no
5				no	no	no
6					no	no
7					no	no
8					no	no
9					no	no
10					no	no
11					no	no
12						no
13						no

Table 5b

Triangular elements						
Quadratic elements, Regular pattern						
Harmonic solution u^H						
h	E'	$(h^{-3}E')$	E''	$(h^{-3}E'')$	E'''	$(h^{-3}E''')$
0.2500	.06063740	(3.88)	.07027678	(4.50)	.04914226	(3.15)
0.1250	.00696365	(3.57)	.00806014	(4.13)	.00565854	(2.90)
0.0625	.00084995	(3.48)	.00098347	(4.03)	.00069111	(2.83)
0.03125	.00010559	(3.46)	.00012217	(4.00)	.00008587	(2.81)

Table 6a

Triangular elements						
Quadratic elements, Regular pattern						
General solution u^G						
h	E'	$(h^{-2}E')$	E''	$(h^{-3}E'')$	E'''	$(h^{-2}E''')$
0.2500	.03445760	(0.55)	.03685704	(2.36)	.03187807	(0.51)
0.1250	.00510295	(0.33)	.00494697	(2.53)	.00525431	(0.34)
0.0625	.00087724	(0.22)	.00062918	(2.58)	.00106923	(0.27)
0.03125	.00018505	(0.19)	.00007899	(2.59)	.00024949	(0.26)

Table 6b

Triangular elements						
Cubic elements, Regular pattern						
Harmonic solution u^H						
h	E'	$(h^{-4}E')$	E''	$(h^{-4}E'')$	E'''	$(h^{-4}E''')$
0.2500	.00205242	(0.53)	.00184893	(0.47)	.00209075	(0.54)
0.1250	.00012563	(0.51)	.00012009	(0.49)	.00012671	(0.52)
0.0625	.00000779	(0.51)	.00000750	(0.49)	.00000785	(0.51)
0.03125	.00000049	(0.51)	.00000047	(0.49)	.00000049	(0.51)

Table 6c

Triangular elements						
Cubic elements, Regular pattern						
General solution u^G						
h	E'	$(h^{-3}E')$	E''	$(h^{-4}E'')$	E'''	$(h^{-3}E''')$
0.2500	.01523855	(0.98)	.00172192	(0.44)	.01667522	(1.07)
0.1250	.00211270	(1.08)	.00011551	(0.47)	.00231377	(1.18)
0.0625	.00027112	(1.11)	.00000734	(0.48)	.00029697	(1.22)
0.03125	.00003411	(1.12)	.00000046	(0.48)	.00003737	(1.22)

Table 6d

Square elements					
Superconvergence points for the class of harmonic solutions					
Points	$p=3$	$p=4$	$p=5$	$p=6$	$p=7$
1	0 $\hat{x}_2 \in [-1,1]$	-0.5587732224 -1.0000000000	-0.7678487865 -1.0000000000	-0.8542303405 -0.9584215542	-0.7415311853 -1.0000000000
2	0.7745966692 0.5773502691	0.5587732224 1.0000000000	0.0000000000 -1.0000000000	-0.5632551950 -1.0000000000	0.0000000000 -1.0000000000
3	-0.7745966692 0.5773502691	0.0000000000 -0.5389584311	0.7678487865 -1.0000000000	0.0000000000 -0.9589718598	0.7415311853 -1.0000000000
4	-0.7745966692 -0.5773502691	-0.6174062248 0.0000000000	-0.5773502692 -0.7990568224	0.5632551950 -1.0000000000	-0.8404899503 0.0000000000
5	0.7745966692 -0.5773502691	0.6174062248 0.0000000000	0.5773502692 -0.7990568224	0.8542303405 -0.9584215542	-0.3896003525 0.0000000000
6		0.0000000000 0.5389584311	-0.5773502692 -0.1678536900	-0.7861575208 0.0000000000	0.0000000000 0.0000000000
7		-0.5587732224 1.0000000000	0.5773502692 -0.1678536900	-0.0538688187 0.0000000000	0.3896003525 0.0000000000
8		0.5587732224 1.0000000000	-0.5494131405 0.0000000000	0.0538688187 0.0000000000	0.8404899503 0.0000000000
9			0.0000000000 0.0000000000	0.7861575208 0.0000000000	-0.7415311853 1.0000000000
10			0.5494131405 0.0000000000	-0.8542303405 -0.9584215542	0.0000000000 1.0000000000
11			-0.5773502692 0.1678536900	-0.5632551950 1.0000000000	0.7415311853 1.0000000000
12			0.5773502692 0.1678536900	0.0000000000 0.9589718598	
13			-0.5773502692 0.7990568224	0.5632551950 1.0000000000	
14			0.5773502692 0.7990568224	0.8542303405 0.9584215542	
15			-0.7678487865 1.0000000000		
16			0.0000000000 1.0000000000		
17			0.7678487865 1.0000000000		

Table 7

Square elements		
(3 × 3) Gauss-Legendre points		
	Cubic tensor-product space $\hat{S}^{(3,3)}$	Cubic intermediate space $\hat{S}^{\square}$
h	E $(h^{-4}E)$	E $(h^{-4}E)$
0.2500	0.000691647 (0.177)	0.00568511 (1.455)
0.1250	0.000043212 (0.176)	0.00035669 (1.461)
0.0625	0.000002686 (0.176)	0.00002229 (1.461)

Table 8a

Square elements		
Cubic serendipity space $\hat{\mathcal{S}}^3$		
	(3×3) Gauss-Legendre points	Points from Table 7
h	E $(h^{-3}E)$	E $(h^{-4}E)$
0.2500	0.05310222 (3.399)	0.002463078 (0.631)
0.1250	0.00664258 (3.401)	0.000156494 (0.641)
0.0625	0.00083252 (3.410)	0.000009786 (0.641)

Table 8b

Square elements				
Quartic serendipity space $\hat{\mathcal{S}}^4$				
Points from Table 7				
	Harmonic solution u^H		General solution u^G	
h	E	$(h^{-5}E)$	E	$(h^{-4}E)$
0.2500	0.0011209	(1.148)	0.0010429	(0.267)
0.1250	0.0000350	(1.147)	0.0000652	(0.267)
0.0625	0.0000011	(1.148)	0.0000041	(0.269)

Table 8c

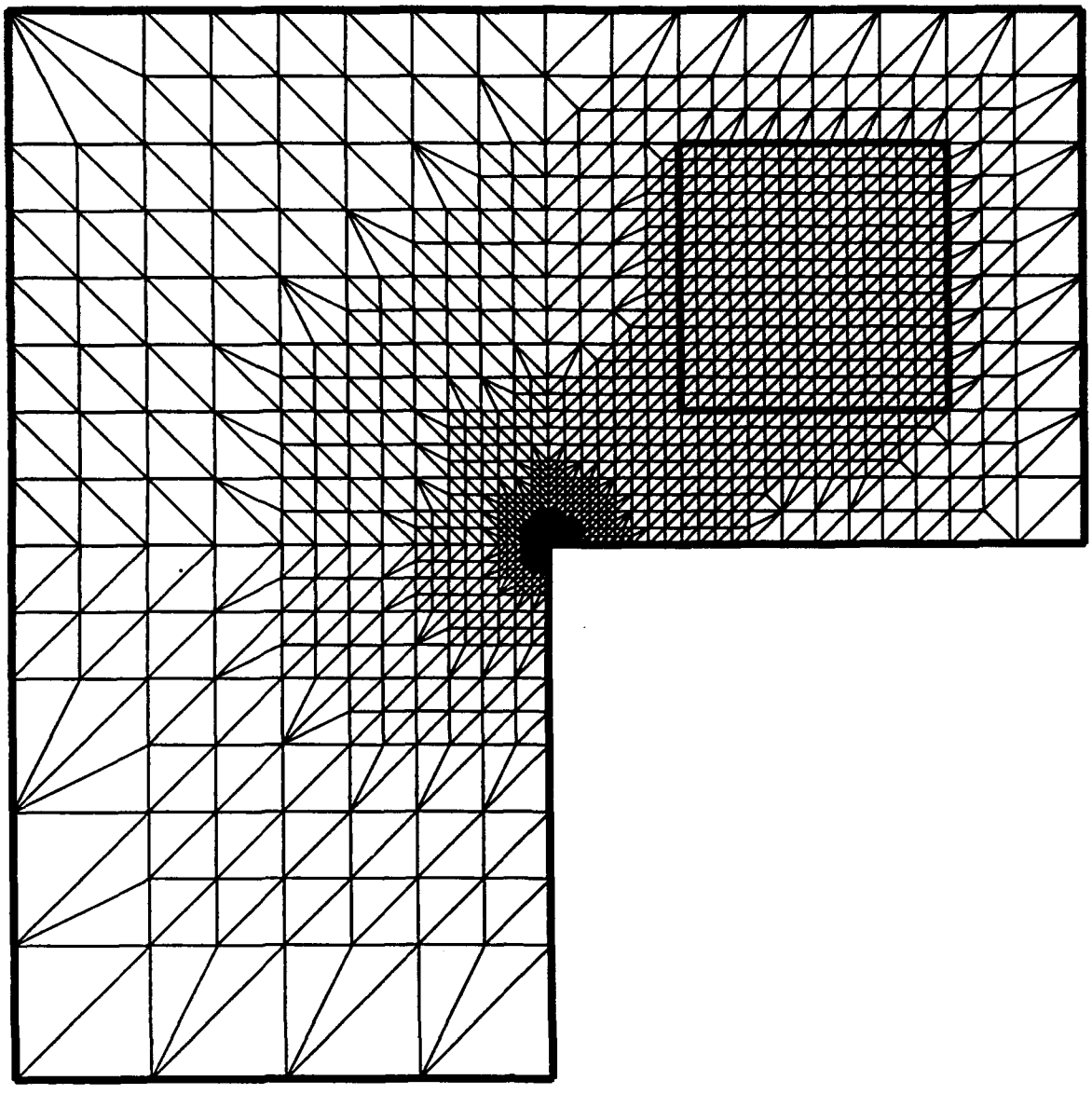

Figure 1a

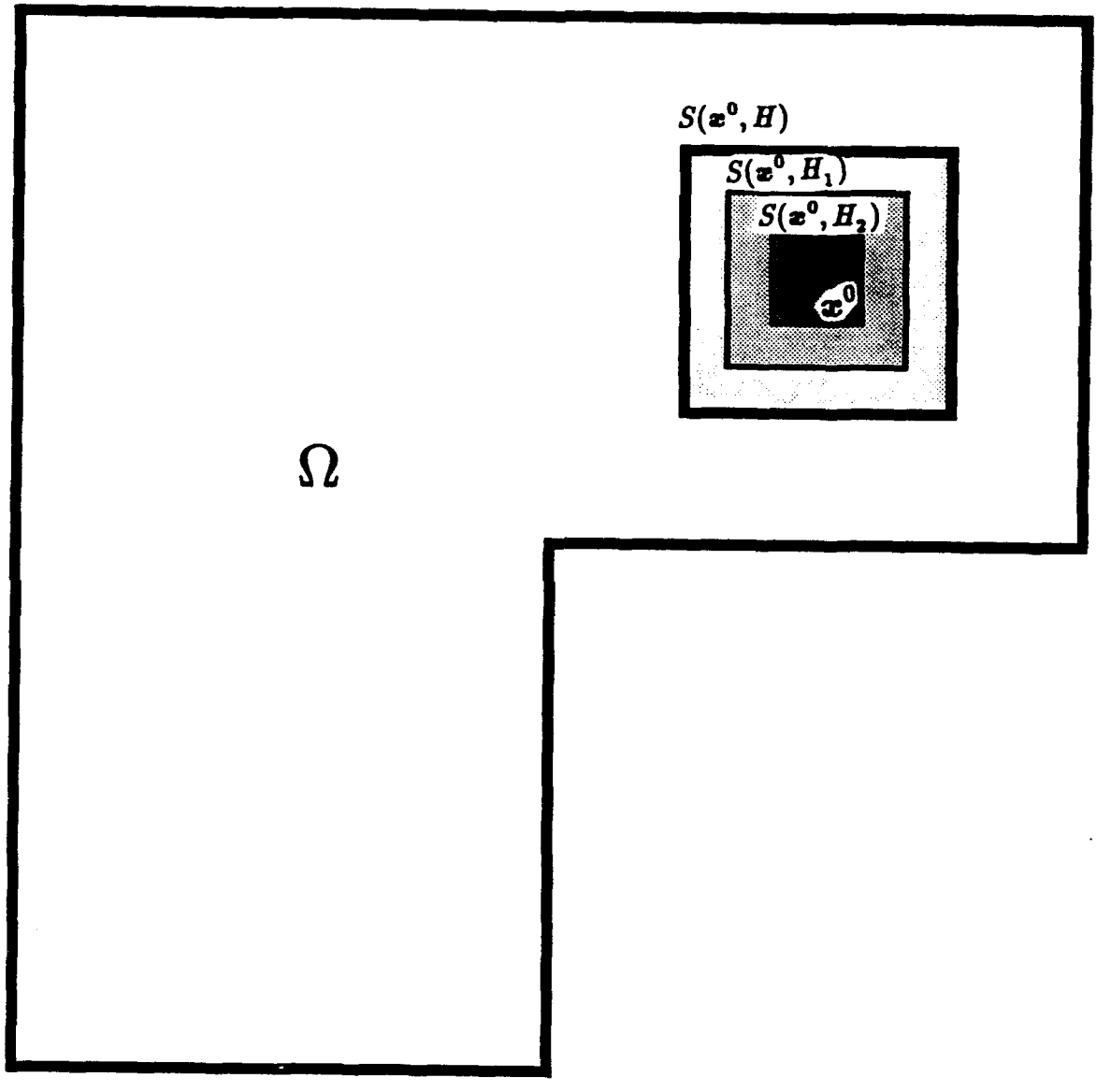

Figure 1b

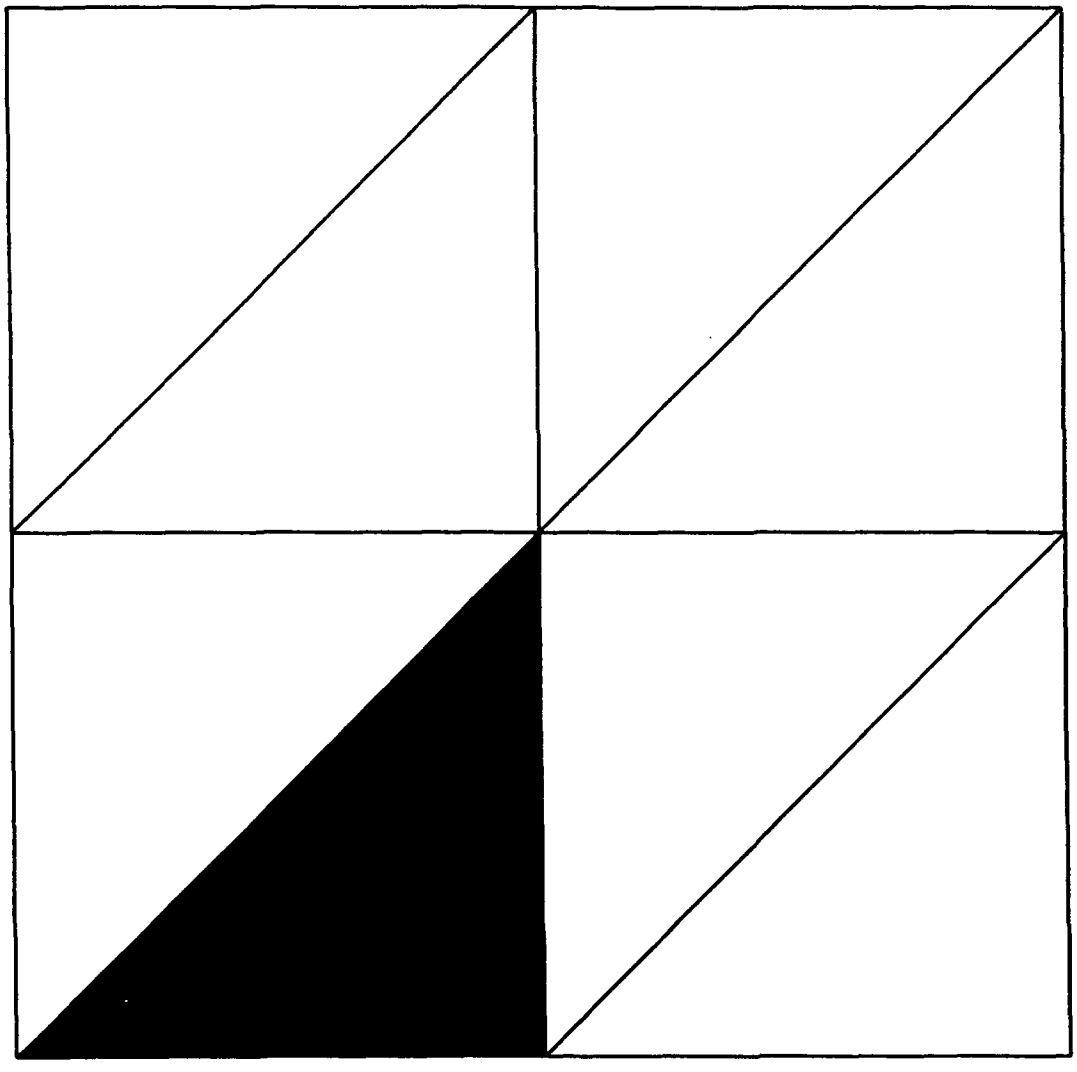

Figure 2a

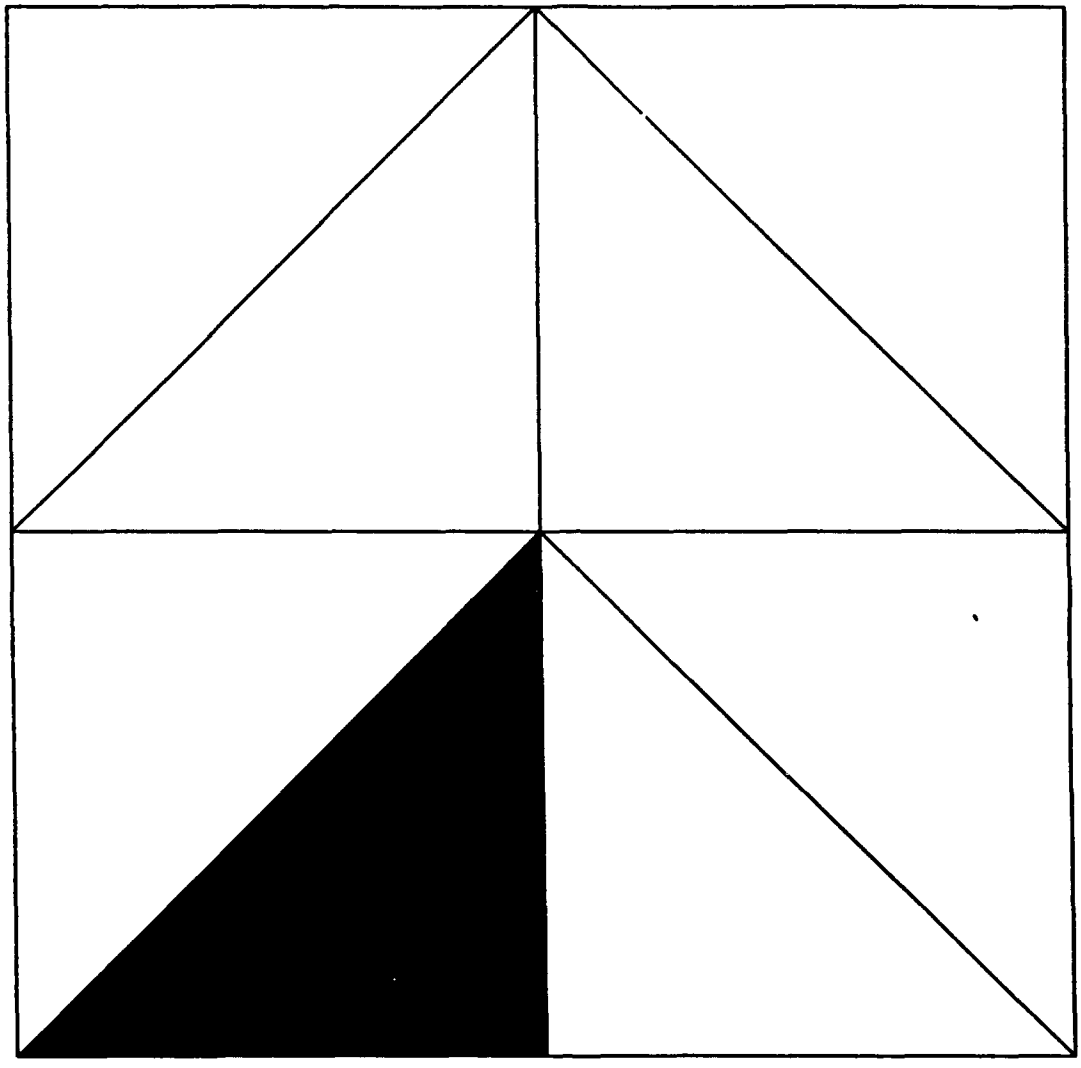

Figure 2b

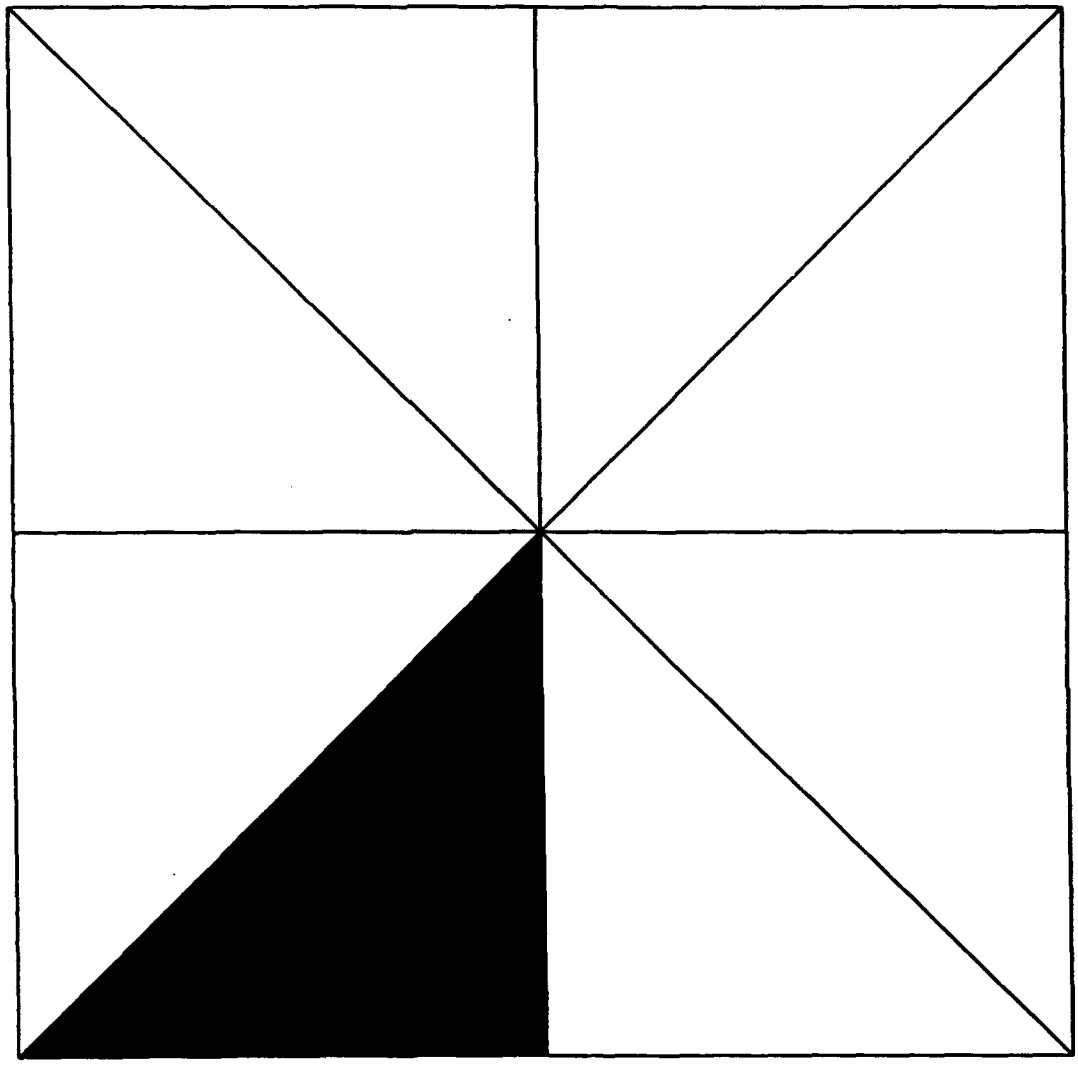

Figure 2c

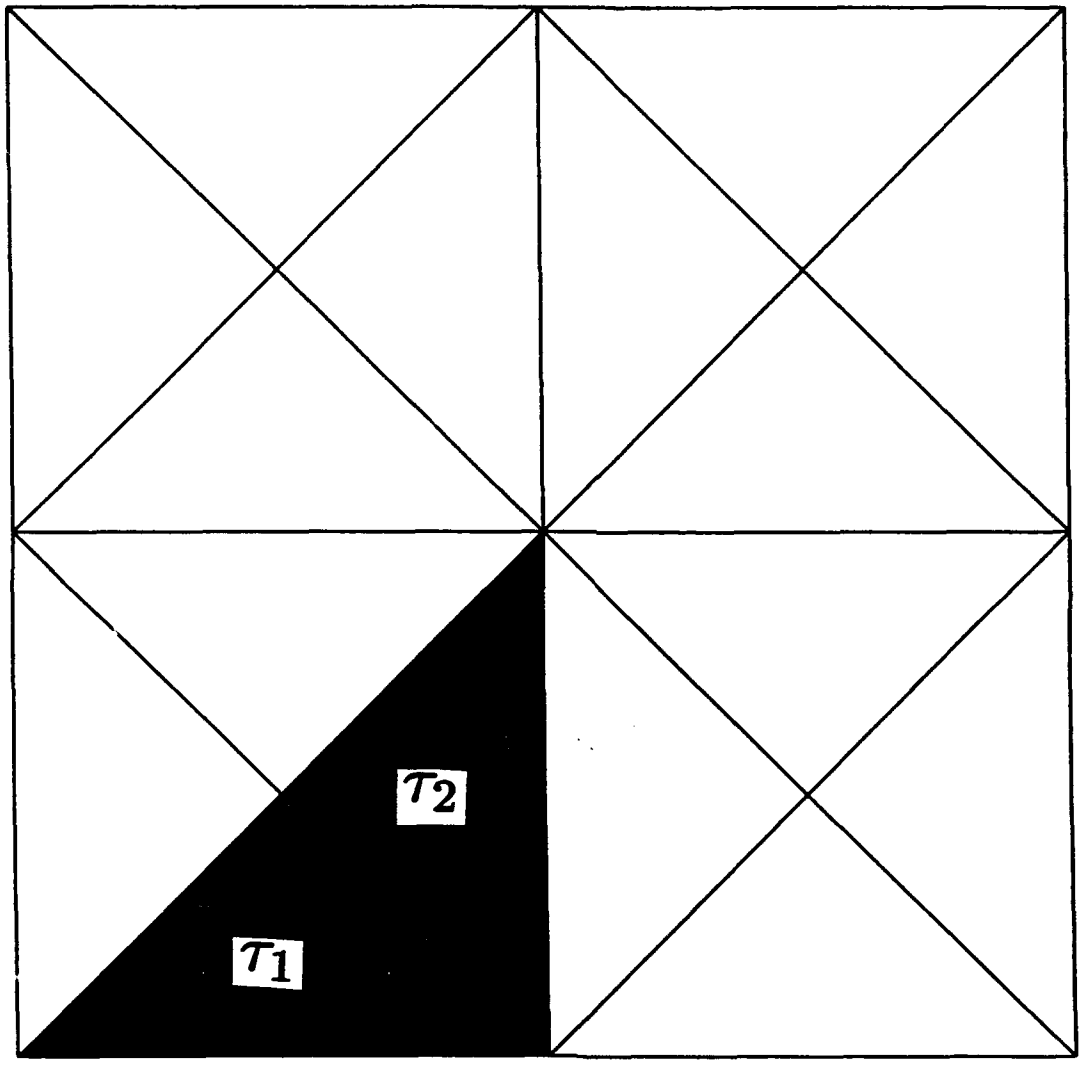

Figure 2d

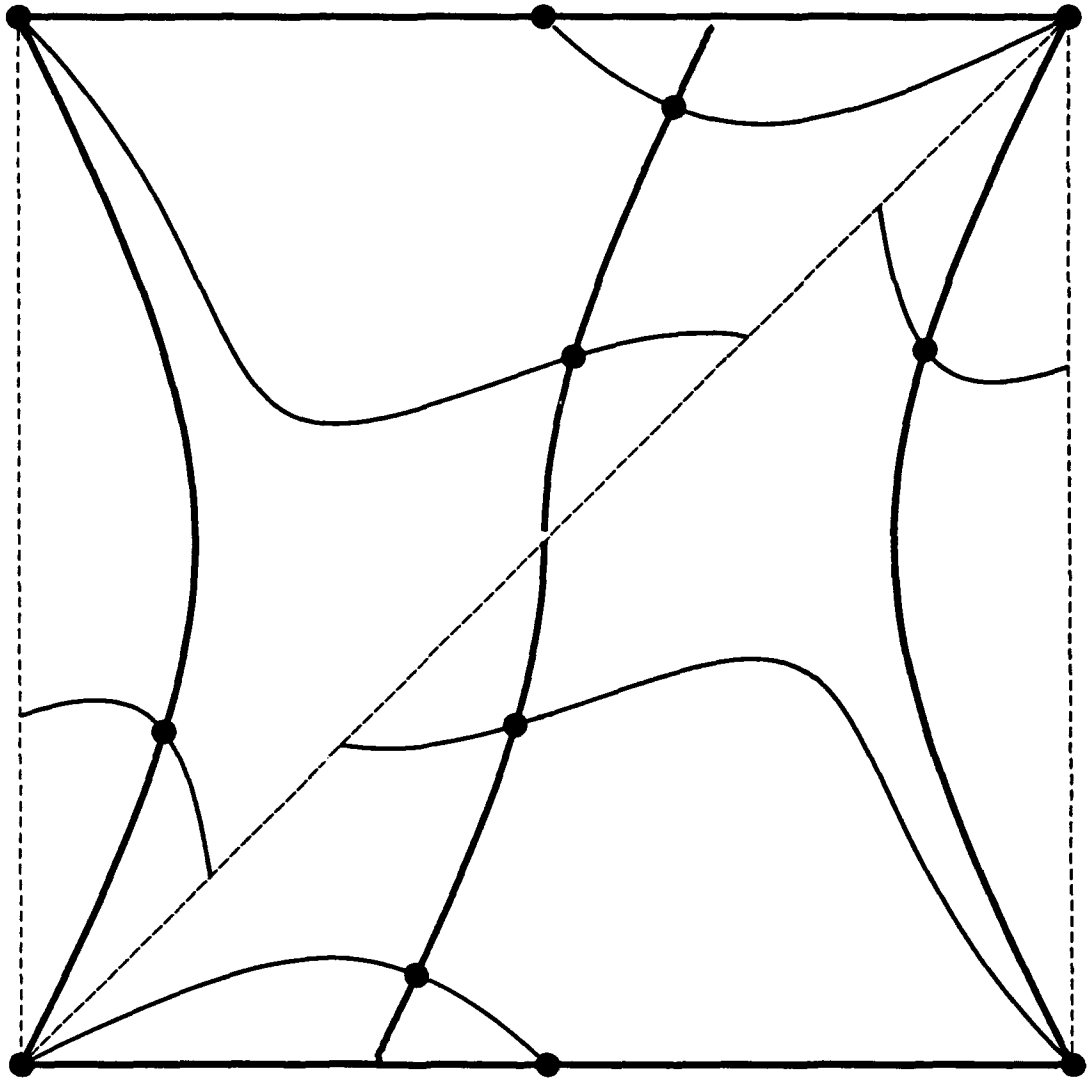

Figure 3a

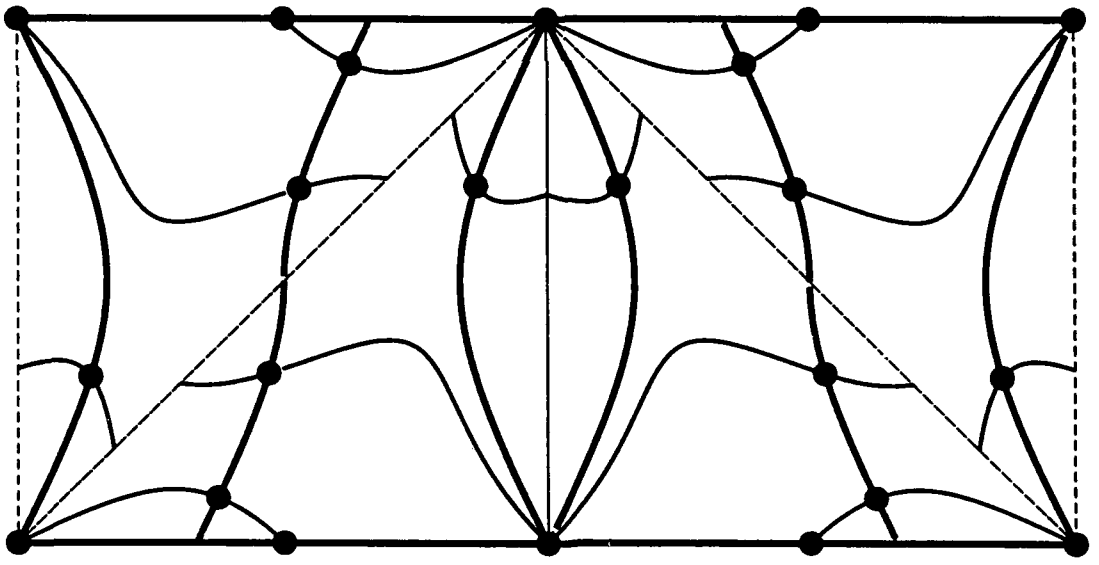

Figure 3b

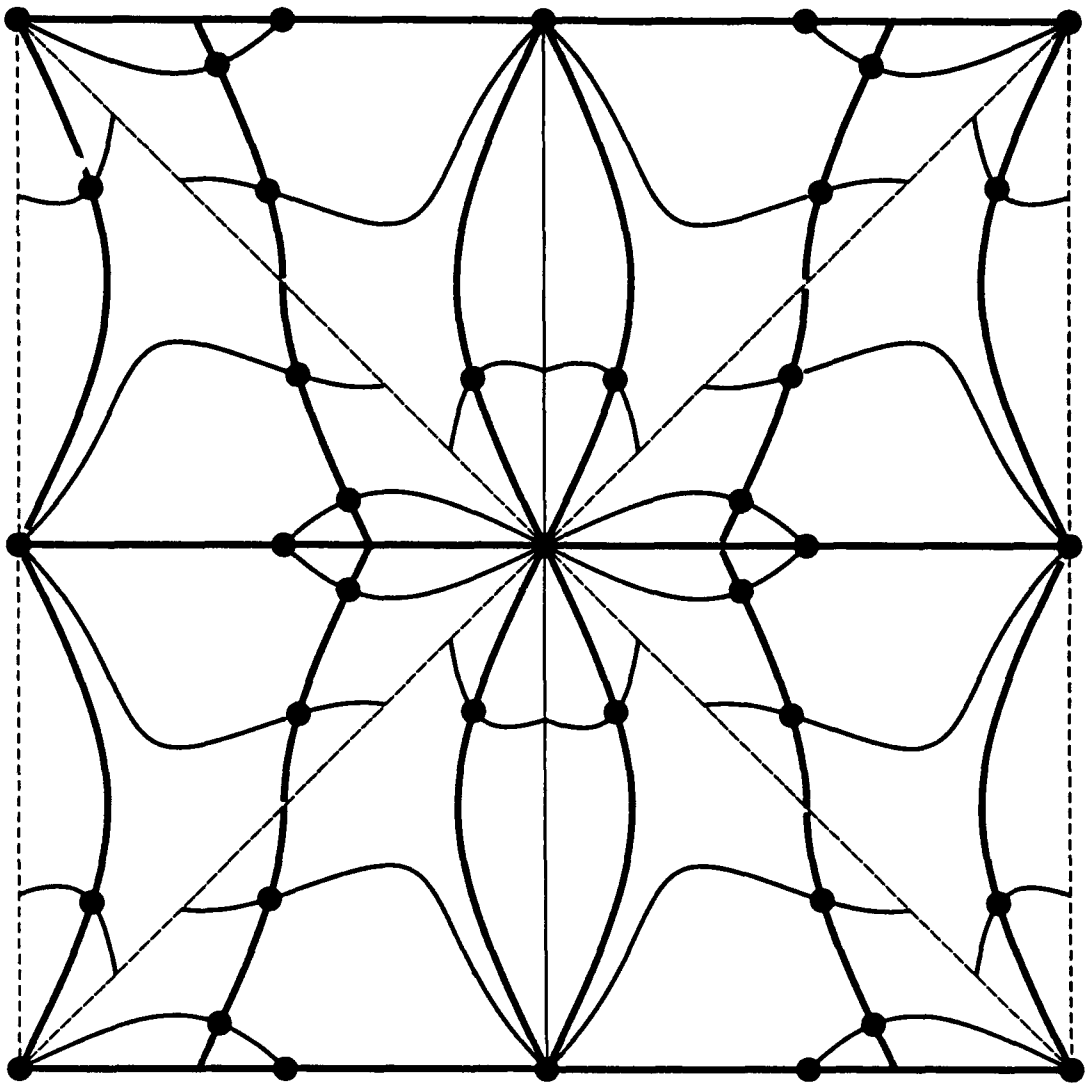

Figure 3c

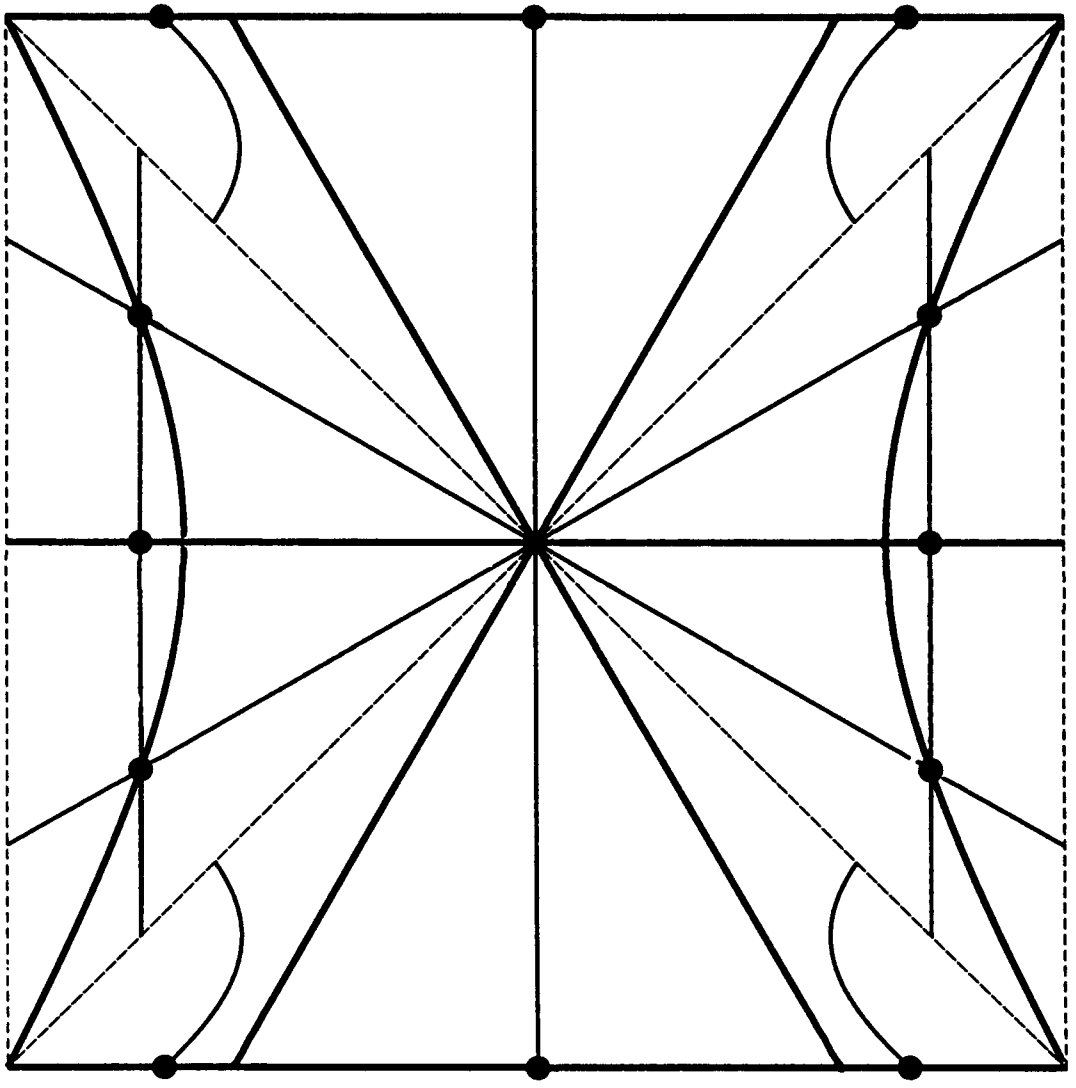

Figure 3d

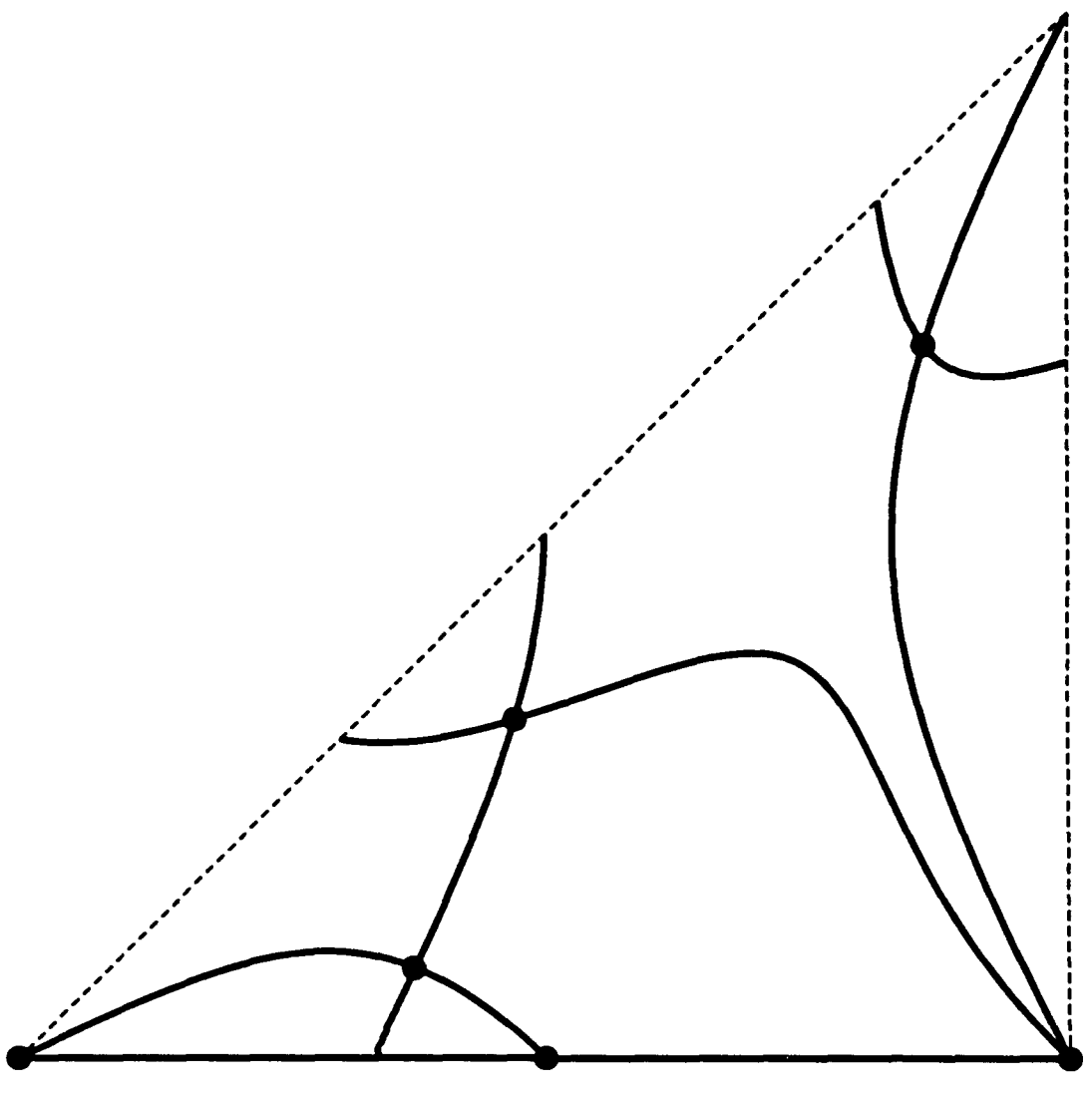

Figure 4a

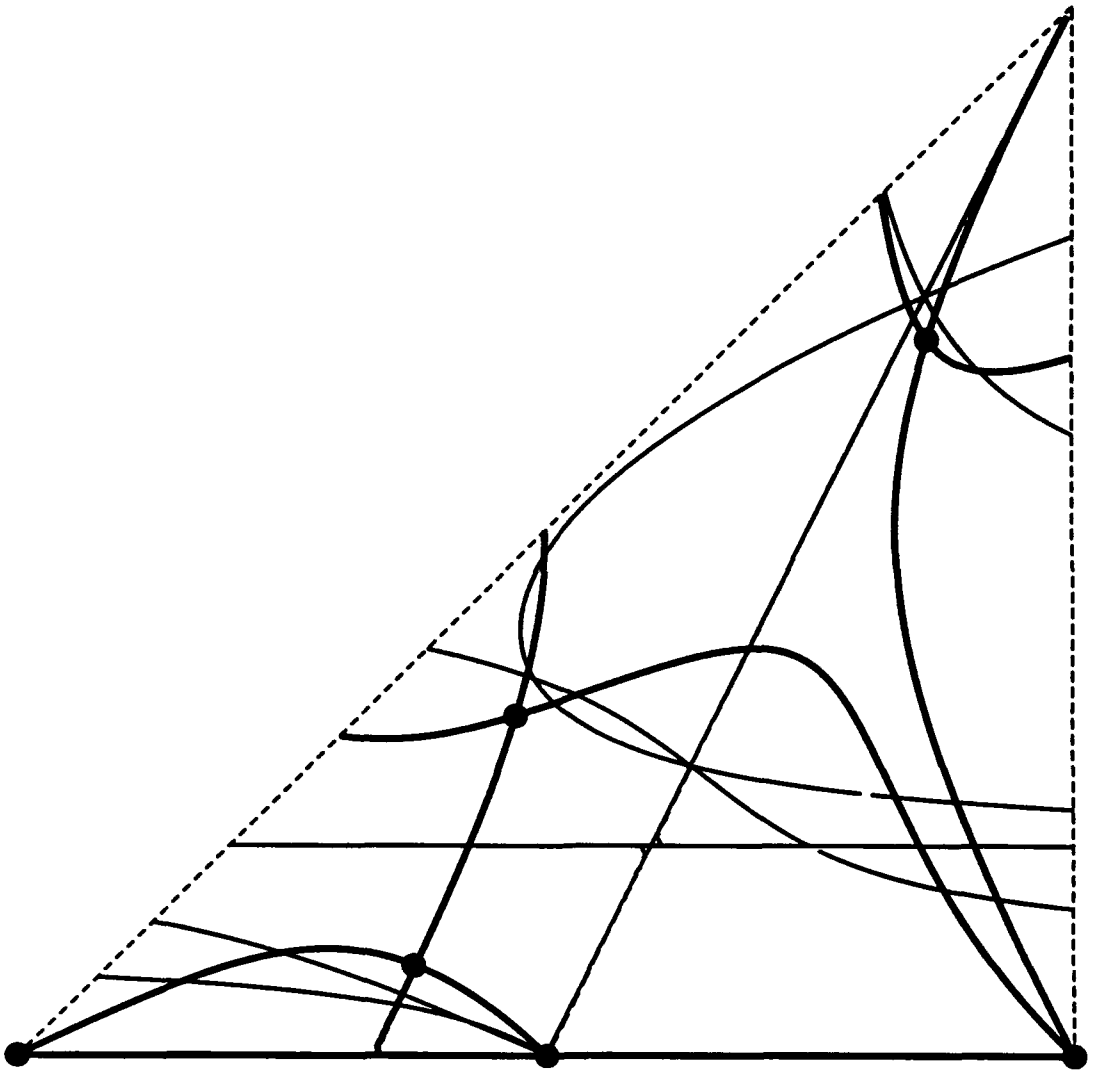

Figure 4b

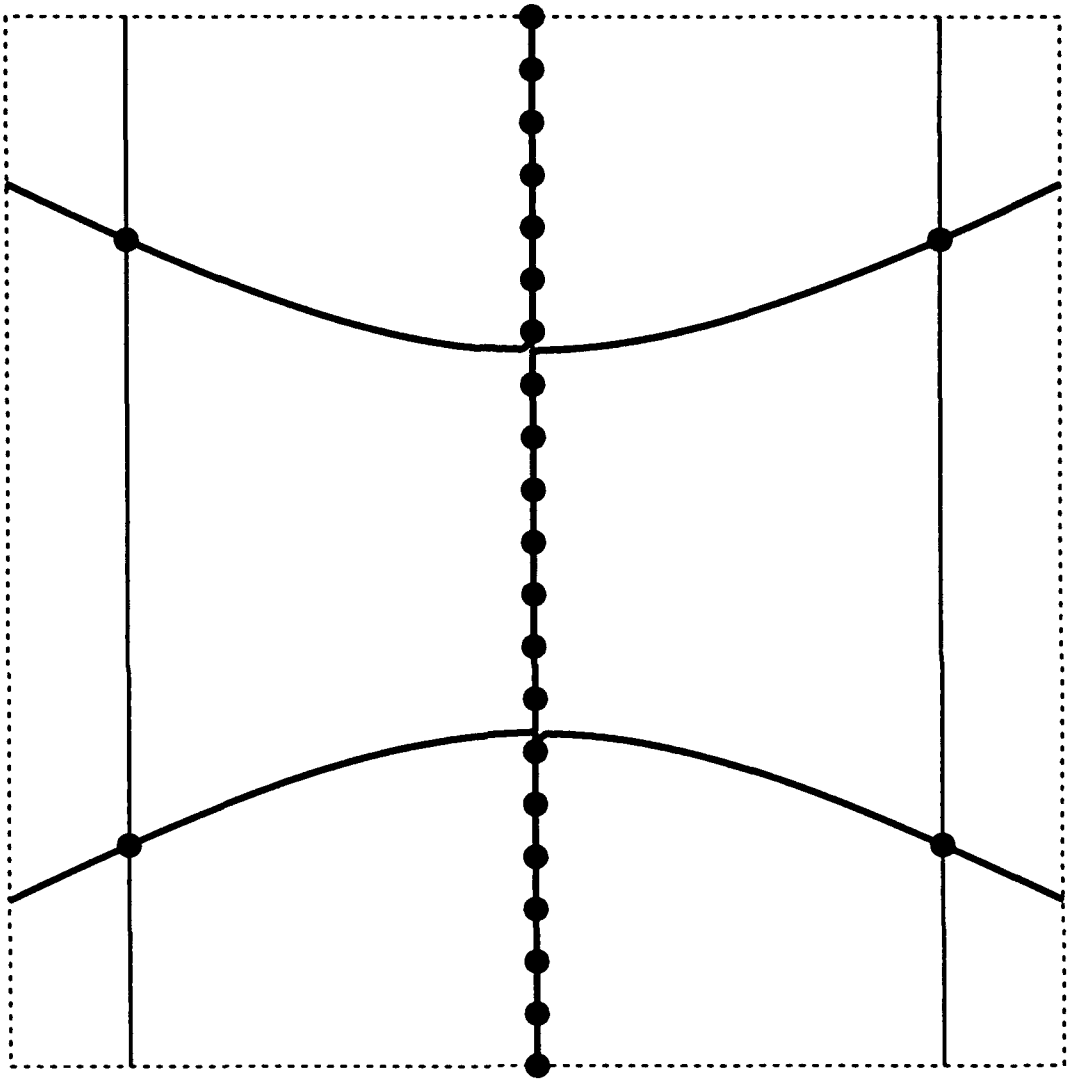

Figure 5

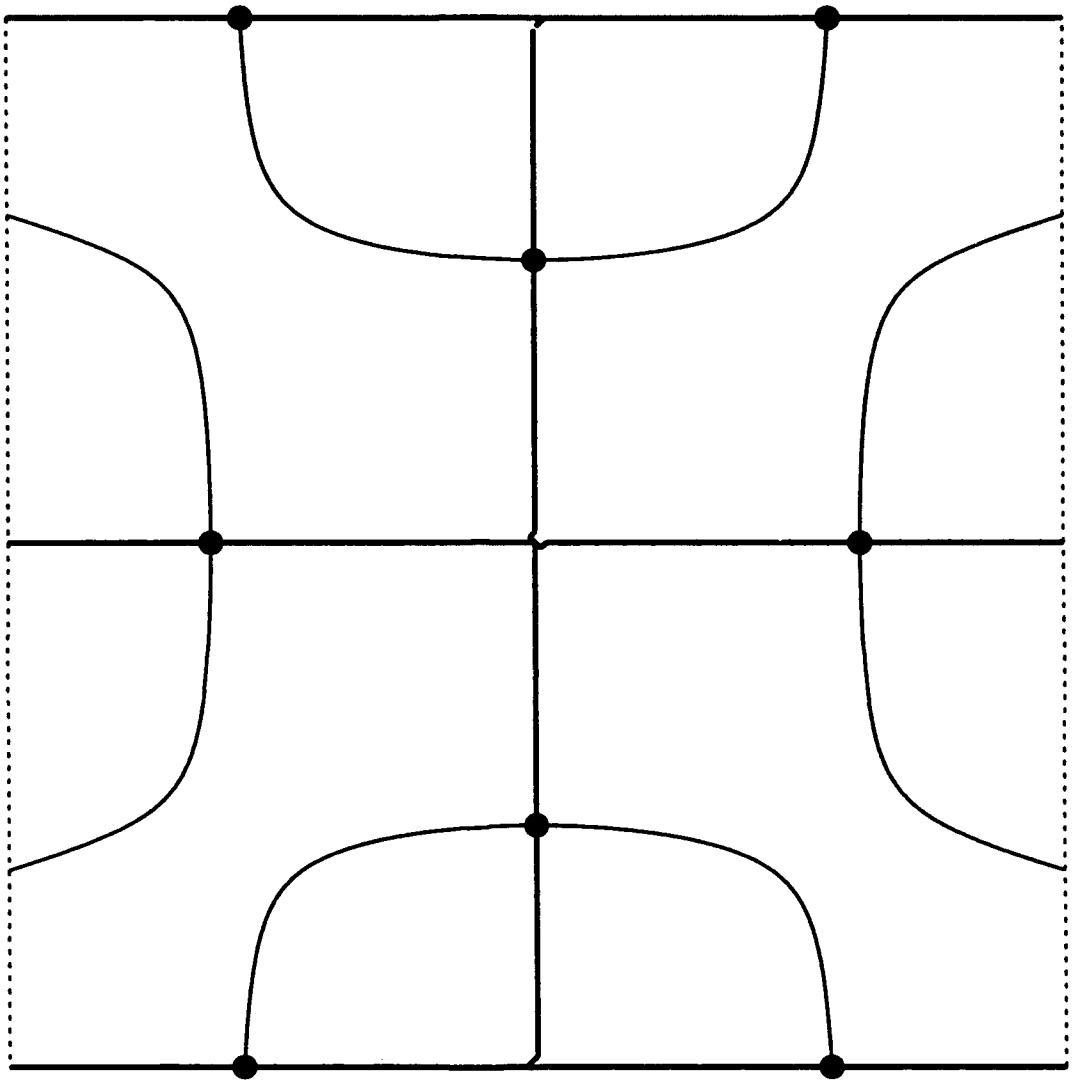

Figure 6a

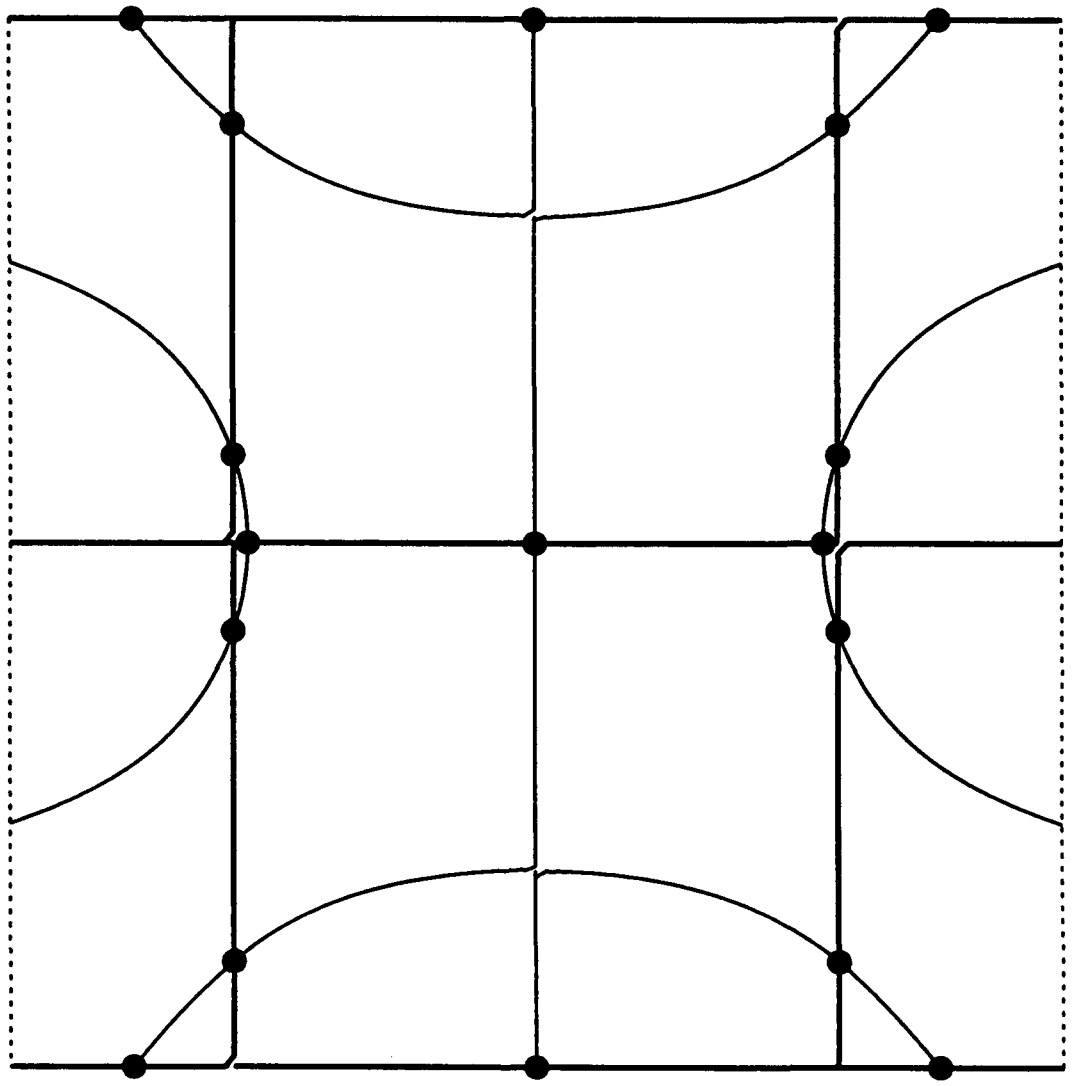

Figure 6b

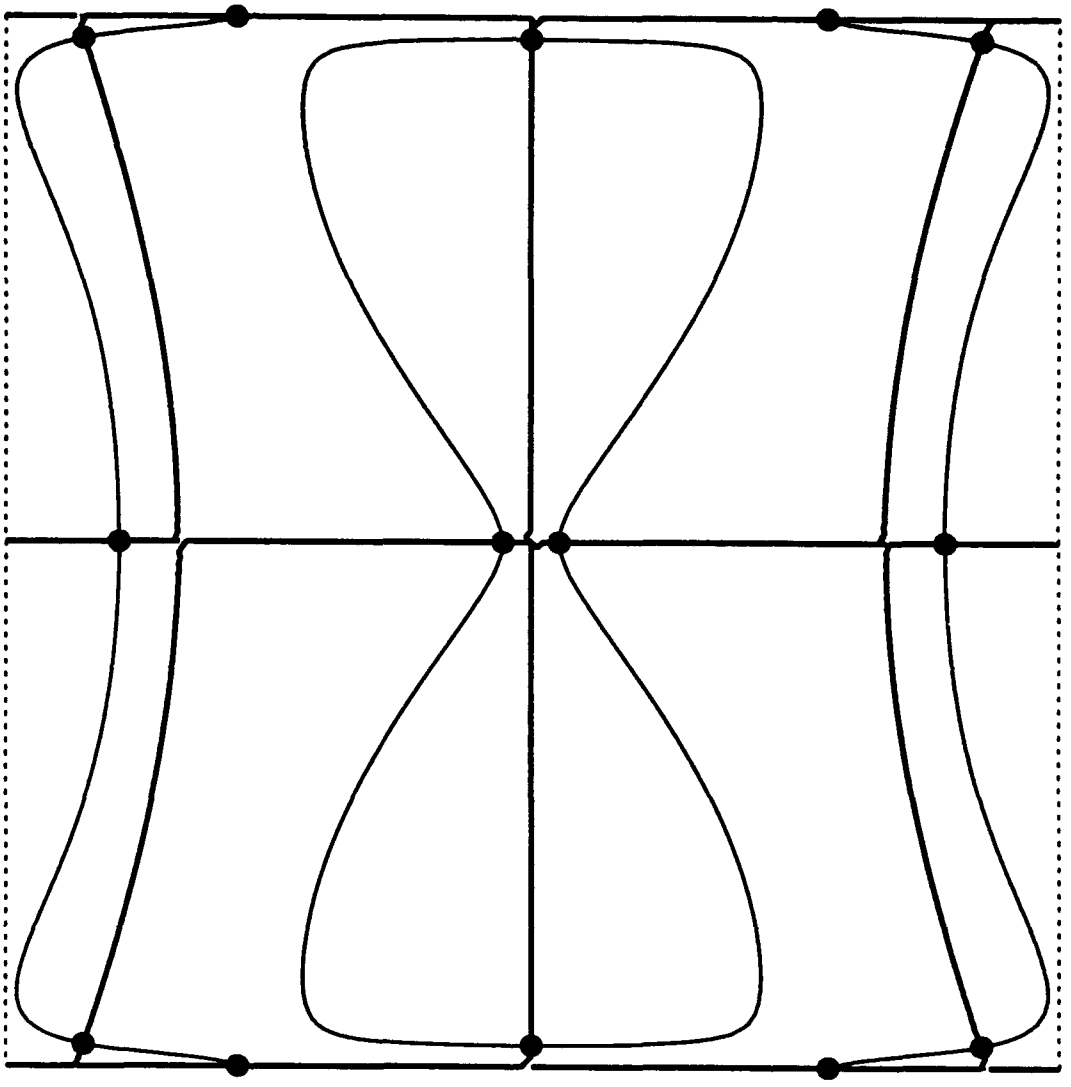

Figure 6c

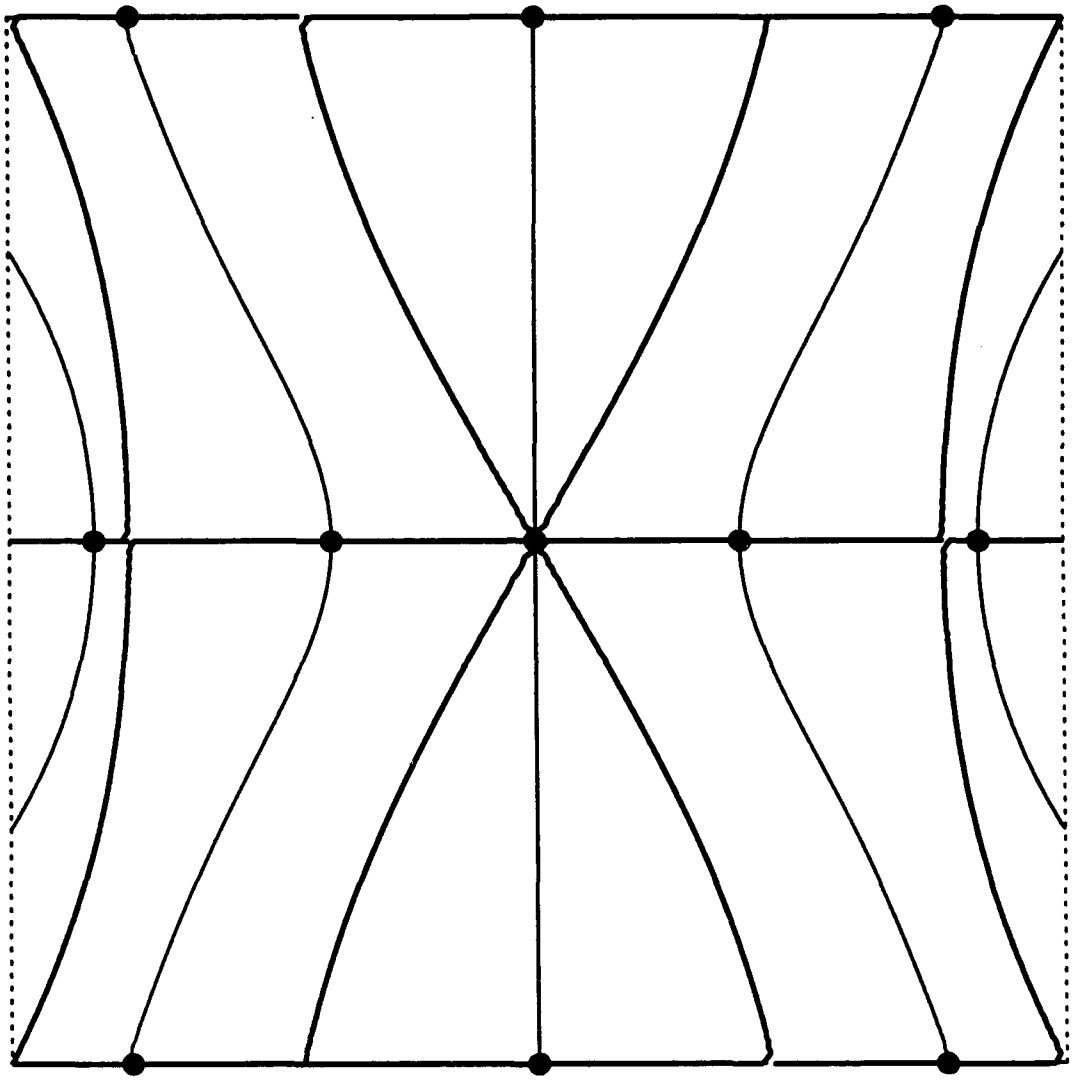

Figure 6d

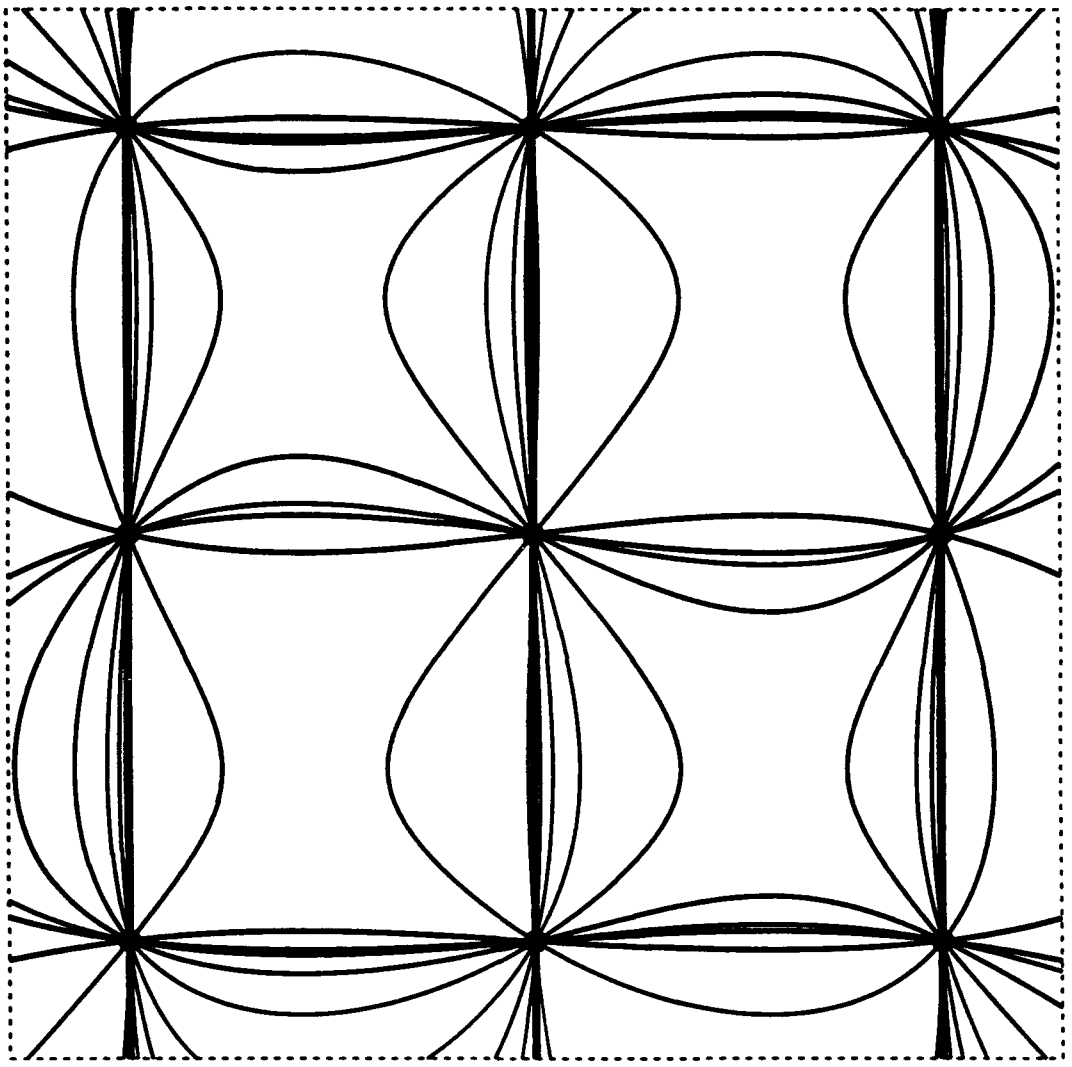

Figure 7a

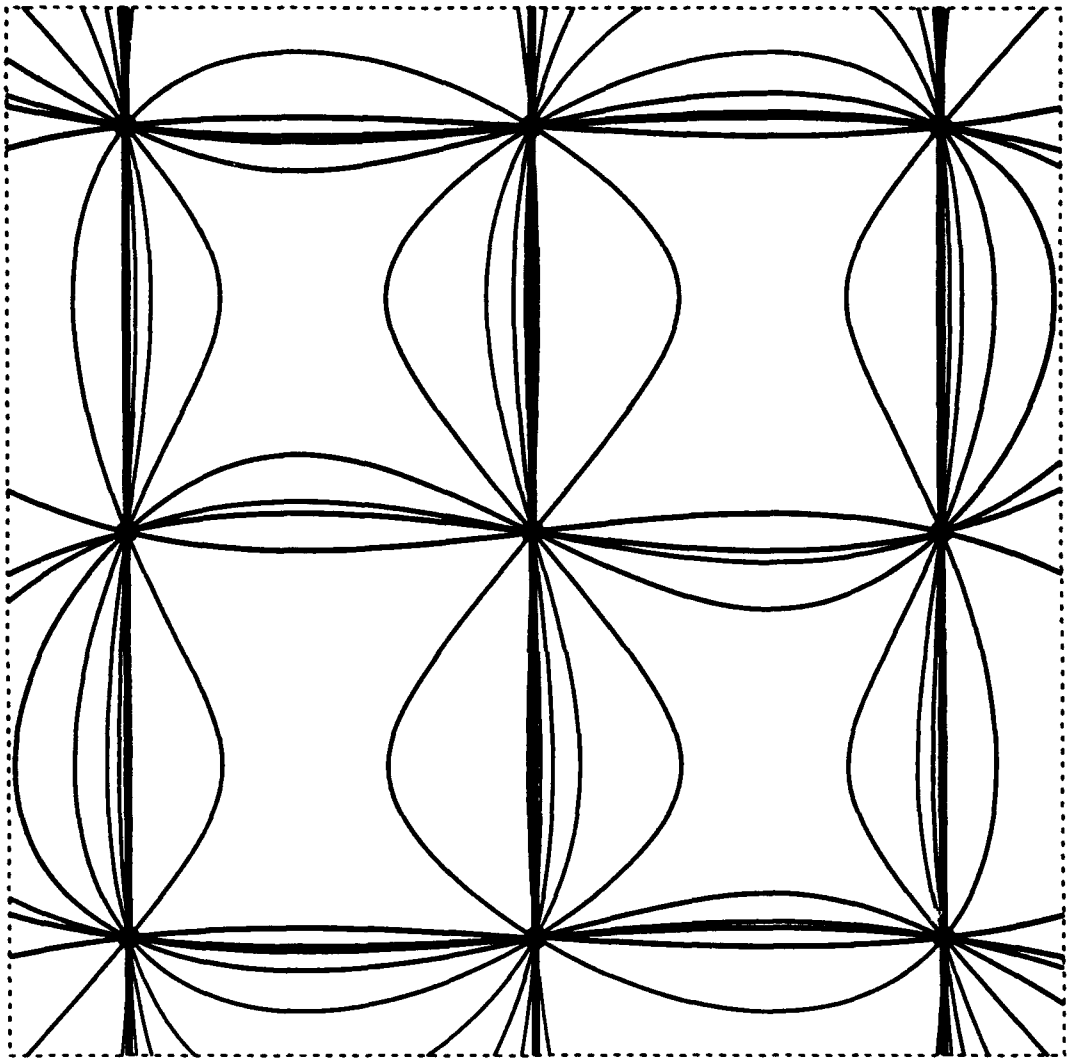

Figure 7b

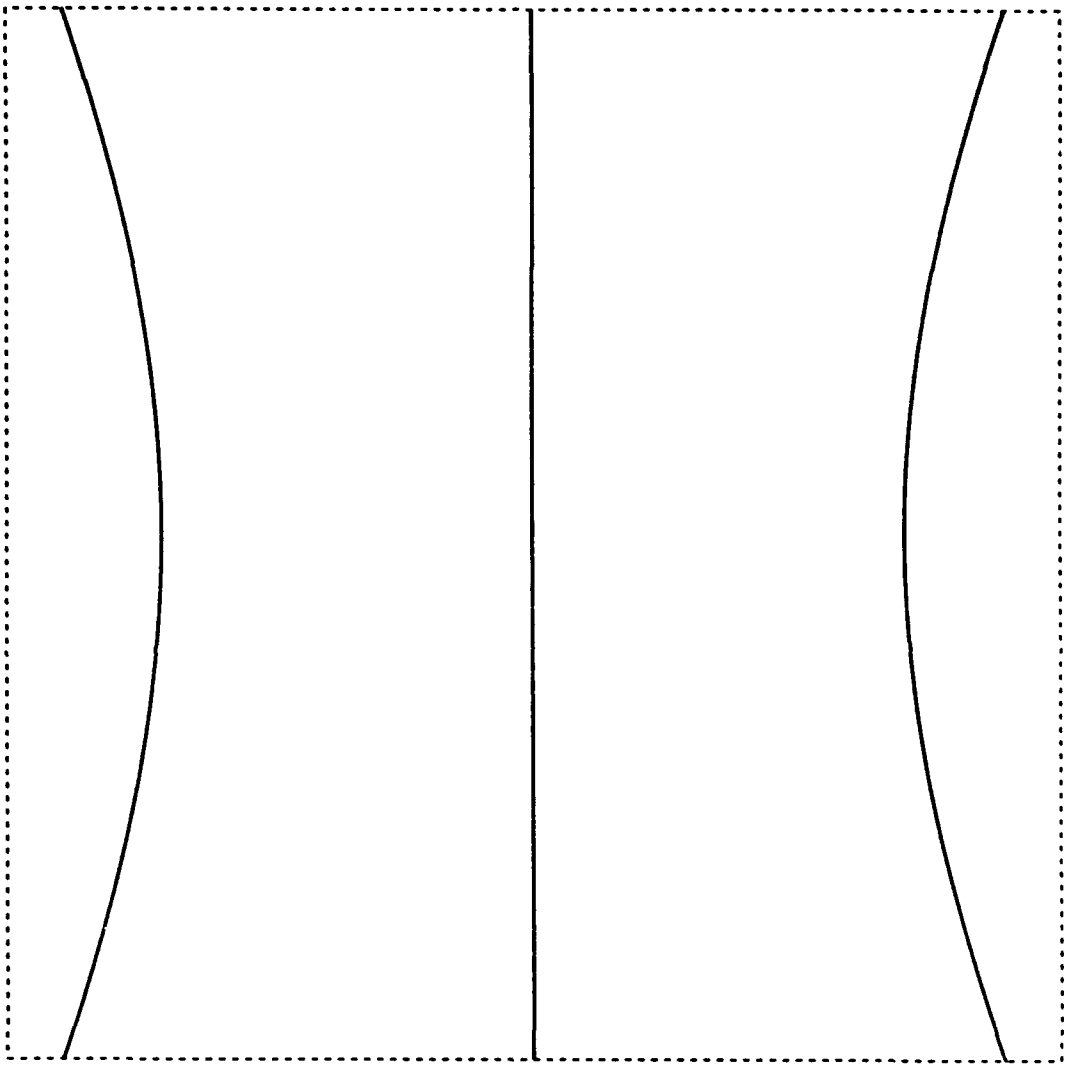

Figure 8a

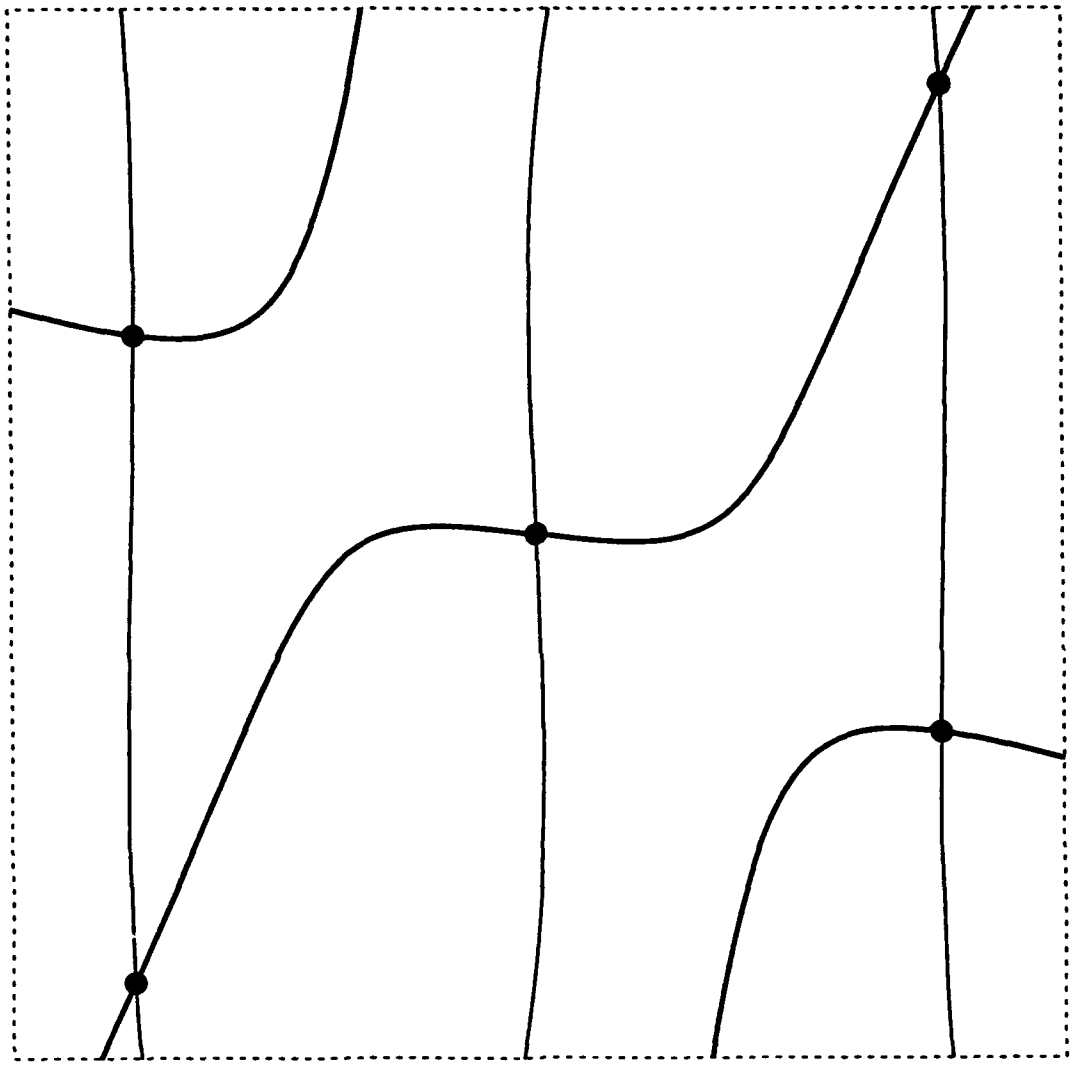

Figure 8b

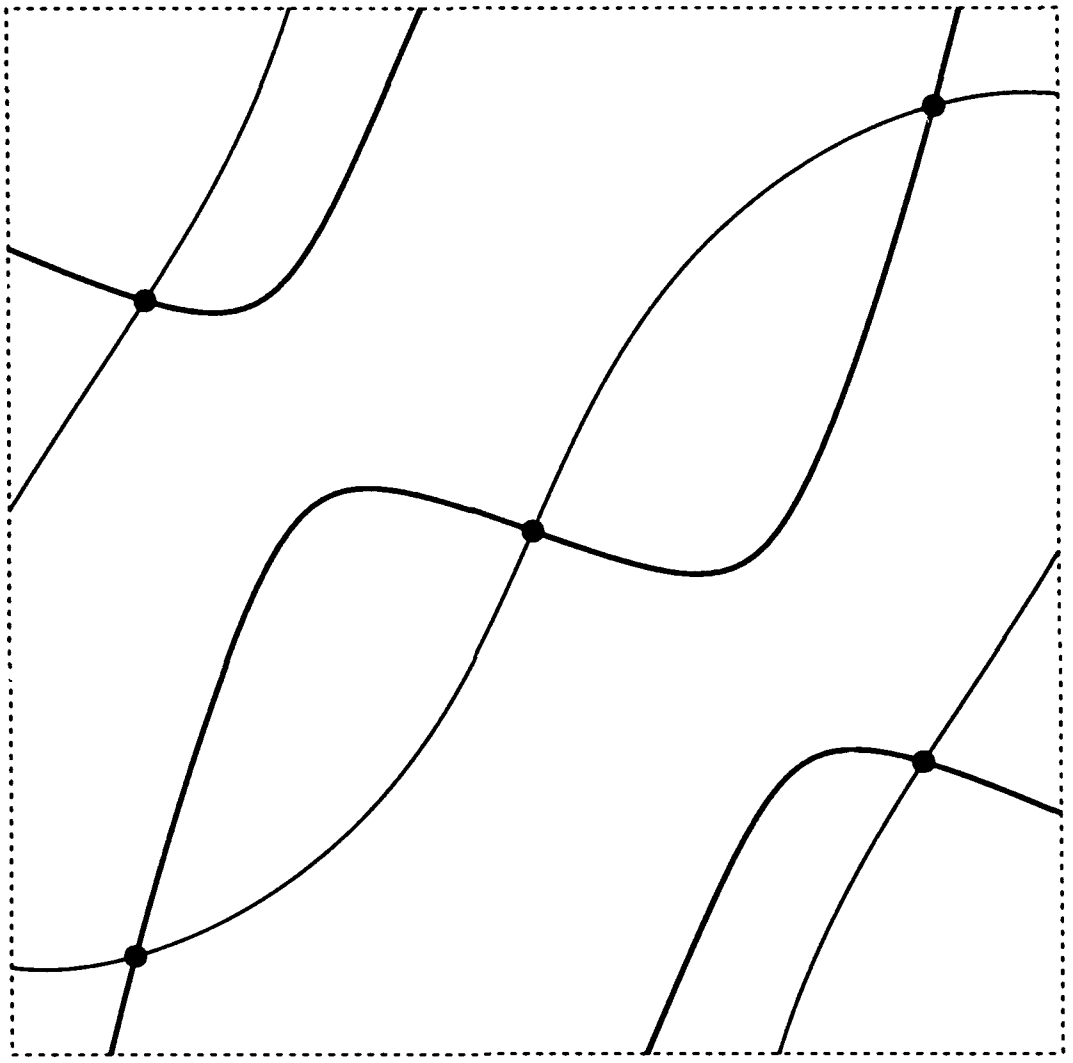

Figure 8c

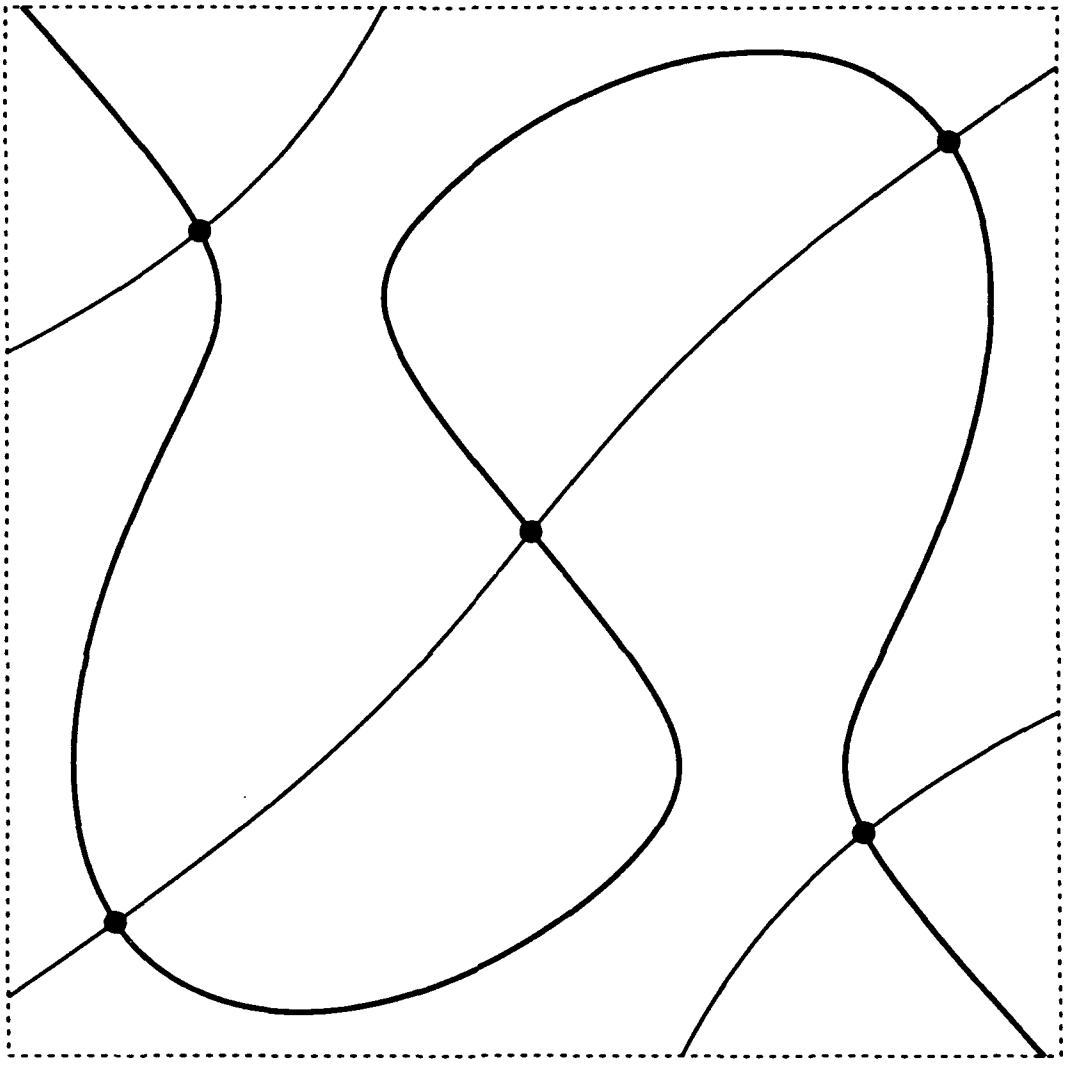

Figure 8d

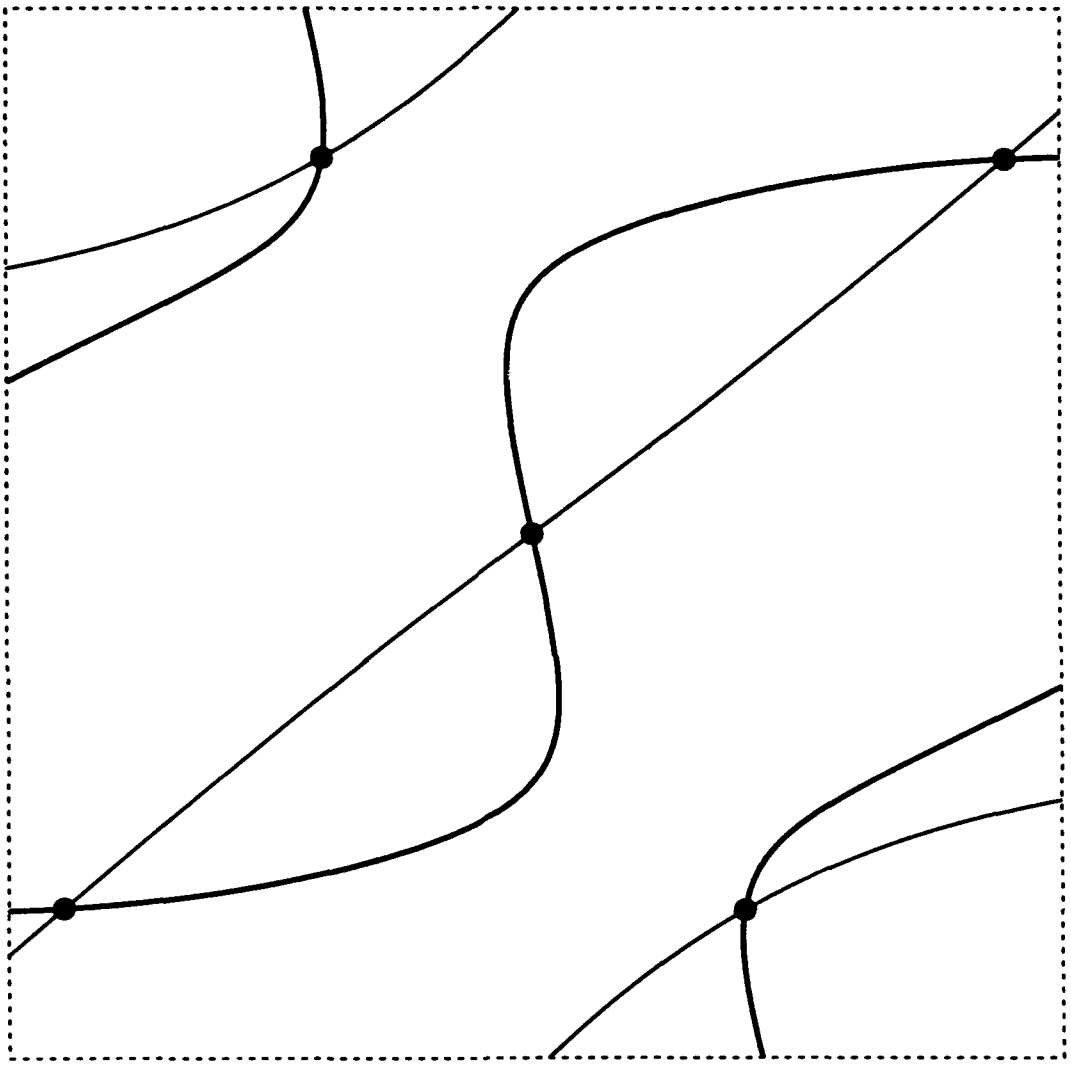

Figure 8e

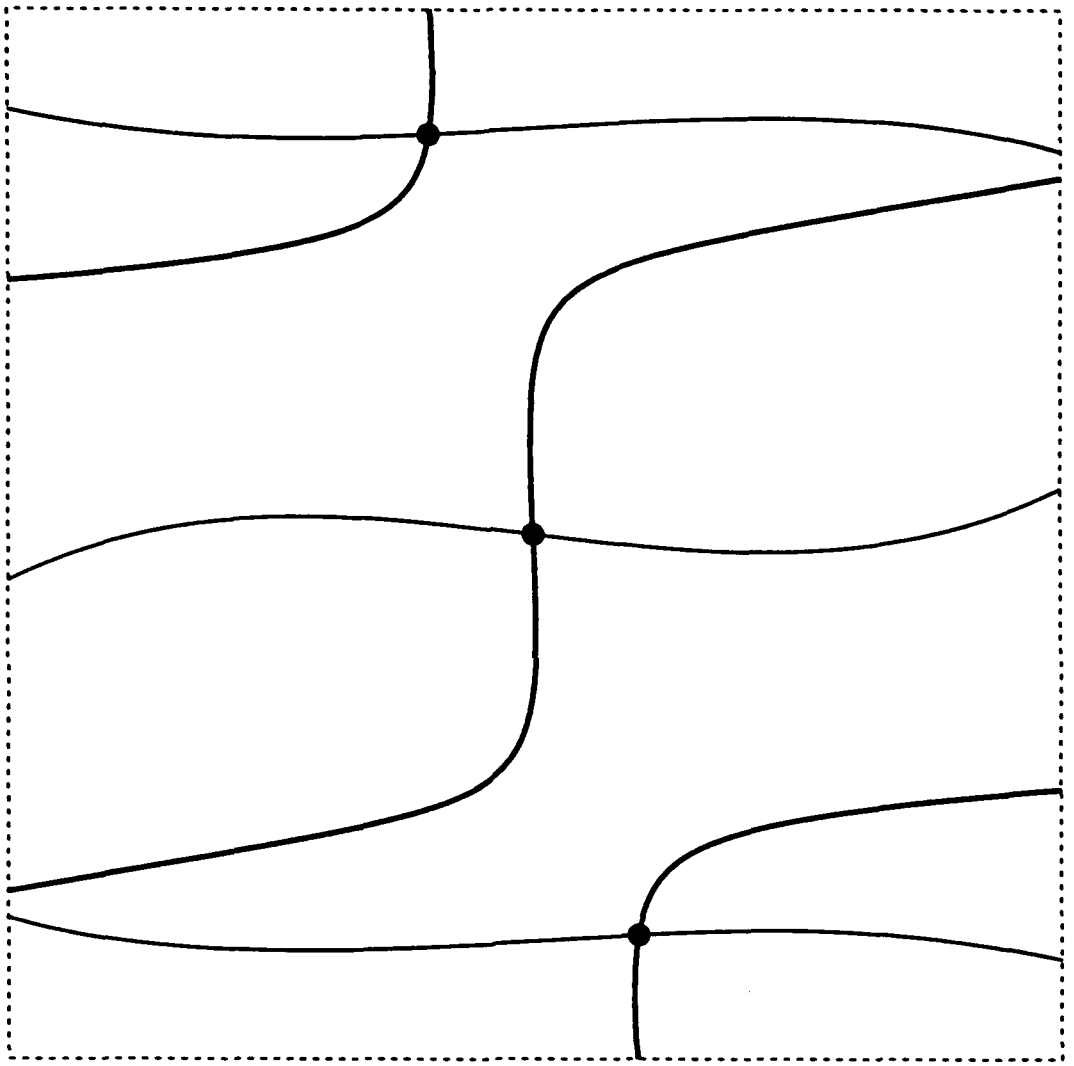

Figure 8f

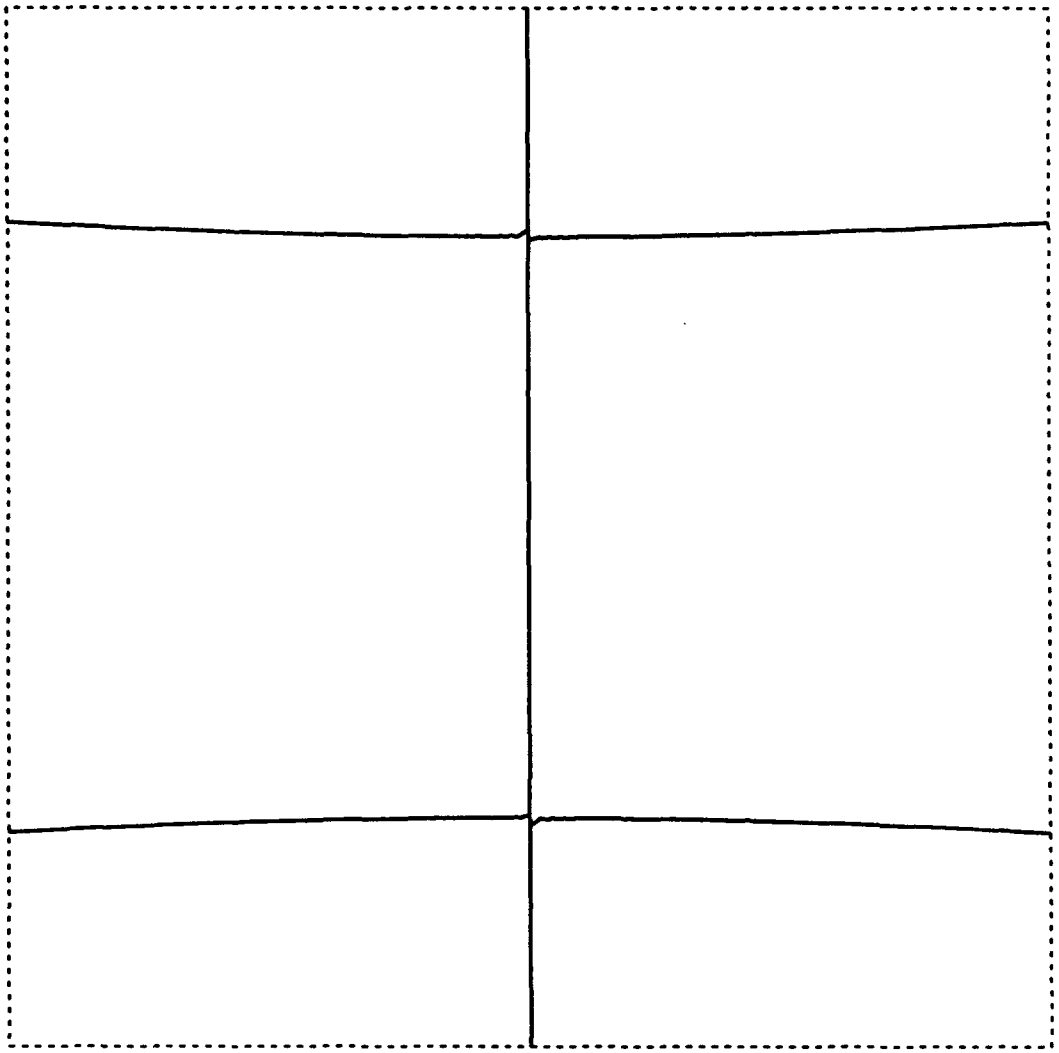

Figure 8g

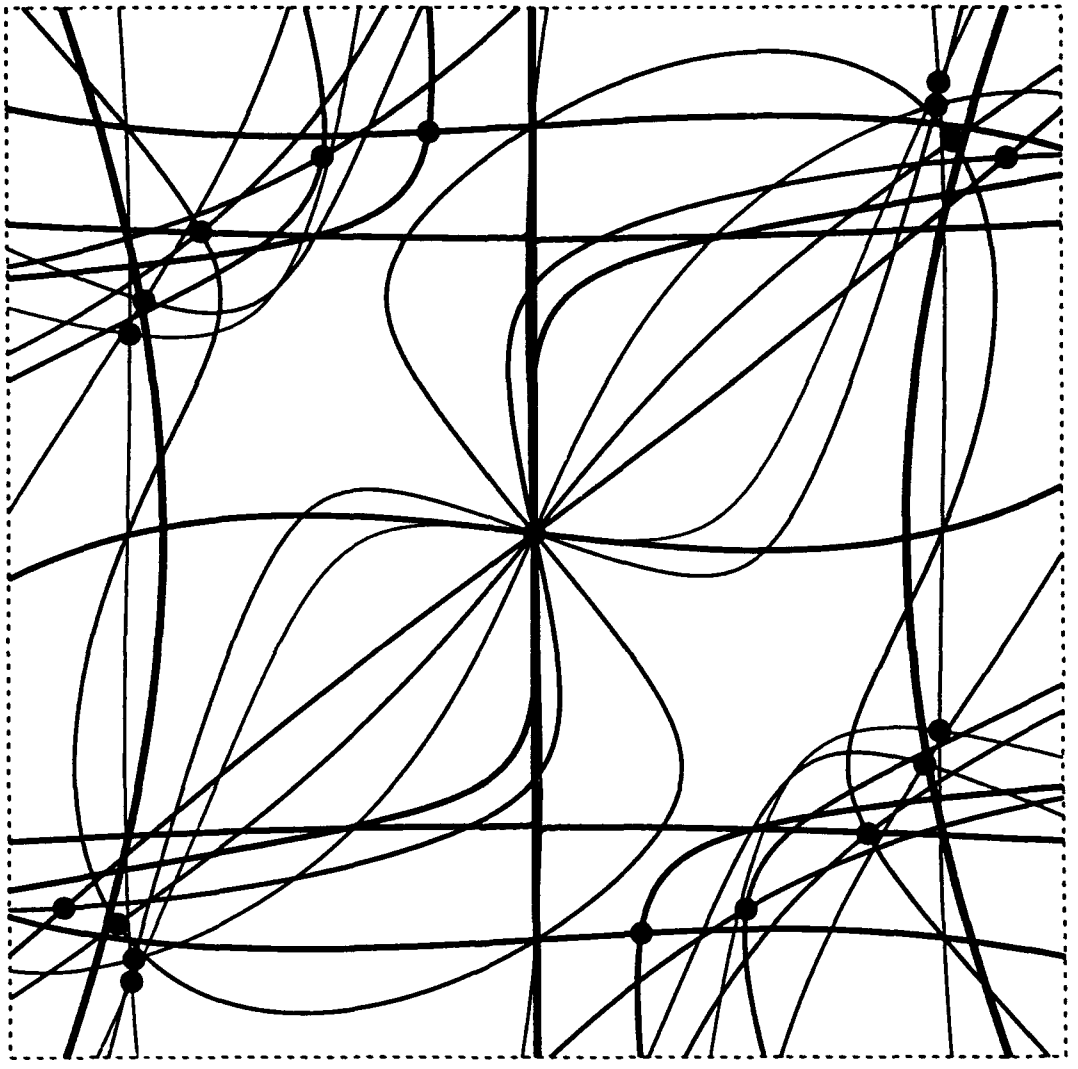

Figure 8h

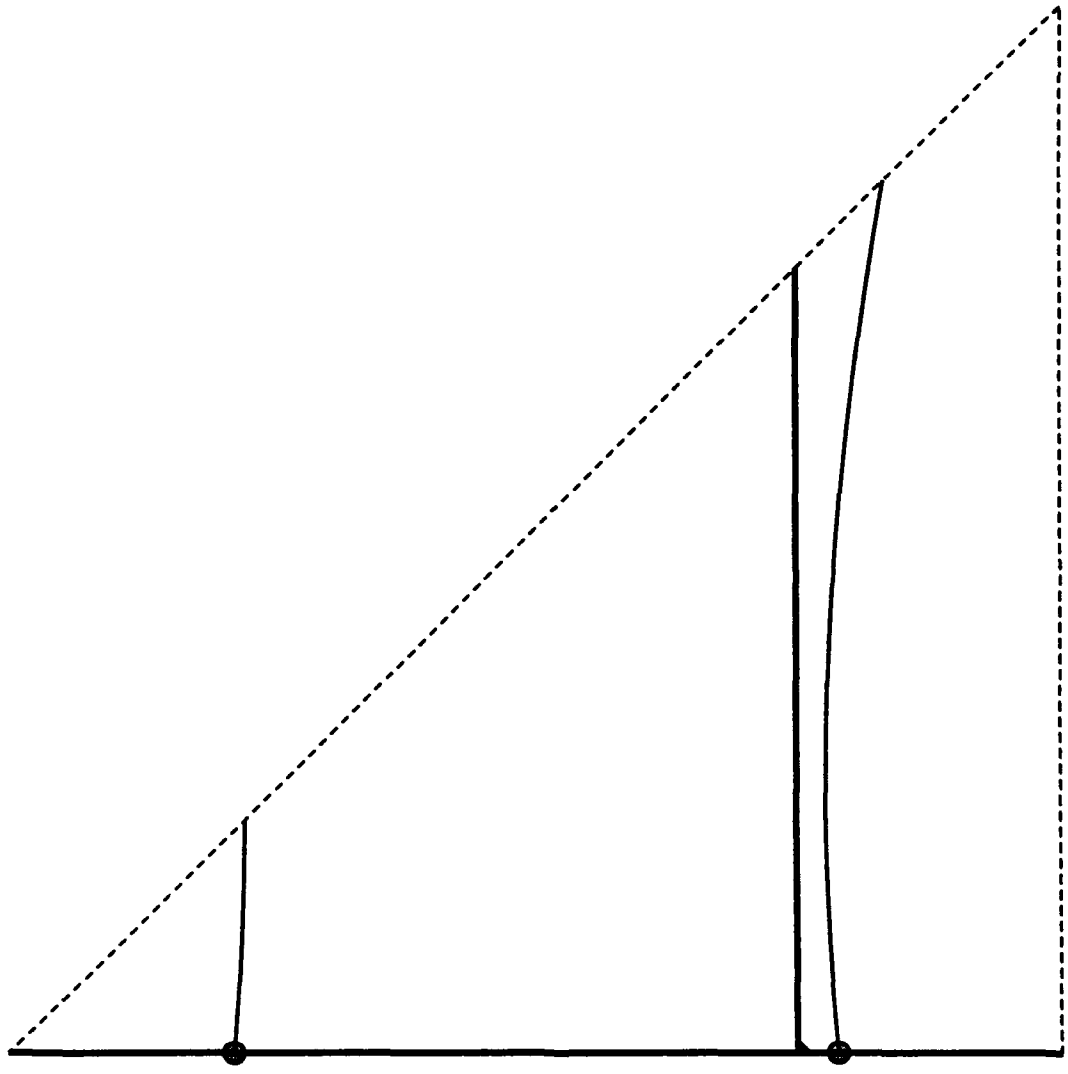

Figure 9a

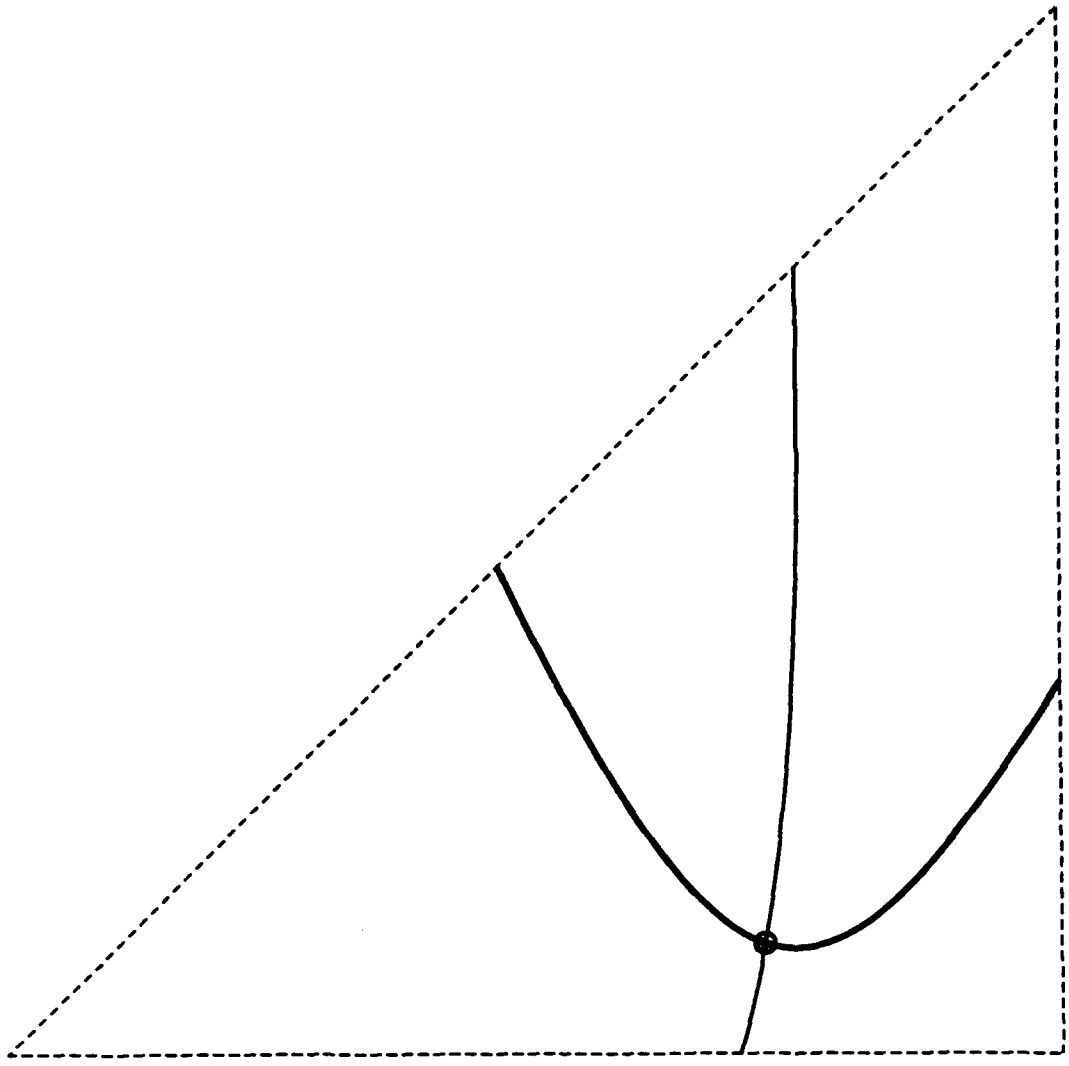

Figure 9b

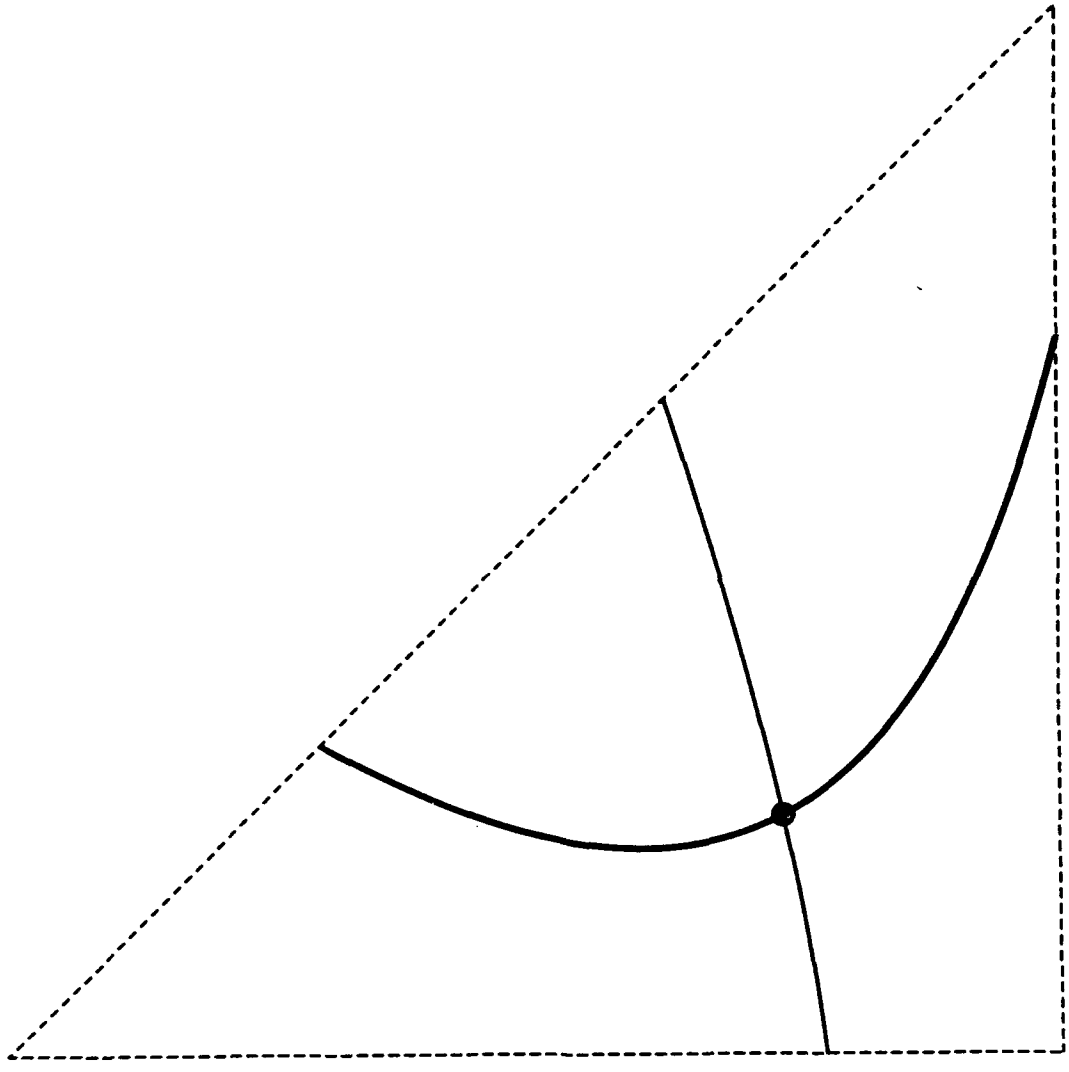

Figure 9c

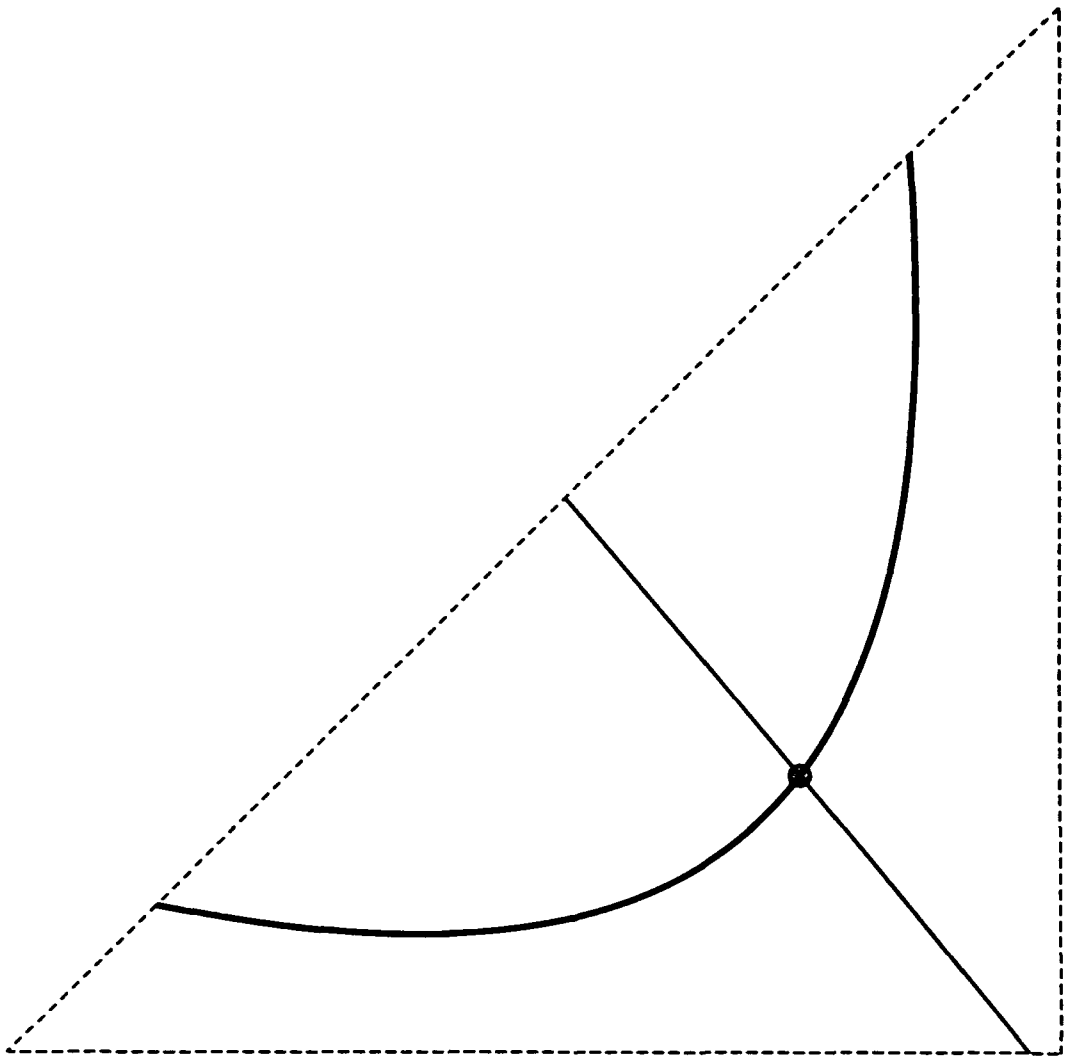

Figure 9d

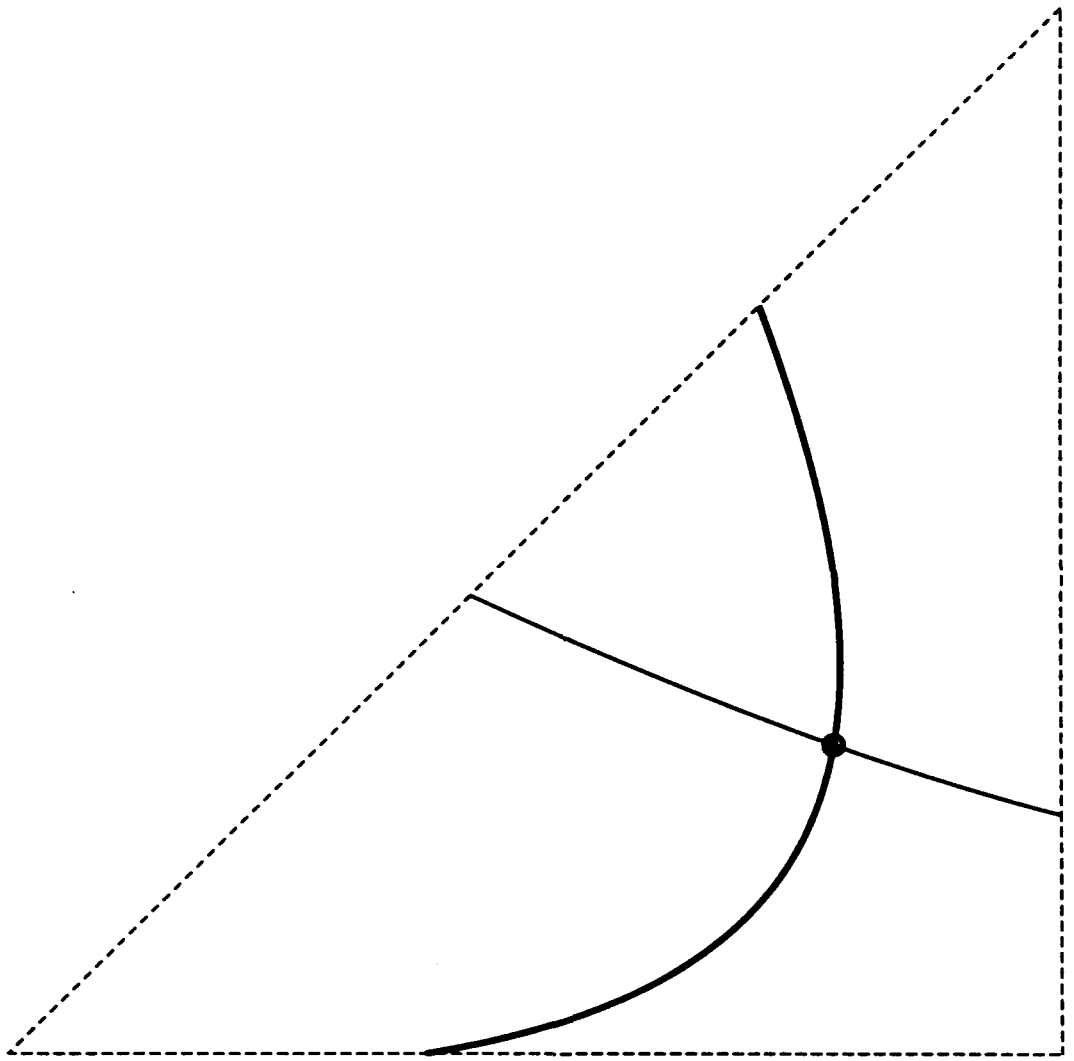

Figure 9e

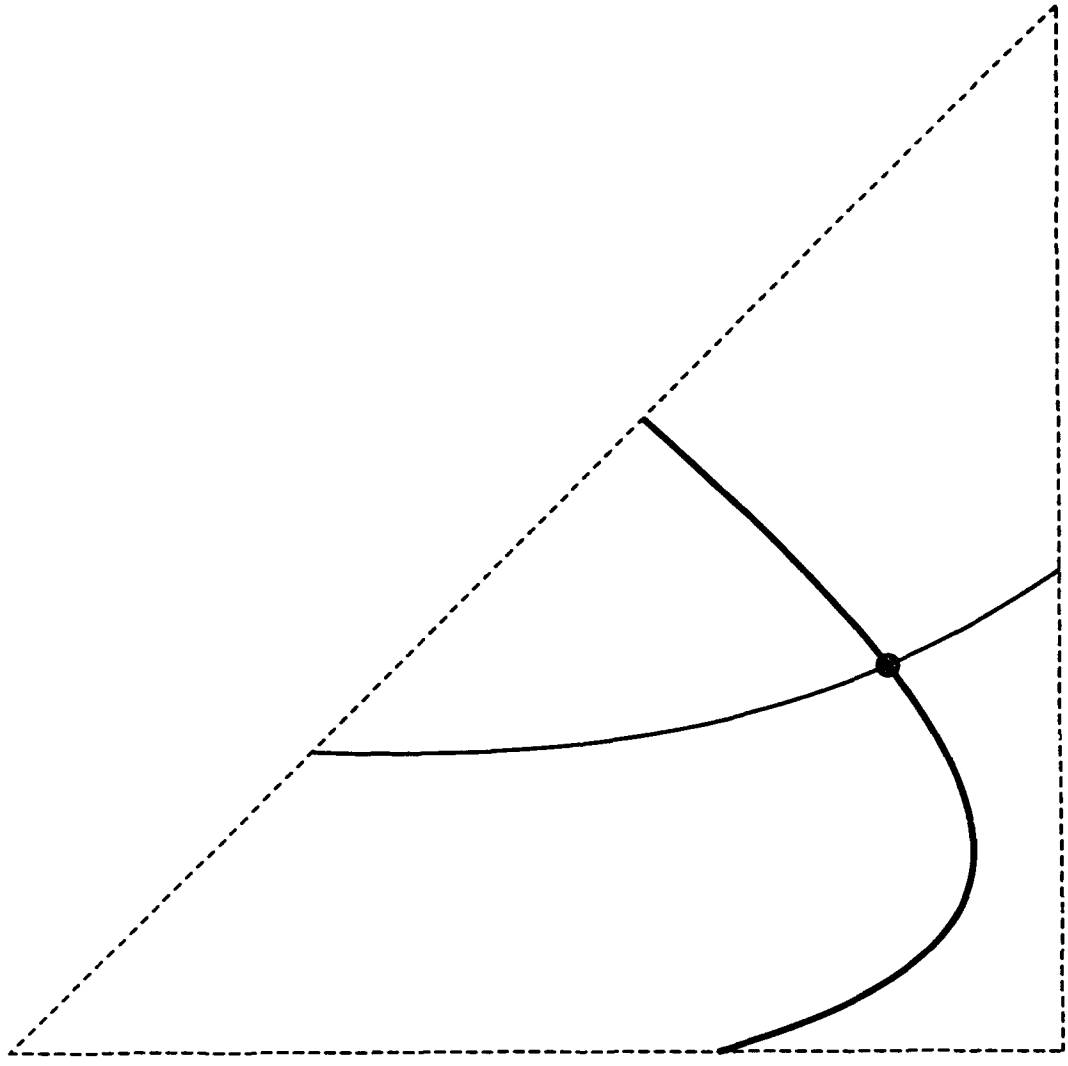

Figure 9f

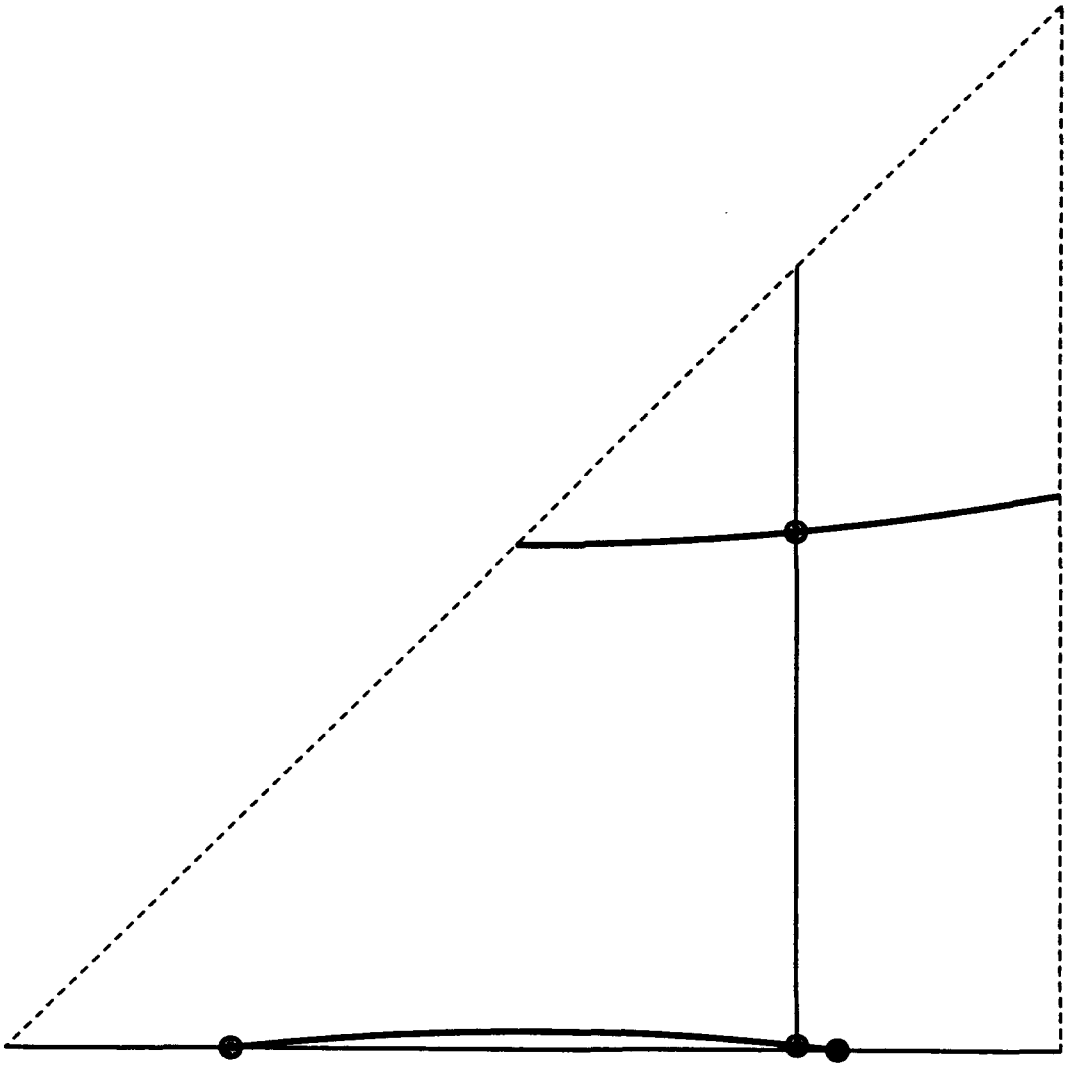

Figure 9g

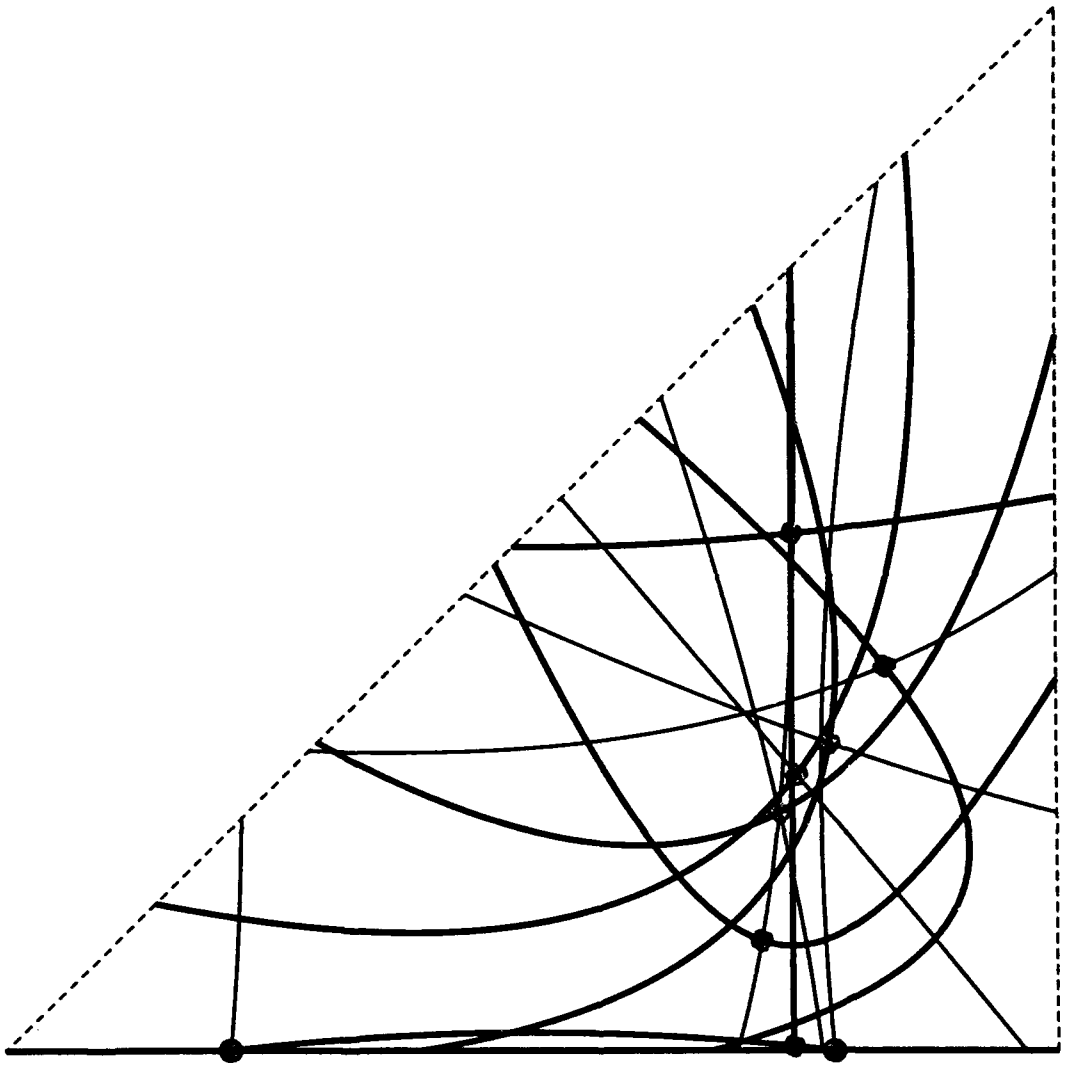

Figure 9h

The Laboratory for Numerical Analysis is an integral part of the Institute for Physical Science and Technology of the University of Maryland, under the general administration of the Director, Institute for Physical Science and Technology. It has the following goals:

- To conduct research in the mathematical theory and computational implementation of numerical analysis and related topics, with emphasis on the numerical treatment of linear and nonlinear differential equations and problems in linear and nonlinear algebra.

- To help bridge gaps between computational directions in engineering, physics, etc., and those in the mathematical community.

- To provide a limited consulting service in all areas of numerical mathematics to the University as a whole, and also to government agencies and industries in the State of Maryland and the Washington Metropolitan area.

- To assist with the education of numerical analysts, especially at the postdoctoral level, in conjunction with the Interdisciplinary Applied Mathematics Program and the programs of the Mathematics and Computer Science Departments. This includes active collaboration with government agencies such as the National Institute of Standards and Technology.

- To be an international center of study and research for foreign students in numerical mathematics who are supported by foreign governments or exchange agencies (Fulbright, etc.).

Further information may be obtained from **Professor I. Babuška**,Chairman, Laboratory for Numerical Analysis, Institute for Physical Science and Technology, University of Maryland, College Park, Maryland 20742-2431.